



## **POLITECNICO DI TORINO**

Master's Degree in Automotive Engineering

### **GFG Style Vision 2030 Rear Frame Design**

Supervisor:

**Prof. Andrea Tonoli**

Candidate:

**Emanuele Maneglia**

*A.A. 2019/2020*



---

# Content

Content.....	3
List of Tables.....	6
List of Figures .....	7
List of Symbols and Abbreviations .....	11
1. CHAPTER 1 – INTRODUCTION .....	15
1.1 L.M. Gianetti Internship .....	15
1.2 GFG Style Vision 2030.....	16
1.3 Vehicle Data.....	18
2. CHAPTER 2 – FUNCTIONAL REQUIREMENTS .....	21
2.1 Suspension Hardpoints.....	21
2.2 Suspension Components .....	26
2.2.1 Upper Control Arm.....	27
2.2.2 Lower Control Arm.....	29
2.2.3 Tie Rod.....	30
2.2.4 Knuckle .....	30
2.2.5 Anti-Roll Bar .....	32
2.2.6 Damper and Spring Group .....	33
2.3 DMU Analysis.....	36
2.3.1 Space Available .....	36
2.3.2 Powertrain.....	38
2.3.3 Battery Pack and BMS.....	39
2.3.4 DC/DC Converter.....	40
2.3.5 Inverter.....	43
3.2.6 Charger Unit.....	45
3.2.7 Rear Wing System .....	47
3. CHAPTER 3 – REAR FRAME.....	49
3.1 Rear Frame Structure .....	49
3.1.1 Material: 25CD4 Steel Alloy .....	49
3.1.2 Geometric Structure .....	50

---

3.2	Rear Frame Components.....	52
3.2.1	Upper Node.....	52
3.2.2	Top Mount.....	54
3.2.3	Upper Control Arm Front Node .....	55
3.2.4	Upper Control Arm Rear Node.....	56
3.2.5	Lower Control Arm Front Node .....	58
3.2.6	Lower Control Arm Rear Node.....	60
3.2.7	Tubes.....	61
3.3	Frame Interface Components .....	63
3.3.1	Inverter and DC/DC Converters Interface.....	63
3.3.2	Motor Mounts.....	66
3.3.3	Central Cell Interface .....	69
4.	CHAPTER 4 – PRODUCTION PROCESS .....	73
4.1	Welding.....	73
4.1.1	TIG Welding.....	73
4.1.2	Defects Detection.....	75
4.1.3	Industrial Radiography .....	77
4.1.4	Industrial Computed Tomography.....	80
4.2	Welding Tools .....	83
4.3	Production Process.....	87
4.4	Rear Frame Weight.....	90
5.	CHAPTER 5 – TEST REFERENCE.....	92
5.1	Dynamics Behavior .....	92
5.1.1	Longitudinal Acceleration 1.2g .....	92
5.1.2	Braking 1.5g.....	93
5.1.3	Cornering 1.5g.....	94
5.2	Impact Behavior .....	96
6.	CHAPTER 6 – FEM ANALYSIS .....	100
6.1	Rear Frame Analysis .....	100
6.1.1	Model and Loadcases.....	100
6.1.2	Acceleration Slip 1.2g.....	103

---



---

6.1.3	Braking 1.5g.....	104
6.1.4	Cornering 1.5g.....	105
6.1.5	Bump 4g .....	106
6.1.6	Lateral Impact .....	107
6.1.7	Longitudinal Impact .....	108
6.1.8	Conclusions .....	109
6.2	Motor Mounts FEM Analysis .....	111
6.2.1	Left Motor Mount .....	111
6.2.2	Right Motor Mount .....	112
6.2.3	Rear Motor Mount.....	113
6.2.4	Conclusions .....	114
7.	CHAPTER 7 – TORSIONAL STIFFNESS .....	116
7.1	Torsional Stiffness Assessment .....	116
7.1.1	Reference and Model.....	116
7.1.2	Rear Frame Torsional Stiffness .....	118
7.1.3	Chassis Torsional Stiffness .....	121
7.2	Torsional Stiffness Validation .....	122
7.2.1	Antiroll Bars.....	122
7.2.2	On Road Testing .....	124
	Annex .....	126
	Bibliography .....	141
	Acknowledgements.....	143

---

## List of Tables

Table 1. Basic Parameters. ....	18
Table 2. Frame & Body.....	18
Table 3. Brakes & Suspensions.....	19
Table 4. Batteries & Powertrain.....	19
Table 5. Rear Suspension Hard Points. ....	23
Table 6. Rotation Points Coordinates. ....	25
Table 7. Setup Parameters. ....	26
Table 8. Suspensions Stroke Data. ....	26
Table 9. ALU 7075 T6 Mechanical Properties. ....	27
Table 10. ALU 7075 T6 Chemical Composition. ....	27
Table 11. ALU 2024 T6 Properties.....	31
Table 12. ALU 2024 T6 Chemical Composition. ....	31
Table 13. 25CD4 Mechanical Properties.....	49
Table 14. 25CD4 Chemical Composition.....	49
Table 15. ALU 5754 Mechanical Properties.....	64
Table 16. ALU 5754 Chemical Composition.....	64
Table 17. ALU 6082 Mechanical Properties.....	69
Table 18. ALU 6082 Chemical Composition.....	69
Table 19. TIG CrMo1 Mechanical Properties.....	74
Table 20. TIG CrMo1 Chemical Composition.....	75
Table 21. S235 Mechanical Properties.....	84
Table 22. S235 Chemical Composition.....	84
Table 23. Vehicle Data for computing Loadcases. ....	92
Table 24. Loadcases Resume. ....	102
Table 25. FEM Analysis Results. ....	109
Table 26, Motor Mounts FEM Analysis Results. ....	114
Table 27. Torsional Test FEM Analysis Results. ....	120
Table 28. Rear Antiroll Bar Data.....	123

## List of Figures

Figure 1. L. M. Gianetti site in northern Turin. ....	15
Figure 2. L.M. Gianetti, plant and Show Room. ....	16
Figure 3. GFG Style Vision 2030 rolling chassis at the Riyadh Car Show 2019. ....	16
Figure 4. The finished GFG Style Vision 2030. ....	17
Figure 5. Double Wishbone Suspension scheme (Left: Long Strut, Right: Short Strut). ....	21
Figure 6. Front and Rear suspension points vs Central Chassis. ....	22
Figure 7. Rear Suspension Points, Left Side. ....	22
Figure 8. Double Wishbone, Instant Center of Rotation for Roll motion. ....	23
Figure 9. Double Wishbone Instant Axis of Rotation. ....	24
Figure 10. Rear Suspension Instant Axis of Rotation (pink) and Control Arms planes (light blue). ..	24
Figure 11. Rear Suspension Rolling Center (RC) ....	25
Figure 12. Pitch Center of Rotation. ....	25
Figure 13. Rear Suspensions Components. ....	27
Figure 14. Upper Control Arm. ....	28
Figure 15. Left: NMB ABYT12-V ball joint. Right: UBJ Detail. ....	28
Figure 16. Powerflex universal bushings PP99-112P. ....	29
Figure 17. Lower Control Arm. ....	29
Figure 18. Tie Rod. ....	30
Figure 19. Toe angle regulation on Tie Rod, detail. ....	30
Figure 20. Front and Rear view of the Knuckle. ....	31
Figure 21. Left: UBJ Carrier; Right: UBJ Camber Shim. ....	32
Figure 22. Left: Anti-Roll Bar Welded Bushing; Right: Anti-Roll Bar Knife. ....	32
Figure 23. Left: Anti-Roll Bar's Connecting Rod; Right: NMB Ball Joint ARYT5-E. ....	32
Figure 24. Anti-Roll Bar Group, Left Half. ....	33
Figure 25. Damper and Spring Group. ....	33
Figure 26. Hydraulics system of the Vehicle: in Red the Groups acting on Damper. ....	34
Figure 27. Mounted Left and Right Rear Suspensions. ....	35
Figure 28. Central Cell Limits. ....	36
Figure 29. Left: Underbody and Diffuser; Right: Sidewall. ....	37
Figure 30. Left: Rear Bumper; Right: Definition of the Rear Volume. ....	37
Figure 31. Vehicle Rear Components placement area. ....	38
Figure 32. Left: Motor Power (Orange) and Torque (Blue); Right: Rear Powertrain. ....	38
Figure 33. Battery Pack layout in CATIA. ....	39
Figure 34. Qualitative reference for change in Batteries Performance. ....	39
Figure 35. BMS Central Unit placed over the Battery Pack. ....	40
Figure 36. Diode behavior and symbol. ....	41
Figure 37. MOSFET behavior and circuit representation. ....	41

Figure 38. DC/DC Converter scheme (a) and waveforms: load Voltage (b), control current(C), load current (d) and current through switch (e).....	42
Figure 39. Components size and holes axes. Left: DC/DC Converter 12V; Right: DC/DC Converter 365V. ....	42
Figure 40. Installed DC/DC Converters. ....	43
Figure 41. Common 3-phased DC/AC Converter circuit. ....	43
Figure 42. PWM. Left: Comparison between Waves; Right: Voltage of each Phase.....	44
Figure 43. Left: Inverter installed on vehicle; Right: Charger above the Battery Pack. ....	44
Figure 44. Recharging Power Paths. ....	45
Figure 45. Final layout of the Power Electric Circuit.....	45
Figure 46. Scheme of the Electric Power System. ....	46
Figure 47. Left: Rear End of the car; Right: Rear End in CATIA. ....	47
Figure 48. Left: Geometric Structure of the Rear Frame; Right: Side view. ....	50
Figure 49. Rear and Top view of the Wireframe.....	51
Figure 50. Half Wireframe with the Nodes. ....	52
Figure 51. Left: Upper Node in CATIA; Right: Machined Upper Node.....	53
Figure 52. Detail of the coupling between Node and Tube. ....	53
Figure 53. Finished Top Mount. ....	54
Figure 54. Left: Detail of the coupling of Top Mount and Damper; Right: Cross section of the Pivot Joint.....	55
Figure 55. UCA Front Node in CATIA.....	55
Figure 56. Finished UCA Front Node on the Welding Tool. ....	56
Figure 57. UCA Rear Node in CATIA. ....	57
Figure 58. Cross section of the Node-Antiroll Bar mounting.....	57
Figure 59. Finished UCA Rear Node on the Welding Tool. ....	58
Figure 60. Cross Section of the Removable Tube mounting.....	59
Figure 61. Finished LCA Front Node.....	59
Figure 62. LCA Rear Node in CATIA. ....	60
Figure 63. Rear Frame: Nodes and Tubes. ....	61
Figure 64. Detail of the Laser Cutting Shapes. ....	62
Figure 65. Shape of the Inverter and DC/DC 365V Converter Support. ....	63
Figure 66. Left: Mounting of the Sheet flaps on the UCA Front Node; Right: Fixing of the Sheet on the Welded Bushings. ....	64
Figure 67 Left: 12V DC/DC Converter Support; Right: Mounting Position. ....	65
Figure 68. Motor Left Mount in CATIA.....	66
Figure 69. Assembly of the Left and Right Motor Mounts. ....	67
Figure 70. Motor Right Mount in CATIA. ....	67
Figure 71. Left: Motor Rear Mount; Right: Fixed Motor Rear Mount. ....	68
Figure 72. Left: Keensert Cross Section; Right: Top Mount Welded Cell Mount.....	70
Figure 73. Higher Welded Cell Mount. ....	70
Figure 74. Lower Welded Cell Mount. ....	71

Figure 75. Welding Scheme. ....	73
Figure 76. TIG Welding Scheme. ....	74
Figure 77. Dye Penetrant Inspection test phases. ....	77
Figure 78. Scheme of the Industrial Radiography. ....	77
Figure 79. Industrial Radiography: Sample OK. ....	78
Figure 80. Industrial Radiography: Different Sample with Defects. ....	79
Figure 81. Tomography, Sample 1, Welding 1. ....	80
Figure 82. Tomography: Sample 1, Welding 2. ....	81
Figure 83. Tomography: Sample 2, Welding 1. ....	81
Figure 84. Tomography: Sample 2, Welding 2. ....	82
Figure 85. Overview of the Welding Tools. ....	83
Figure 86. Welding Tools: Base. ....	84
Figure 87. Welding Tools: Rear Frame Tool. ....	85
Figure 88. Welding Tools: Rear Frame Toll, details. ....	85
Figure 89. COP Chassis before and after the Trim. ....	87
Figure 90. Assembly of the Rear Frame on the Welding Tools. ....	88
Figure 91. Welding of the Cell Interface. ....	89
Figure 92. Left: Rear Frame with some Electric System Components; Right: Rear Frame with Powertrain and part of the Rear End. ....	89
Figure 93. Rear Frame Components Weight. ....	90
Figure 94. Vehicle Parts Weight. ....	90
Figure 95. Loadcase: Acceleration 1.5g. ....	93
Figure 96. Loadcase: Braking 1.5g. ....	94
Figure 97. Loadcase: Cornering 1.5g. ....	95
Figure 98. Loadcase: Bump 4g. ....	96
Figure 99. Loadcase: Lateral Impact. ....	97
Figure 100. Loadcase: Longitudinal Impact. ....	97
Figure 101. FEM Model with Suspensions interface. ....	100
Figure 102. Left: Detail of Suspension rigids spider; Right: Detail of SPC rigids spider. ....	101
Figure 103. Left: Longitudinal Impact Model; Right: Detail of Rear End rigids spider. ....	101
Figure 104. Acceleration 1.2g Displacements. ....	103
Figure 105. Acceleration 1.2g Stresses. ....	103
Figure 106. Braking 1.5g Displacements. ....	104
Figure 107: Braking 1.5g Stresses. ....	104
Figure 108: Cornering 1.5g Displacements. ....	105
Figure 109: Cornering 1.5g Stresses. ....	105
Figure 110: Bump 4g Displacements. ....	106
Figure 111: Bump 4g Stresses. ....	106
Figure 112: Lateral Impact Displacements. ....	107
Figure 113: Lateral Impact Stresses. ....	107
Figure 114: Longitudinal Impact Displacements. ....	108

---

Figure 115: Longitudinal Impact Stresses. ....	108
Figure 116. Left Motor Mount FEM Analysis Model.....	111
Figure 117. Left Motor Mount FEM Analysis Results. ....	112
Figure 118. Right Motor Mount FEM Analysis Model. ....	112
Figure 119. Right Motor Mount FEM Analysis Results. ....	113
Figure 120. Rear Motor Mount FEM Analysis Model. ....	113
Figure 121. Rear Motor Mount FEM Analysis Results. ....	114
Figure 122. Torsional Bar Model.....	116
Figure 123. 3-Springs Torsional Model. ....	117
Figure 124. Benchmark Models: Left: Audi R8; Right: Bugatti Veyron. ....	117
Figure 125. Torsional Test FEM Model. ....	118
Figure 126. Torsional Test. Left: Test on the Testbench; Right: Scheme of the correct SPCs. ....	119
Figure 127. Rear Frame Torsional Stiffness Results and Mean Value. ....	120
Figure 128. Pilbeam Model and Formula.....	122

## List of Symbols and Abbreviations

a: CoG Front Distance .....	92
AC: Alternating Current.....	43
Al: Aluminum.....	passim
Al <sub>2</sub> O <sub>3</sub> : Aluminum Oxide .....	28
b: CoG Rear Distance.....	92
BEV: Battery Electric Vehicle.....	39
BMS: Battery Management System.....	39
C: Carbon.....	49
C <sub>c</sub> : Central Cell Compliance.....	117
C <sub>eq</sub> : Equivalent Carbon Content .....	75
C <sub>f</sub> : Front Frame Compliance.....	117
C <sub>r</sub> : Rear Frame Compliance.....	117
C <sub>tot</sub> : Chassis overall Compliance .....	117
CAE: Computer Aided Engineering .....	36
COP: Carry Over Parts .....	49
Cr: Chromium .....	49
C <sub>tot</sub> : Overall Chassis Compliance. ....	117
Cu: Copper.....	passim
d: Antiroll Bar Diameter .....	122
DC: Direct Current.....	40
DMU: Digital Mockup Analysis.....	36
DoF: Degrees of Freedom .....	102
d <sub>w</sub> : Wheel Diameter .....	92
E: Young Modulus .....	27
E: Young Modulus [MPa].....	passim
EPB: Electric Park Brake .....	30
f: Maximum Displacement. [mm] .....	passim
Fe: Iron .....	49
FEM: Finite Element Method .....	92
fvsa: Front View Swing Arm .....	24
HB: Brinell's Hardness .....	27
HB: Brinell's Hardness [HB] .....	31; 64; 69; 84
h <sub>G</sub> : CoG Height.....	92
HLS: HYdraulic Lift System, by KW .....	33
IC: Instant Center of Rotation .....	23
I <sub>p</sub> : Polar Inertia. ....	116
ITR: Inner Tie Rod.....	23

K: Leverage Ratio (Pilbeam Model).....	122
K <sub>ARB</sub> : Antiroll Bar Stiffness. ....	122
K <sub>C</sub> : Central Cell Torsional Stiffness. ....	117
K <sub>f</sub> : Front Frame Torsional Stiffness. ....	117
K <sub>r</sub> : Rear Frame Torsional Stiffness. ....	117
L: Antiroll Bar semi-length. ....	122
l: Torsional Bar Length. ....	116
LBJ: Lower Ball Joint .....	23
LCA: Lower Control Arm.....	29
LCAf: Lower Control Arm Front.....	23
LCAr: Lower Control Arm Rear .....	23
LH: Left Handed Side .....	94
Mg: Magnesium .....	passim
MIG: Metal-Arc Inert Gas.....	87
Mn: Manganese .....	49
Mo: Molybdenum .....	49
M <sub>t</sub> : Torsional Momentum. ....	116
OCV: Open Circuit Voltage .....	39
OTR: Outer Tie Rod .....	23
P: Phosphorus .....	49
PC: Pitch Center of Rotation .....	23
PWM: Pulse Width Modulation. ....	43
Q: Antiroll Bar Stiffness.....	122
qty: quantity.....	61
R: Antiroll Bar effective arm.....	122
RC: Rolling Center.....	23
RCH: Rolling Center Height .....	23
RH: Right Handed Side .....	94
S: Sulphur .....	49
Si: Silicon .....	49
SoC: State of Charge.....	40
svsa: Side View Swing Arm.....	24
t: Track.....	92
T: vehicle Track (Pilbeam Model).....	122
Ti: Titanium .....	64; 69
TIG: Tungsten Inert Gas.....	73
UBJ: Upper Ball Joint .....	23
UCA: Upper Control Arm.....	28
UCAf: Upper Control Arm Front.....	23
UCAr: Upper Control Arm Rear .....	23
UTS: Ultimate Tensile Strength .....	27



---

UTS: Ultimate Tensile Strength [MPa] .....	passim
$V_a$ : DC/DC load Voltage, or output voltage.....	42
$W$ : Vehicle Weight.....	92
$w_b$ : Wheelbase .....	92
$W_f$ : Front Axle Weight Distribution .....	92
$W_r$ : Rear Axle Weight Distribution .....	92
Zn: Zinc .....	passim
$\delta$ : Switch Duty Cicle.....	42
$\theta$ : Angular Displacement.....	116
$\mu_{x,max}$ : Max Tyre Friction Coeff. X .....	92
$\mu_{y,max}$ : Max Tyre Friction Coeff. Y .....	92
$\nu$ : Poisson's Ratio.....	101
$\rho$ : Density .....	27
$\rho$ : Density [kg/dm <sup>3</sup> ] .....	passim
$\sigma_{MAX}$ : Maximum Stress [MPa].....	passim



# 1. CHAPTER 1 – INTRODUCTION

## 1.1 L.M. Gianetti Internship



Figure 1. L. M. Gianetti site in northern Turin.

Starting from the end of September 2019 I had the opportunity to work as an intern in the *L. M. Gianetti* company, where I was able to develop the project for my Master's degree thesis. *L.M. Gianetti* is a mechanical workshop company operating in the field of the automotive industry founded in 1966 and based in northern Turin. The main focus of the company is towards the field on Motorsport, with a personnel of around 40 people between engineers, operators and managers, counting 30 work centers it is capable to provide from the production of prototype components for motorsport up to the design and manufacturing of complex vehicles. In the past it partnered with *Abarth* company to create models of success such as the *Lancia 037*, the *Lancia S4*, *Delta group A* and its evolutions, manufacturing components for suspension groups, engine, gearbox, rollcage and monocoque. Later it was involved in the project of the winning *Alfa Romeo 155* and *156*, manufacturing monocoques, suspension groups and gearboxes. In the last years it began collaborating also with foreign manufacturers challenging in categories like *Formula 1* and World Rally Championship *WRC*. The company was able to obtain the UNI EN ISO 9001 certification of quality and can boast the Fia/Csai Manufacturer License type B/A. Moreover, today it also serves the most important firms of Automotive Design, thanks to these collaborations I was able to get involved with a project of *GFG Style* by *Giorgetto* and *Fabrizio Giugiaro*, the *GFG Style Vision 2030* prototype.





Figure 2. L.M. Gianetti, plant and Show Room.

## 1.2 GFG Style Vision 2030

The GFG Style Vision 2030 is a prototype one-off car designed by *GFG Style* company by Giorgetto and Fabrizio Giugiaro originally intended to be presented at the 2020 *Geneva International Motor Show*. It was then revealed during the Spring at GFG Style site in Moncalieri (TO) and in July 2020 took part to the *Poltu Quatu Classic 2020*, a *Concours d'elegance* for classic cars held in the Sardinian locality of Arzachena (SS). The prototype bodywork on the other hand was presented during Riyadh Car Show in Saudi Arabia State capital during autumn 2019.



Figure 3. GFG Style Vision 2030 rolling chassis at the Riyadh Car Show 2019.

The prototype is a 2-seated 4-wheel drive coupé, powered with one electric motor per axle for an aggregate Power of 320 kW (435 CV) and Torque of 680 Nm, in boost conditions. The capacity of the battery pack is 80 kWh and it allows a range of more than 380 km considering the NEDC test



cycle. The chassis, as discussed forward, is formed by a central cell in aluminum alloy, a front frame in steel 25CD4 alloy and a rear frame in steel 25CD4 alloy. Notably, the bodywork is entirely made of Carbon fiber with some parts (wheel arches) made of Kevlar. The vehicle maximum speed is set to be slightly above 200 km/h and the performance over the 0-100 km/h sprint is 4.4 sec. The total mass of the vehicle is 2200 kg with a weight distribution between axles of 48% Front - 52% Rear.

The prototype is based on the existing central cell in aluminum alloy, so it was needed to design the all new Front and Rear frames. Overall, the car needed 6 months to be designed, manufactured, assembled and tested, starting in September 2019 and finishing in the end of February 2020. For what concerns the Rear Frame subject of this thesis the design began in middle October 2019 once the suspension points were close to be defined except for minor adjustments, the CAD software involved was *CATIA V5* by *Dassault Systems*. The design of all components was ended by middle November with the model undergoing FEM Analysis by means of software *Hypermesh (Optistruct)* by *Altair*.



Figure 4. The finished GFG Style Vision 2030.

The manufacturing process was long and to start it had to wait the end of the production of the Front Frame components, therefore while the Front Frame was already assembled on the Central Chassis the last few components of the Rear Frame were still under milling process. Finally, the Rear Frame was assembled on the Chassis in middle January 2020.

The main topics touched by my Thesis will deal about the constraints of the design, starting from the new chosen suspension's points to the size occupied by all components sited in the back of the car, to the limit formed by the bodywork; the actual structure of the chassis, its integration with the

other components of the Rear end and the solution of the main layout issues; the production process with particular focus on the Welding Process; the Load cases considered in order to verify the structure and the FEM analysis based on them; finally, the evaluation and validation of the Torsional Stiffness.

### 1.3 Vehicle Data

Basic Parameters	
Length	4619.1 mm
Height	1279.7 mm
Wheelbase	2830 mm
Tyres	275/50 R20
Track	1751 mm
Curb Weight	2200 kg

Table 1. Basic Parameters.

Frame & Body	
Frame	
Central Cell	All-Aluminum alloy
Front Frame	Steel 25CD4
Rear Frame	25CD4
Body	
Front and Rear bumpers	Carbon fiber
Sides and Doors	Carbon fiber
Roof and Door Wings	Carbon fiber
Wheel arches	Kevlar
Rear Wing	Carbon fiber
Trunk	Carbon fiber
Splitter and Diffuser	Carbon fiber

Table 2. Frame & Body.

<b>Brakes &amp; Suspensions</b>	
<i>Brakes</i>	
Front Disc	Ø 405 x 34 mm
Rear Disc	Ø 380 x 28 mm
Calipers	Brembo M6 Front + Brembo M4 Rear
<i>Suspensions</i>	
Front + Rear Suspension	Double Wishbone
Upper Control Arm	ALU 7075 T6
Lower Control Arm	Steel 15CDV6
Knuckles	ALU 2024 T6
Damper + Coil + Helper	Custom form KW Suspension

Table 3. Brakes &amp; Suspensions.

<b>Batteries &amp; Powertrain</b>	
<i>Batteries</i>	
Type	NCM Lithium Ion – Liquid Cooled
Capacity	80 kWh
<i>Powertrain</i>	
Motors	Permanent Magnetic Synchronous
Maximum Power	320 kW (160 F + 160 R)
Maximum Torque	680 Nm (340 F + 340 R)
Transmission	Single Stage Reduction
Maximum Speed	200 km/h
0-100	4.4 sec
Range on NEDC cycle	+380 km

Table 4. Batteries &amp; Powertrain.





## 2. CHAPTER 2 – FUNCTIONAL REQUIREMENTS

### 2.1 Suspension Hardpoints

Usually the suspension points, known as Hardpoints, are defined and analyzed with the aim for best handling and vehicle performance. In the considered case, in which it is requested the design of the front and the rear frames, the position of stated points and the derived shape of the suspension's components affect heavily the following steps of the design process: in fact the Rear Frame will be designed around the Hardpoints and then modified to be compliant with others functional requirements.

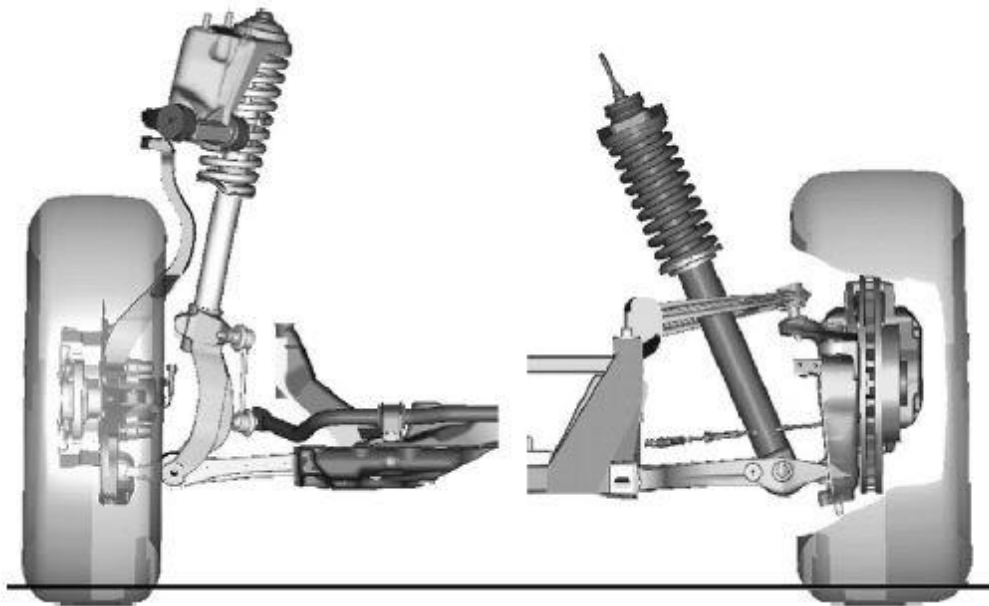


Figure 5. Double Wishbone Suspension scheme (Left: Long Strut, Right: Short Strut).

Given the required performance of the prototype the chosen structure for the suspensions is a Double Wishbone Suspension for both axles. This kind of structure is formed by two triangles, upper and lower, acting between the chassis and a common Knuckle (Short Strut), which is also the support for the Hub and the Braking System. Considering the Rear Axle along with the two triangles there is also a third arm which acts as a Tie Rod for the aim of controlling the Toe angle of the rear wheels. The Damper and the Spring are working on the same axis and mounted directly from the Lower Arm to the Chassis (via Rear Frame), since there are no issues with the components size alternative solutions like Push-Rod or Pull-Rod have been discarded, the result is a simpler suspension. Finally, the Anti-Roll Bar is linked to the Damper-Spring group by means of a Connecting Rod and passes through the Rear Frame in transversal direction.

Focusing on the Rear Suspension from now on, the number of fundamental points can be computed as follows: 3 for the Upper Control Arm, 3 for the Lower Control Arm, 2 for the Spring-Damper group, 2 for the Tie Rod and 2 for the wheel. The points needed to describe the Knuckle are already within the other components since they correspond to the joints between the parts, along with the Hard

points it is useful to define also the ground plane, in particular the point of contact between ground and the wheel.

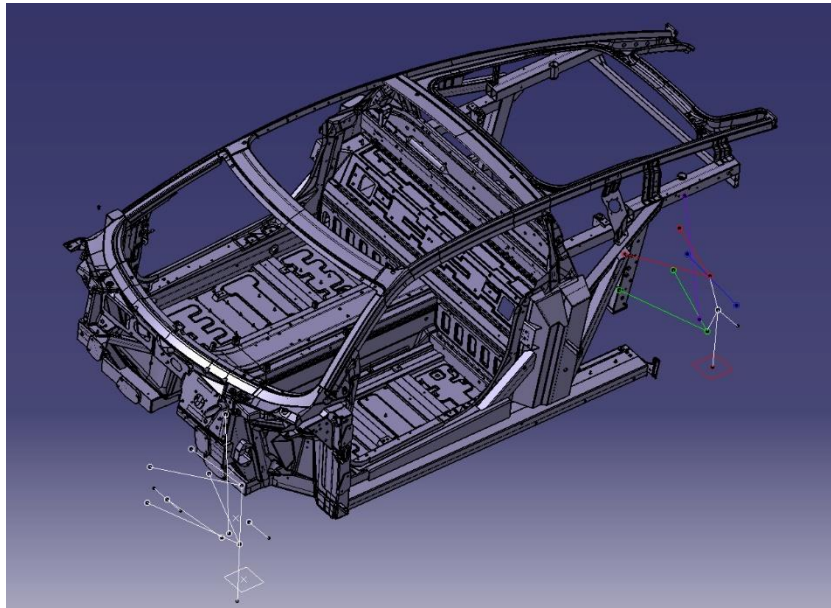


Figure 6. Front and Rear suspension points vs Central Chassis.

In total 6 points for each side will be involved later in the design of the frame: 4 inboard points of the 2 Control Arms, the inner point of the Tie Rod and the Top point of the damper-spring group (in Figure7: Point 1, 2, 4, 5, 8 and 10).

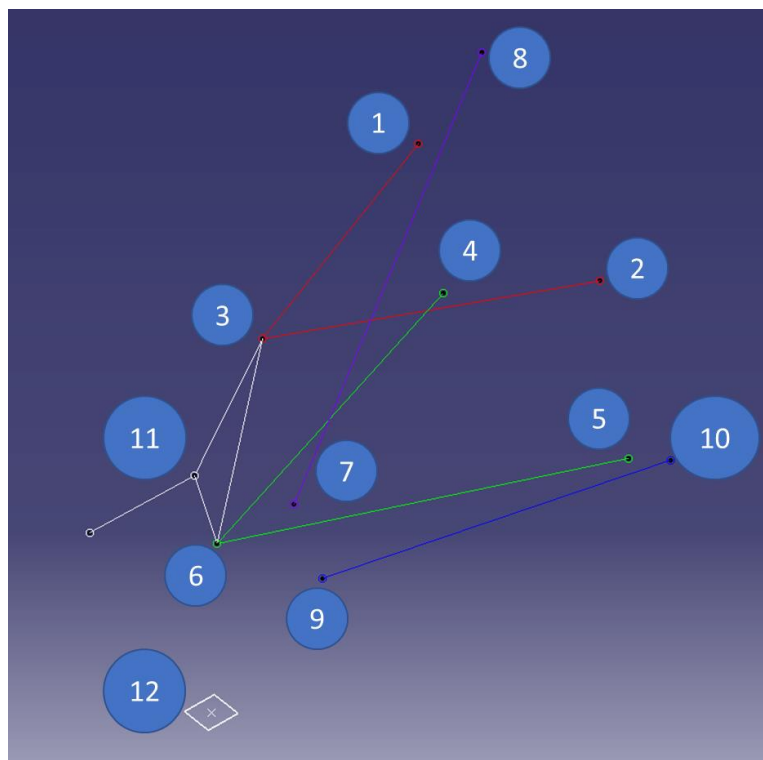


Figure 7. Rear Suspension Points, Left Side.

N°	Name	Symbol	X [mm]	Y [mm]	Z [mm]
1	Upper Wishbone Front Pivot	UCAf	2520,00	-400,00	95,00
2	Upper Wishbone Rear Pivot	UCAr	2847,00	-400,00	105,00
3	Upper Wishbone Outer Ball Joint	UBJ	2720,00	-790,00	140,00
4	Lower Wishbone Front Pivot	LCAf	2520,00	-380,00	-140,00
5	Lower Wishbone Rear Pivot	LCAr	2850,00	-380,00	-170,00
6	Lower Wishbone Outer Ball Joint	LBJ	2690,00	-840,00	-150,00
7	Damper Wishbone End		2702,82	-760,00	-122,00
8	Damper Body End		2760,66	-530,00	415,00
9	Outer Track Rod Ball Joint	OTR	2870,00	-829,17	-80,00
10	Inner Track Rod Ball Joint	ITR	2930,00	-380,00	-110,00
11	Wheel Center		2711,50	-880,08	-0,24
12	Ground Point		2711,50	-880,08	-354,24

Table 5. Rear Suspension Hard Points.

Furthermore, defining the Hardpoints it is possible to get the position of the suspension's Instant Center of Rotation (IC), so the vehicle's Rotation Center Height (RCH) and Pitch Center (PC). Considering a simplified scheme, the Rolling Center of Rotation (RC) can be depicted like in *Figure 8*, where the axes of the Control Arms are projected, defining the center of rotation of the Knuckle at their intersection (IC). The further intersection of the connection between those Centers and the ground points of the wheels gives the Rolling Center.

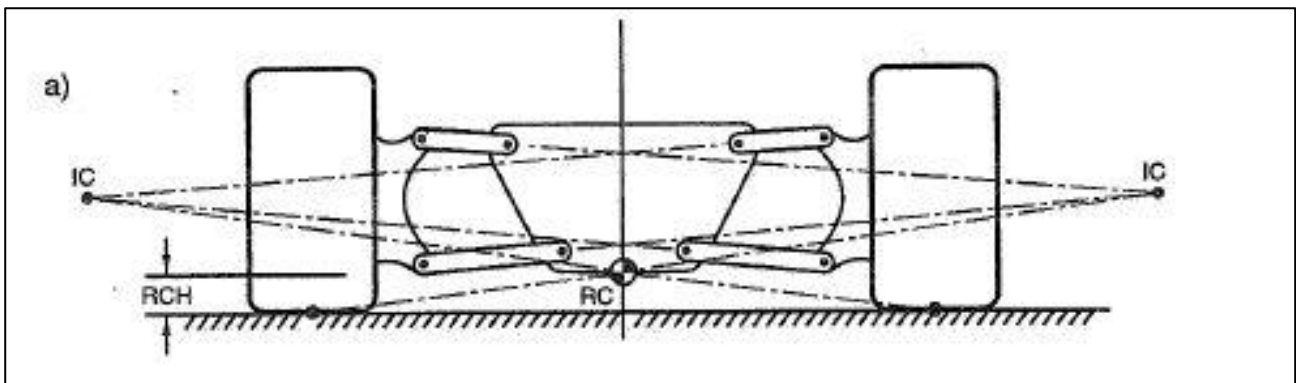


Figure 8. Double Wishbone, Instant Center of Rotation for Roll motion.

The real scheme of the suspension in a 3-dimensional space is different and must consider the slope of the Control Arms in both Longitudinal and Lateral directions: therefore it is defined an Instant Axis of Rotation instead of an Instant Center. As a first step are considered the planes generated by the Upper and Lower Control Arms: the intersection between the 2 planes is the Instant Axis of Rotation of the suspension (*Figure 9*). Considering Front and Side view it is possible to define the

relative Swing Arms (fvsa, svsa) and then the Roll and Pitch centers, following the construction depicted in the scheme.

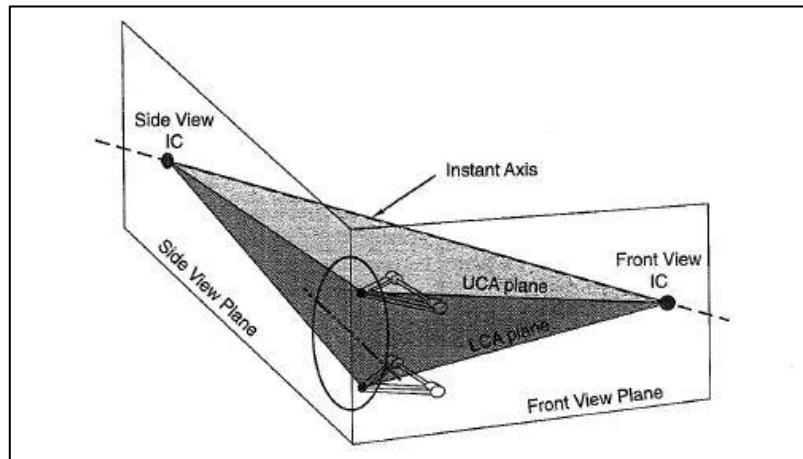


Figure 9. Double Wishbone Instant Axis of Rotation.

To define the Rolling Center it is necessary to consider the line connecting the ground point of the wheel and the IC of the suspension, then accounting the symmetry of the vehicle its intersection with the vertical symmetry axis of the vehicle defines the Rolling Center (*Figure11*).

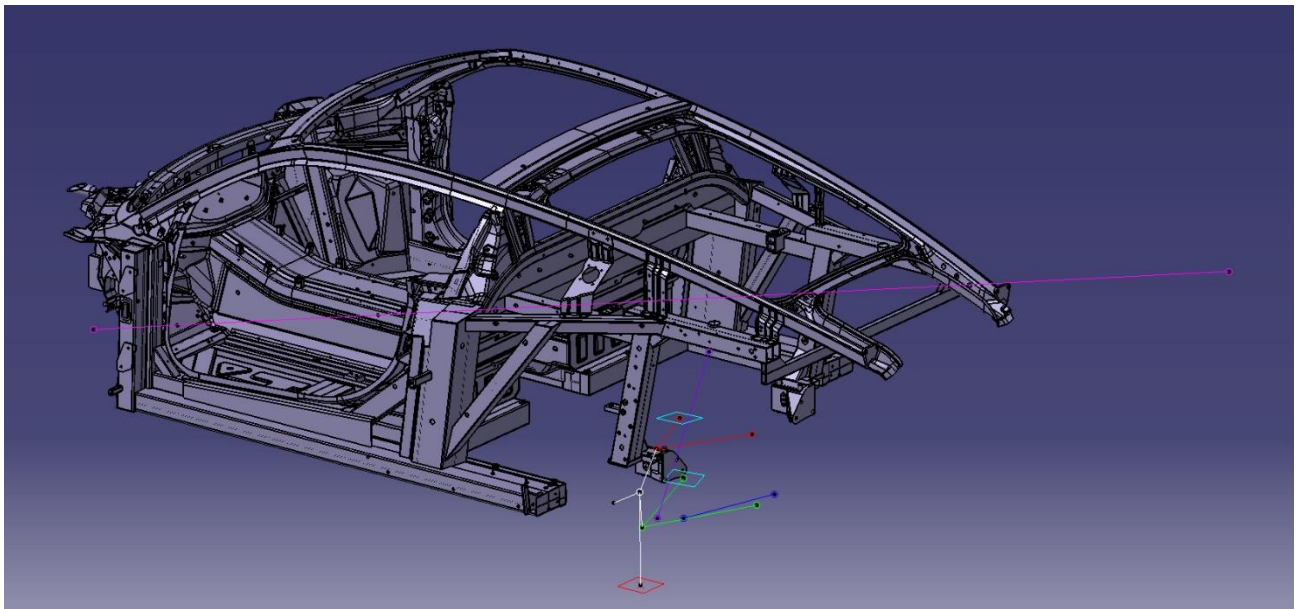


Figure 10. Rear Suspension Instant Axis of Rotation (pink) and Control Arms planes (light blue).

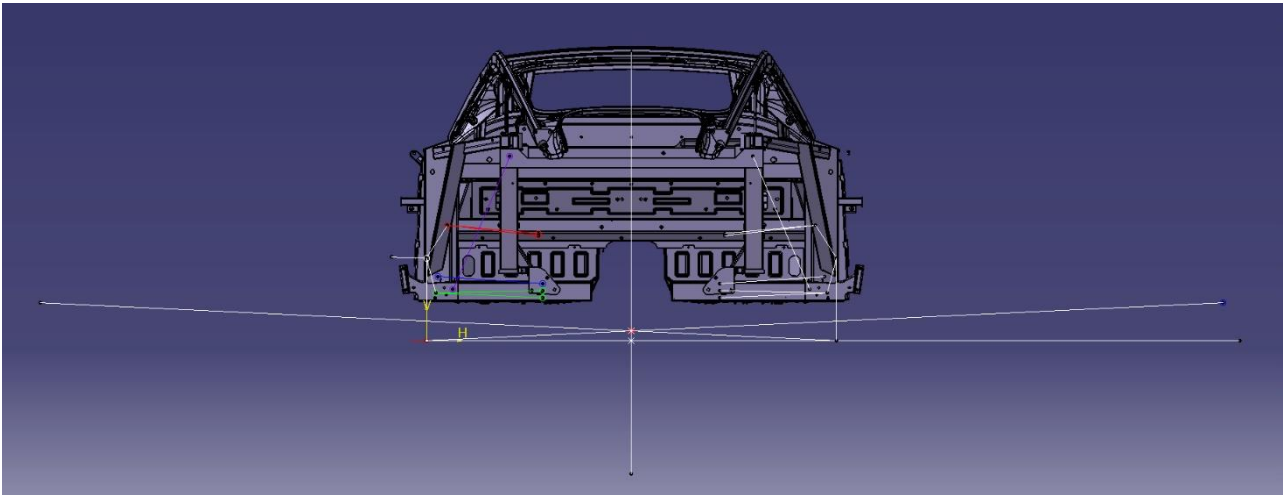


Figure 11. Rear Suspension Rolling Center (RC)

As a side note, in *Figure11* is shown that the IC of the Suspensions are much wider and away from the chassis: this means that the fvsa are long and as a result the change in Camber due to a certain Roll Angle will be much smaller with respect to a solution with shorter fvsa.

Furthermore, it is possible to define the Pitch Center of Rotation (PC) starting from the considerations made about *Figure9* and *Figure10* but considering the Side View plane: in this way the IC for Rear suspension is already defined. The process is repeated also for the Front suspension and again drawing the lines from the ground points of the wheels to its relative IC the Pitch Center is defined as the intersection between the lines (*Figure12*).

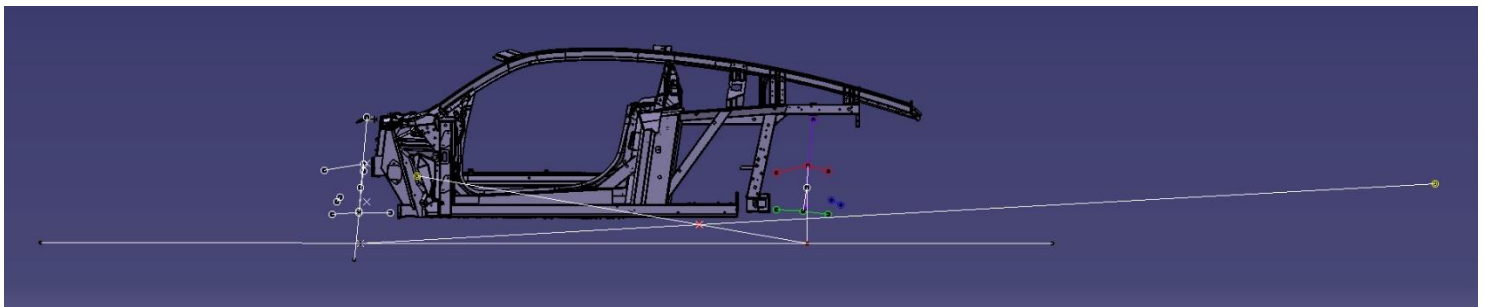


Figure 12. Pitch Center of Rotation.

As a remind, the presented Hardpoint are to be considered as a result of a series of revisions and not as a given input, in order to confirm the set of points it was also necessary, for example, to analyze the kinematic behavior of the suspensions geometry.

Point	Symbol	X [mm]	Y [mm]	Z [mm]
Rear Rolling Center	RC	2711.5	0	-312.5
Pitch Center	PC	2029	0	-236

Table 6. Rotation Points Coordinates.

## 2.2 Suspension Components

The Hardpoints define the suspensions geometry, it is implied that they work as a reference only for static conditions, at resting position. To further evaluate the portion of space occupied by the Suspensions it is required to consider the overall stroke of the Damper, in Bounce and Rebound directions, along with the shapes and dimensions of the Suspensions Components.

As requested by the Customer it is possible to set the Prototype on 3 different Heights from the ground, the lower setup "RACE" is suited for maximum performance and in-track racing; the standard setup "ROAD" is the neutral position between the other two and is suited to travel on common roads; the higher setup "OFF-ROAD" is aimed to allow the vehicle of driving on all type of roads, may them be made of dirt, sand or ice.

All 3 Setups are obtained through regulation done by a hydraulic system acting on Spring-Damper group: "RACE" setup is got shortening the overall length of the group by action of an actuator mounted between the group and the LCA, without modify the length of Spring and Damper, while "OFF-ROAD" setup is set with the HLS system in-built into the Damper-Spring group (later described) which increases the length of the group.

In conclusion, the 3 Setups (*Table7*) are the possible resting points for the vehicle, and they are covering only a part of the total stroke available for the Damper and Spring Group, as reported in *Table8*.

SETUP	Front Stroke – D-S Group [mm]	Rear Stroke – D-S Group [mm]	Front Stroke - Wheel [mm]	Rear Stroke - Wheel [mm]	Front Max Stroke [mm]	Rear Max Stroke [mm]
OFF-ROAD	45	45	56,25	50	85	90
ROAD	0	0	0	0		
RACE	-30	-30	-37,5	-33,33	-62	-66

*Table 7. Setup Parameters.*

Stroke Data		
Bump Travel	80	mm
Rebound Travel	135	mm
Steering Travel	70	mm

*Table 8. Suspensions Stroke Data.*

After having set the Hardpoints and defined the Stroke of the Suspensions the final observation to do about Suspensions is regarding the actual size of the components and how they will be jointed with the Rear Frame in design. Like mentioned the components of the Rear suspension are the Upper and Lower Control arm, the Tie Rod, the Knuckle, the Damper and Spring Group and the Anti-Roll Bar Group.

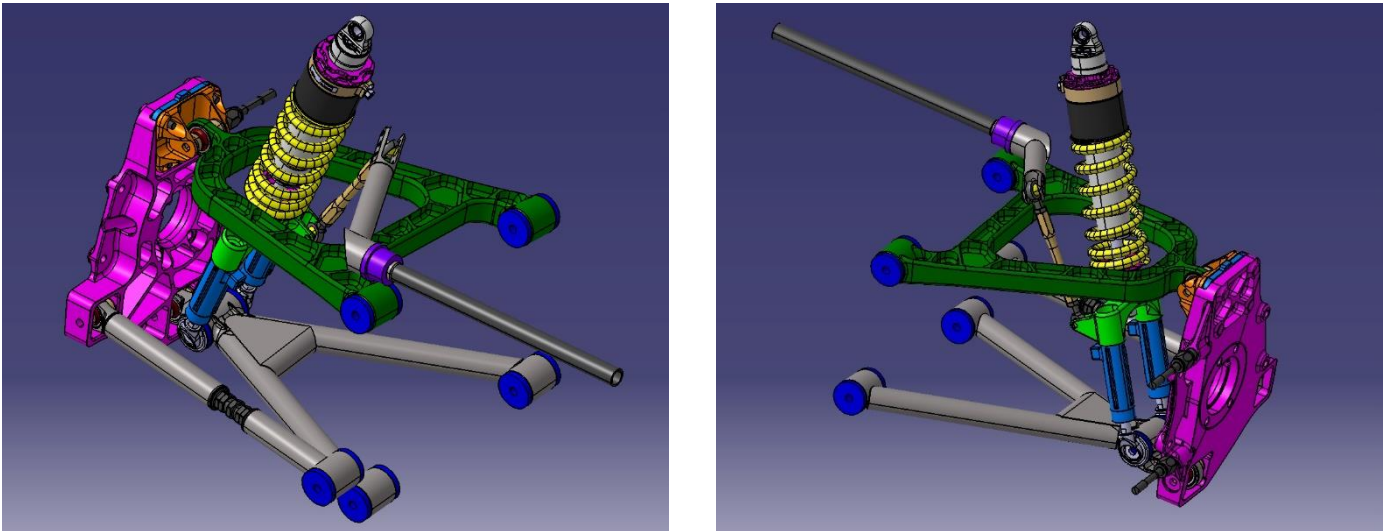


Figure 13. Rear Suspensions Components.

### 2.2.1 Upper Control Arm

Between the 3 arms of the suspension the one with lower dynamic loads is the Upper control arm, this is the main reason for the choice of material i.e. the Aluminum alloy ALU 7075 T6. This alloy made primely of Aluminum and Zinc, with noticeable content of Magnesium and Copper, is vastly used in Aeronautics and Motorsport applications for the good compromise between weight and mechanical properties. In fact considering for the Aluminum a rough value of density of  $2.7 \text{ kg/dm}^3$  the value of Yielding Stress  $R_{p0,2}$  can reach almost 500 MPa. The ALU 7075 T6 can be produced in slabs, plates or bars, hence the Upper Control Arm has been designed to be produced by Milling.

ALU 7075 T6		
Density	$\rho$	$2.81 \text{ kg/dm}^3$
Young Modulus	E	72 GPa
Ultimate Tensile Strength	UTS	530 MPa
Yielding Stress	$R_{p0,2}$	460 MPa
Elongation	--	5%
Hardness	HB	158 HB

Table 9. ALU 7075 T6 Mechanical Properties.

Name	Mg	Cu	Zn	Impurity	Al
ALU 7075 T6	2.10-2.90%	1.20-2.00%	5.10-6.10%	0.05-0.15%	Remaining

Table 10. ALU 7075 T6 Chemical Composition.



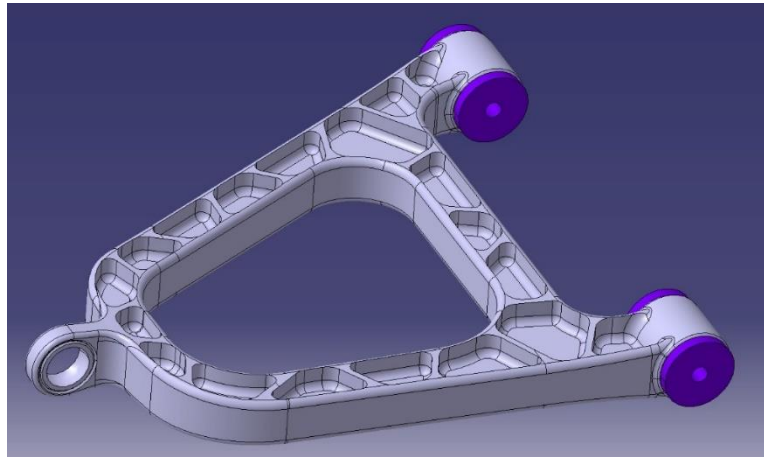


Figure 14. Upper Control Arm.

After the Milling process the Arm is finished with a surface treatment named OX-A which has two function: a layer made of Aluminum Oxide  $Al_2O_3$  is a protection against corrosion and at will it can be colored, so it can replace the painting.

The UCA is linked to the Knuckle by means of the UBJ, chosen to be a ABYT12-V by *NMB*, with the fixed part mounted on the UCA and moving part on Knuckle, kept still by means of dedicated bushings and a screw acting like a pin.

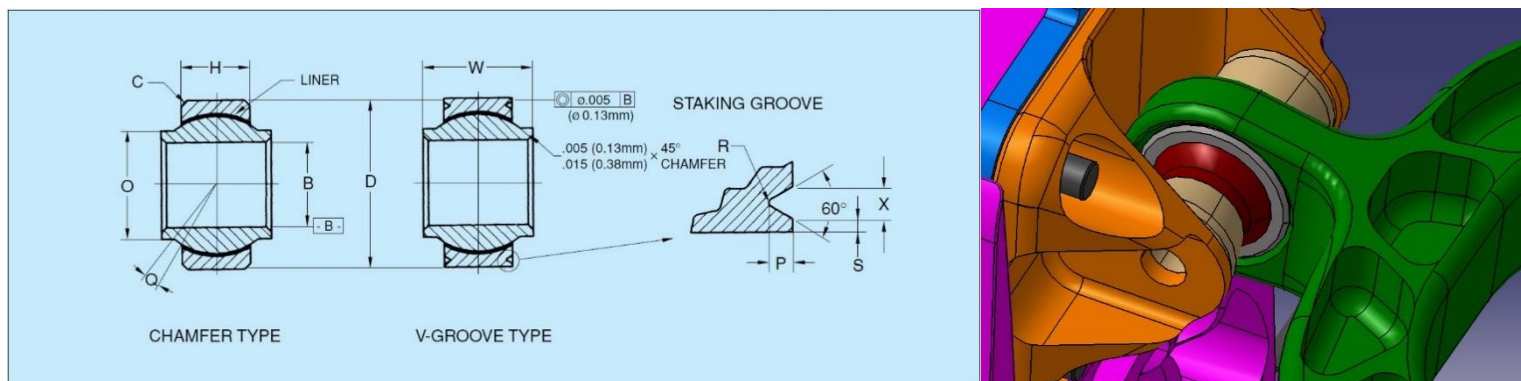


Figure 15. Left: NMB ABYT12-V ball joint. Right: UBJ Detail.

On the other side the UCA is mounted on the Rear frame with a Pivot joint made with PP99-112P bushings by *Powerflex*, which consist in two bushings in polyurethane with a central sleeve originally in stainless steel replaced with an aluminum one. A screw acts as the pivot axis passing through the sleeve and the Rear frame interface fastening the frame, the bushings and the UCA together (forward illustrated in chapter dedicated to the frame).

Altogether the UCS occupies a volume of 450x380x50 mm that rotates about the pivot axis of the joint on the side of the Chassis, following the stroke of the suspension.



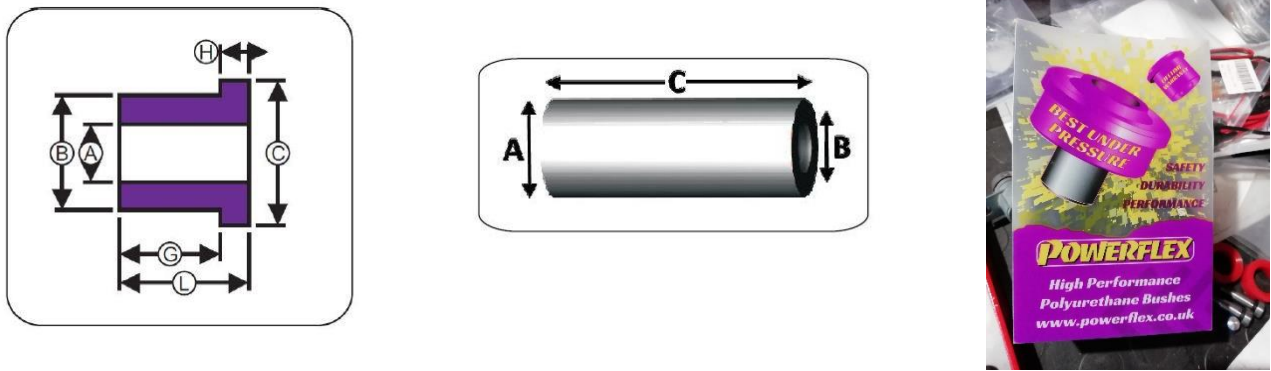


Figure 16. Powerflex universal bushings PP99-112P.

### 2.2.2 Lower Control Arm

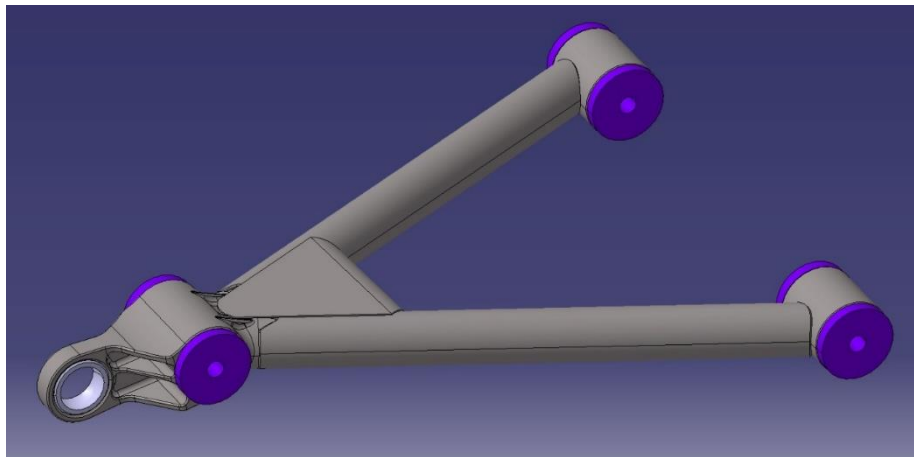


Figure 17. Lower Control Arm.

The Lower Control Arm must face a higher dynamic load with respect to the UCA, therefore the material chosen is Steel, in particular Steel Alloy 25CD4, which will be described in detail while dealing with the Rear Frame itself. The 25CD4 came in both tubes and billets so the LCA is obtained welding several components together. A joint shaped with milling to hold the LBJ and the lower end of the damper is welded with two tubes reinforced with a gusset. The ends toward the frame are made with two bushings worked on the lathe. The components are the same adopted for the UCA: the ball joint is an ABYT12-V and the pivot joint are two PP99-112P. Another pivot joint is used to connect the LCA with the damper, through a dedicated housing for the bushings molded in the machined joint. The whole component has a size of 500x400x50 mm and as the other control arm it is free to move around the pivot axis on the frame side.

### 2.2.3 Tie Rod

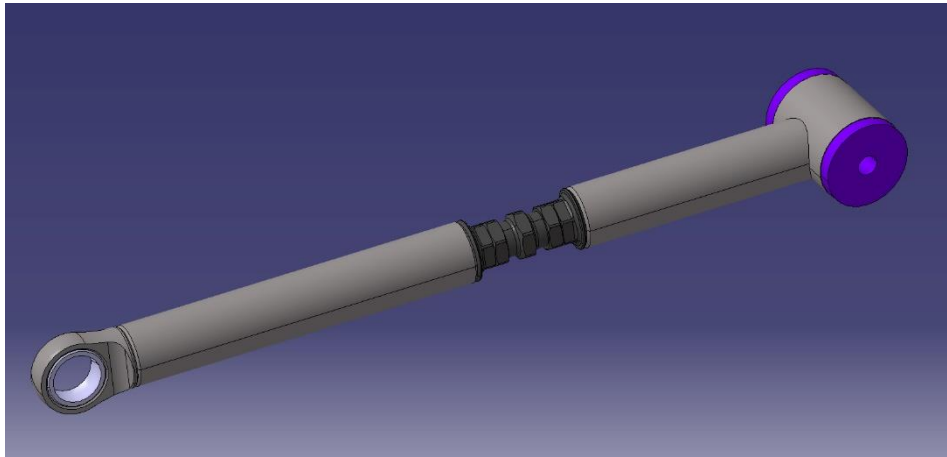


Figure 18. Tie Rod.

The Tie rod is basically a two pieces element made in Steel alloy 25CD4: the first one linked to the Knuckle via ball joint ABYT10-V is obtained welding a machined eye for the joint with a tube; the second one is a tube welded with a bushing housing a pivot joint PP99-112P. The Tie rod is essential for Toe angle regulation: it occurs acting on a special screw with two threaded end, one right-handed and one left-handed. Welded on the two tubes ends there are two nuts with specific thread, while another two nuts are used to lock the position once the setup is done. The Tie Rod is a smaller component with respect to the Control Arm, considering the dimensions of 70x70x500 mm.

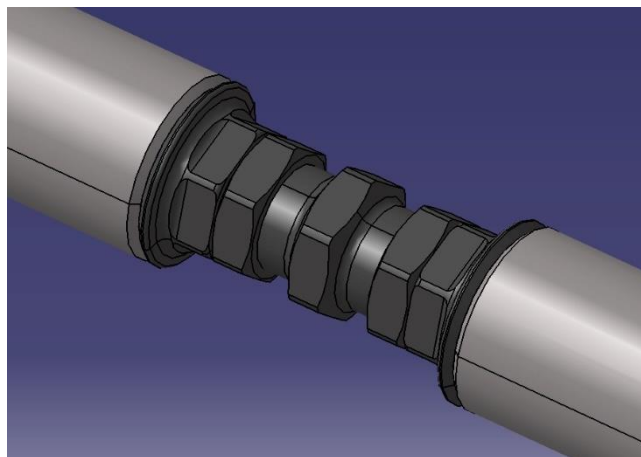


Figure 19. Toe angle regulation on Tie Rod, detail.

### 2.2.4 Knuckle

In a suspension system the Knuckle has several duties, starting from the obvious one: on the Knuckle is machined the housing for the Hub, hence the Knuckle works as a support for the wheel and transmits loads to the rest of the vehicle. Moreover on the Knuckle are fitted the still parts of the braking system: in this case the Braking Caliper and the Electric Park Brake (EPB); and finally specific design of the Knuckle makes possible the regulation of Toe angle and Camber angle. The former as already described is achieved by acting on Tie Rod linked to the Knuckle with a ball joint, the latter

is implemented separating the UBJ from the Knuckle and placing between them Shims of different thickness, made of Stainless steel or Aluminum depending on the thickness.

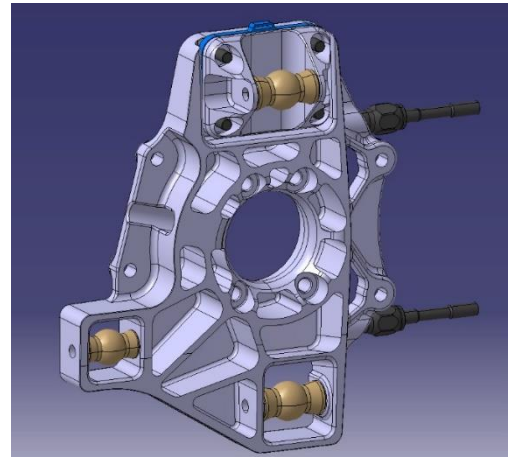
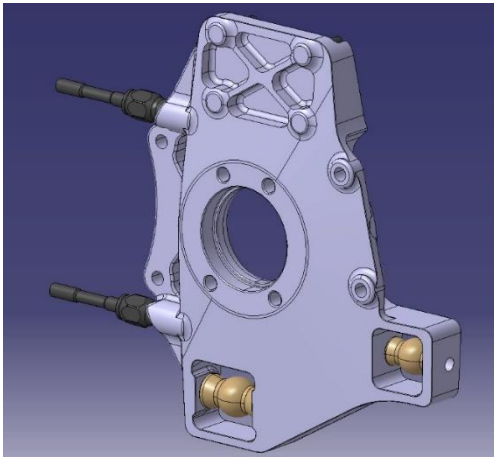


Figure 20. Front and Rear view of the Knuckle.

The main body occupies a volume of 375x310x45mm and it is made of Aluminum-Copper alloy ALU 2024 T6, used for Aeronautic applications, which major quality is to be lightweight, maintaining acceptable mechanical properties. The finish of the main body is a color neutral OX-A-N which adds a thick layer of aluminum oxide. Other elements are made of different Steel Alloys: the ball joint bushings and the UBJ carrier are in 30NCD12 while the Studs are in FDMS Steel (30NCD16), two High-Carbon alloys with Nickel, Chromium and Molybdenum, suited for high load applications.

ALU 2024 T6		
Density	$\rho$	2.78 kg/dm <sup>3</sup>
Young Modulus	E	75 GPa
Ultimate Tensile Strength	UTS	430 MPa
Yielding Stress	R <sub>p0,2</sub>	290 MPa
Elongation	--	11%
Hardness	HB	122 HB

Table 11. ALU 2024 T6 Properties.

Name	Mg	Cu	Zn	Impurity	Al
ALU 2024 T6	1.2-1.8%	3.8-4.9%	<0.25%	0.05-0.15%	Remaining

Table 12. ALU 2024 T6 Chemical Composition.

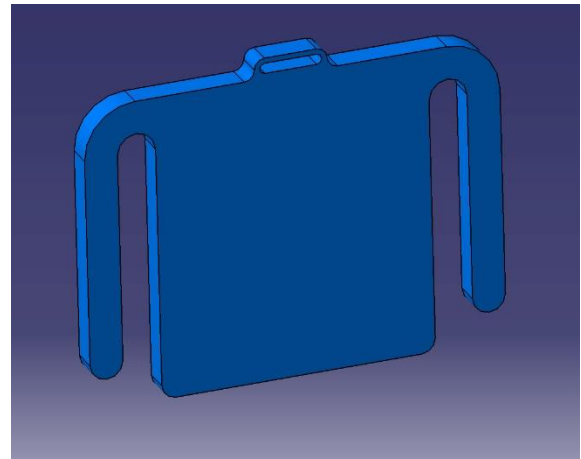
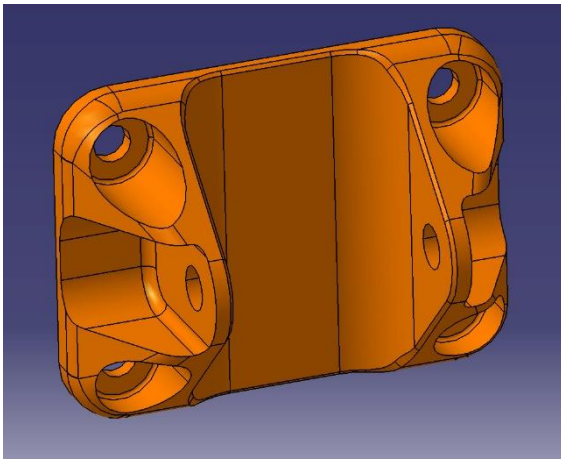


Figure 21. Left: UBJ Carrier; Right: UBJ Camber Shim.

### 2.2.5 Anti-Roll Bar

The Prototype is provided with Anti-Roll Bars on both axles, since it is an element mounted in transversal direction between the two sides of the vehicle clearly it will affect the Rear Frame design. The Bar itself is a tube 823 mm long in Steel alloy 25CD4  $\varnothing 25 \times 2.5$ , with special bushings welded at both ends. The bushing presents an octagonal cut for sake of regulation of the group and through the cut it is coupled with the Anti-Roll Bar Knife, 200 mm long, an element which acts like an arm transforming the vertical movement of the wheel into a Torque and transmits it to the Bar.

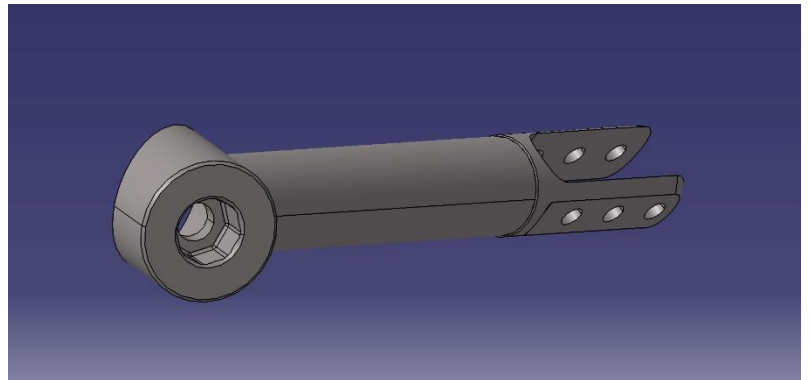
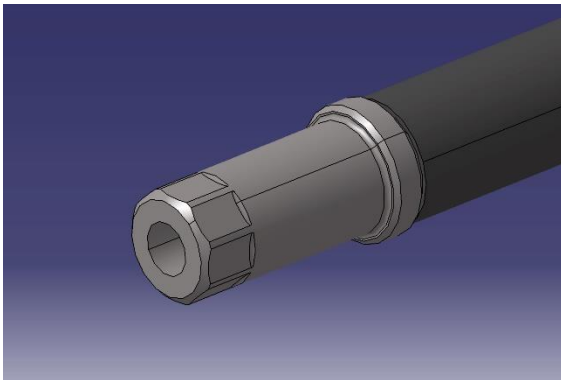


Figure 22. Left: Anti-Roll Bar Welded Bushing; Right: Anti-Roll Bar Knife.

On the Bar side the Knife there is a special bushing compliant with the one on the bar and over them it is placed a polyurethane sleeve like the one of the PP99-112P which will work as interface with the Rear Frame: the elastic material will prevent impact and reduce the noise of the Anti-Roll Bar.

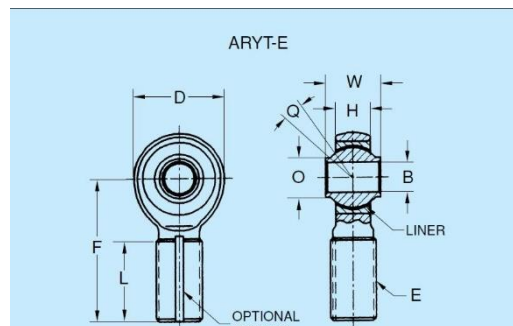
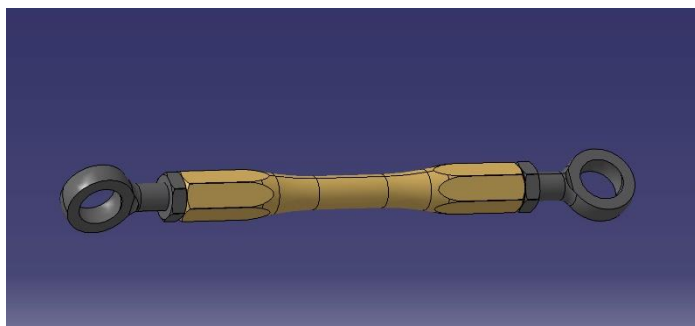


Figure 23. Left: Anti-Roll Bar's Connecting Rod; Right: NMB Ball Joint ARYT5-E.

On the other side the Knife has a Fork element with several holes on which it is connected the following element of the group: the Connecting Rod. Acting between the Knife and the Damper Group the Con Rod is an element made in ALU 7075 by both lathe and milling with a ball joint at each end locked by means of a nut. The ball joint is again by *NMB* and the model chosen is the ARYT5-E, which is a ball joint with included threaded pin.

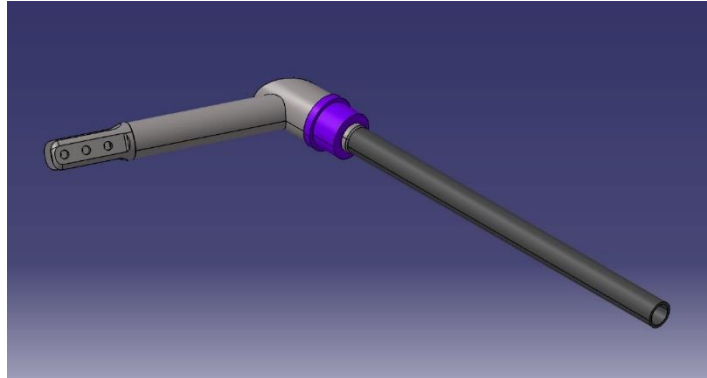


Figure 24. Anti-Roll Bar Group, Left Half.

### 2.2.6 Damper and Spring Group

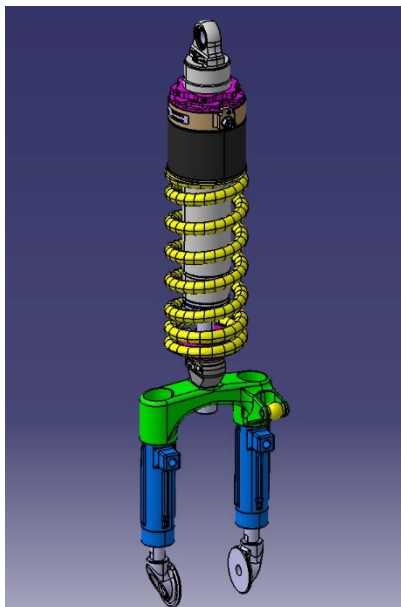


Figure 25. Damper and Spring Group.

The Damper and Spring Group is in fact quite complex featuring several elements, overall occupying the volume of cylinder with diameter 85 mm and length 420 mm, plus a fork of 175x150x40 mm. The Group changes its length but always staying on its axis that slightly moves around the Top Mount. The Damper present a ball joint in-built by *KW Suspensions* which works as main link to the Rear Frame. Below is placed the Hydraulic Lift System (HLS), a system developed by *KW* that allows to change the height of the car, modifying the length of both Damper and Spring. The Spring itself is made by two pieces: the first is the main Coil that is a usual spring for suspension, in series with it there is second spring way softer, the Helper, that does not increase overall stiffness but works in

order to prevent the main spring from swaying in condition of sudden rebound. The Group is then mounted on a special manufactured Fork with two hydraulic actuators that can lift the whole system in order to change the vehicle height. On the fork it is also filled the fastening element for the Anti-Roll Bar Connecting Rod. At the ends of the stems are screwed up two elements that couple with the LCA machined joint by means of a screw acting like a pin.

The hydraulic system of the suspension allows the car to ride on 3 different setups, like previously discussed: in "ROAD" setup the actuators on the fork are completely extended and the HLS is compressed; in "RACE" setup both actuators and HLS are at lower point; in "OFF-ROAD" setup actuators are fully extended and HLS are in stretched. Both systems are controlled via one-way hydraulics: the power of the pump is used to lift the car while to lower it the valves will open, then the weight of the car alone will empty the actuators and HLS chambers.

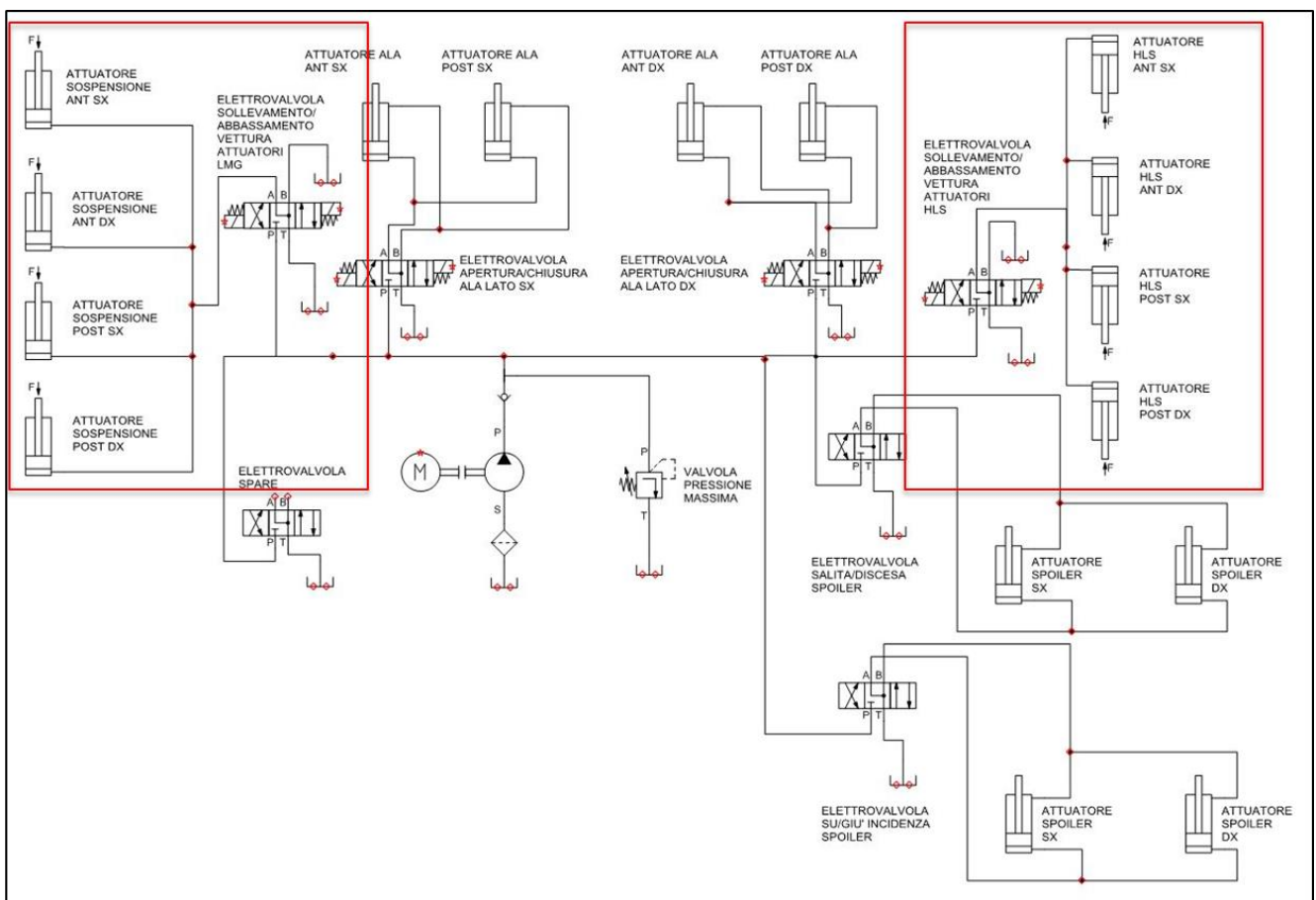


Figure 26. Hydraulics system of the Vehicle: in Red the Groups acting on Damper.



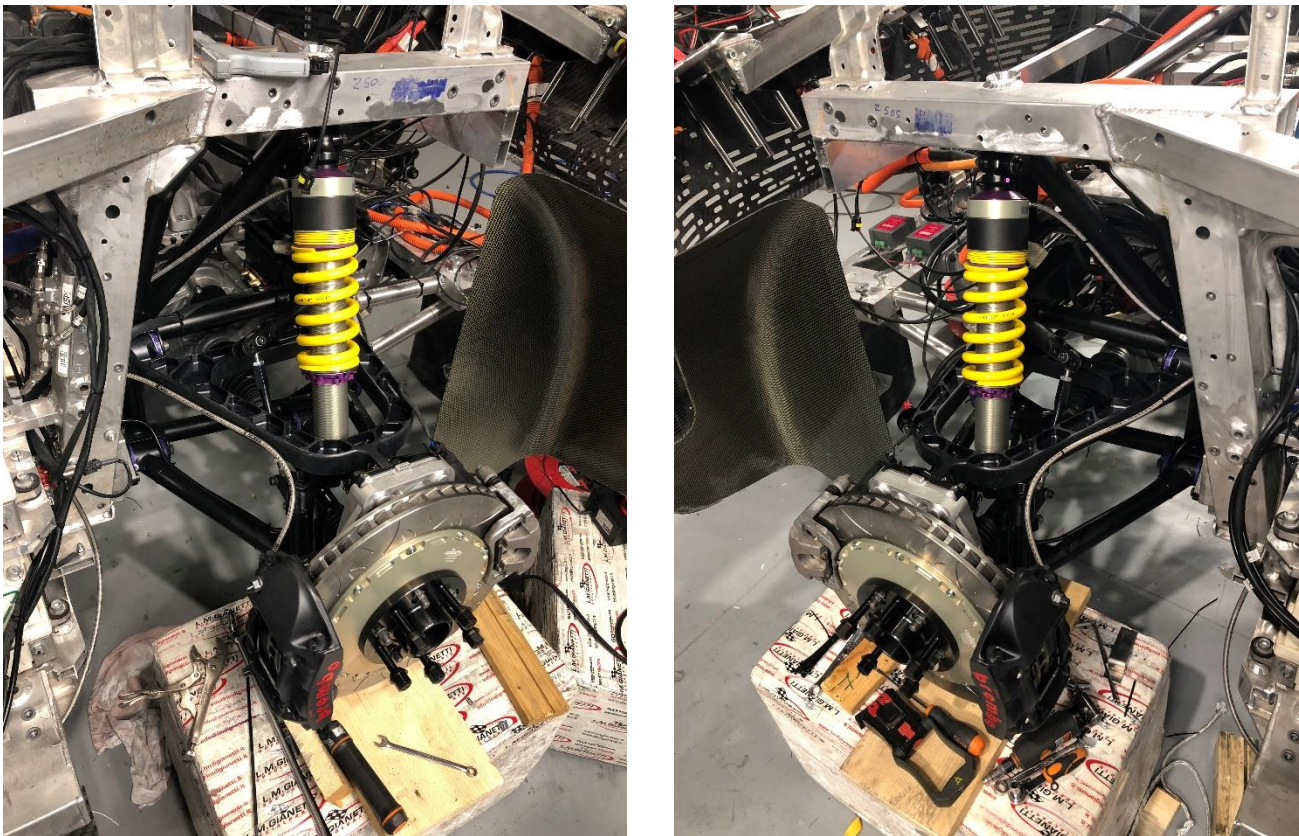


Figure 27. Mounted Left and Right Rear Suspensions.

## 2.3 DMU Analysis

The DMU Analysis, Digital Mockup Analysis, is a part of the Design activities aimed to create the representation in 3D by means of the CAE (Computer Aided Engineering) tools of the object of a product. In the case of this project all the components are designed in CAD environment and their feasibility is analyzed before they are sent to the Production Process queue. The DMU allows to reduce the time needed for completing the project outlining possible issues very early in the process; it also reduces the costs of the design since it reduces the number of pre-production prototypes for each component, moreover it also generates a higher perceived quality of the product granting the possibility to evaluate different solutions and then choose the best suited for the requirements. This DMU will mainly focus on the definition of the space available in the Rear Engine Bay, on the size occupied by all the components there fitted, with a brief description of their function, and the approximate position of said components.

### 2.3.1 Space Available

Fixed the suspension point the next step towards Frame design is to establish the requirements for the Frame itself: define in first place the maximum space available in the rear of the vehicle, and then which components in the Rear Frame will affect the shape of the Frame, in terms of size, shape, interface and functions.

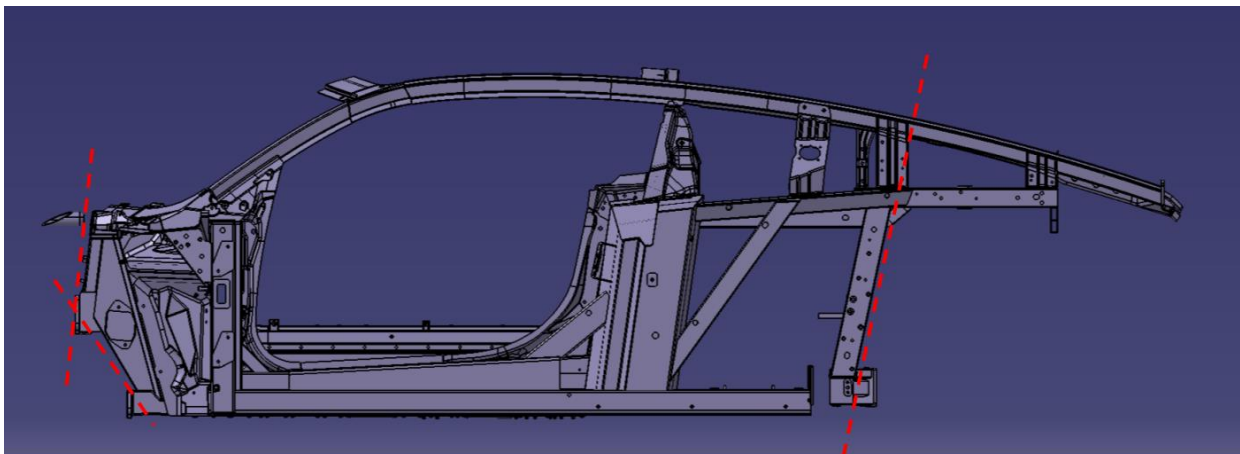


Figure 28. Central Cell Limits.

The Central Cell of the vehicle represent the main edge from rear engine bay towards the center of the car, as shown in *Figure28* on the Cell are drawn the trim-lines that divide in a sharp way the Passenger's Cabin from the outside. In the Front the lines clearly follow the Firewall while in the Rear the trim-line is moved away from the cell: in this vehicle the Battery Pack is integrated with the Central Cell, hence the Rear Frame will attach to the Cell past the Battery Pack.



The rest of the available space is limited basically by the bodywork, all made of Carbon Fiber with wheel arches in Kevlar, here follow the components. The lower area is occupied by the Underbody, which links the covers of the central Cell with the rear; the Diffuser, it is involved in both esthetic and aerodynamics tasks and moreover it supports the rear fog light, it is fixed with the Underbody to form a single component.

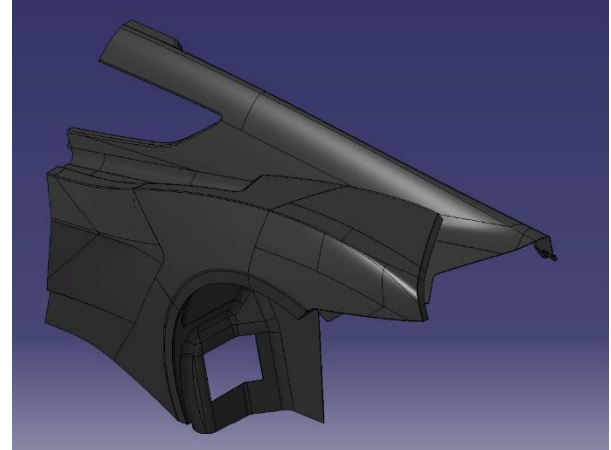
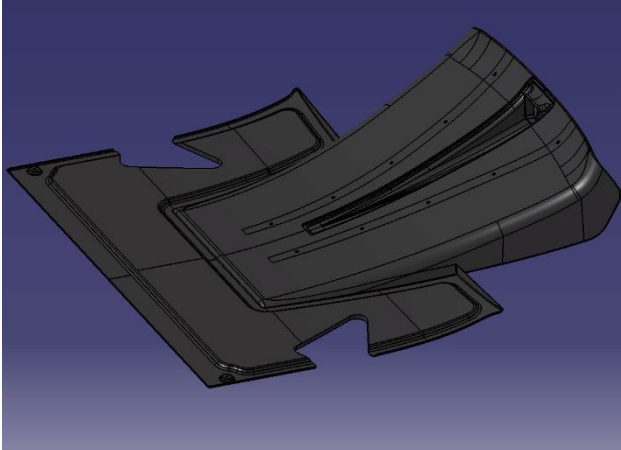


Figure 29. Left: Underbody and Diffuser; Right: Sidewall.

On the sides are placed the Sidewalls, for Style demand they are a two-pieces component and they seal the Front and Top parts of the Wheel arches with embedded parts in Kevlar. The back end of the control volume under analysis is closed by means of two elements: the first is the already described Diffuser, which acts along with the second one, the Rear Bumper. This is a complex component, it closes the Back part of the wheel arches, it supports all the back lights and on top it works together with a milled aluminum component to house the recharge sockets and the closing mechanism of the Trunk. The Trunk volume and Trunk Door, finally, act as the upper limit of the available space for the Rear Frame.

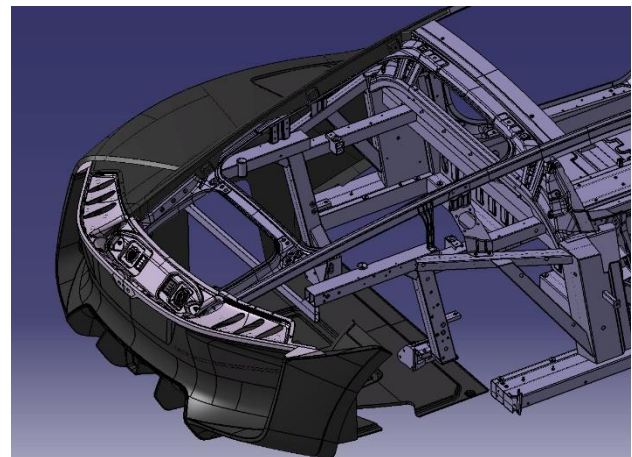
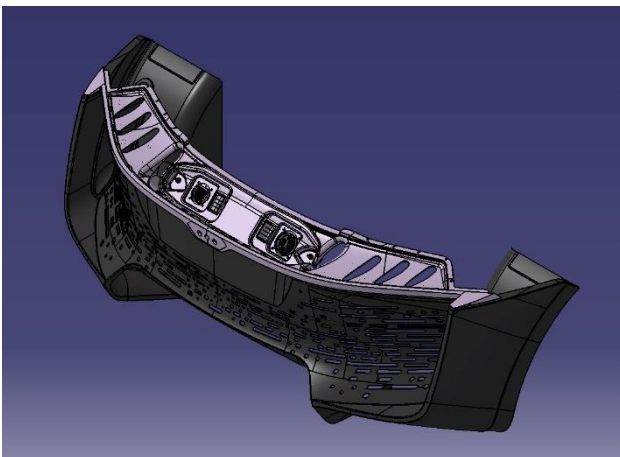


Figure 30. Left: Rear Bumper; Right: Definition of the Rear Volume.

The defined volume therefore will be the available space for the design of mainly two components: the Rear Frame, the central topic of the analysis, and the Rear End, which will be mounted on the Rear Frame to work as a support for the Rear Wing System.

After having defined the available space in the back of the car it is needed to identify all the components there placed. Due to the design of the car in rear are found components of one of the two drivelines and almost all elements of the Electric Power System.

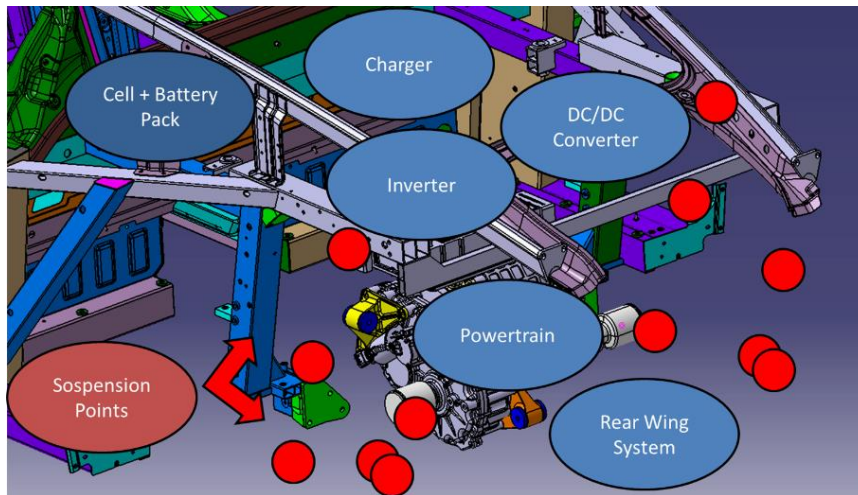


Figure 31. Vehicle Rear Components placement area.

### 2.3.2 Powertrain

As already mentioned, the Powertrains of the Front and the Rear axles of the vehicle are two identical elements. The Motor is a 3-phases Permanent Magnetic Motor delivering 160 kW (220CV) of Power and 340 Nm of Torque, considering Transient peak values. The motor is linked to the wheels through the gearbox, which is a *Borg Warner eGearDrive*, a 3 Axis-2 Stages Reducer with overall Reduction Ratio of 9.07, 2.68 on the first stage, 3.38 at differential. The driveline is mounted in transversal direction, with Motor axis shifted with respect to the Halfshafts axis due to interposition of the Reducer. The Rear Frame will be designed around the Powertrain group leaving space for the drive shafts and including the interface to house the Motor and Reducer Mounts.

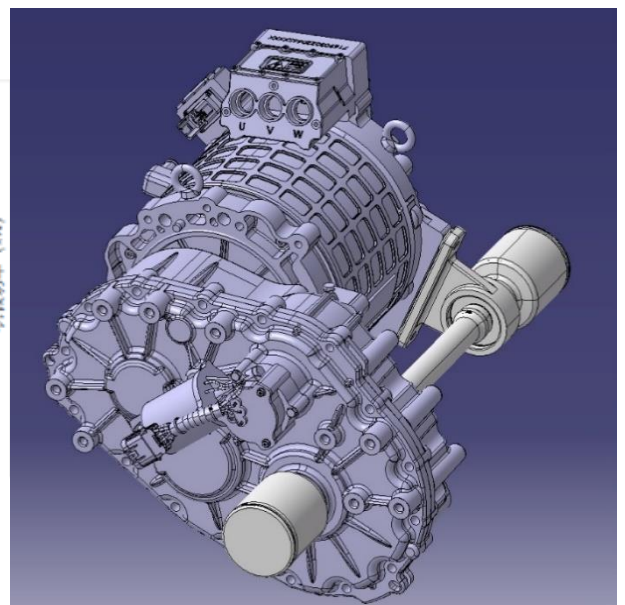
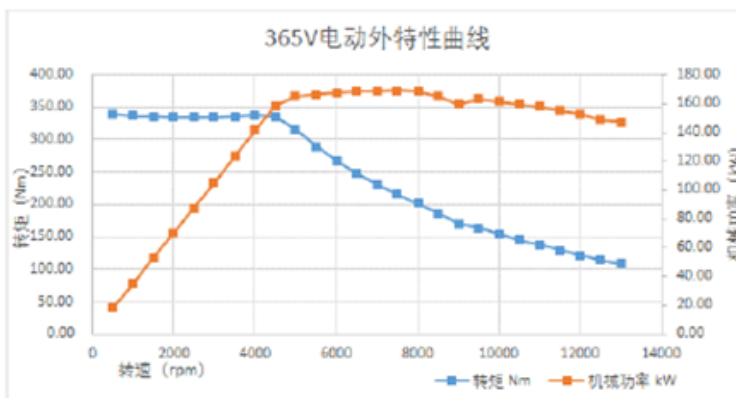


Figure 32. Left: Motor Power (Orange) and Torque (Blue); Right: Rear Powertrain.

### 2.3.3 Battery Pack and BMS

The Battery Pack is key component for an electric vehicle, not only for the primary task of being the only energy storage device, in fact its weight and dimensions are not negligible deeply affecting the design of the whole car. The Battery Pack of this Prototype is made of a total of 10 cell connected in Series, each of which counts 36.5 V tension and 7.884 kWh capacity. Therefore the Battery Pack delivers a Voltage of 365 V and almost 80 kWh of Energy. A single cell occupies  $710 \times 276 \times 200 \text{ mm}^3$  and weights 55.6 kg, that makes the total Battery Pack weight 556 kg hence the Specific Energy can be evaluated as roughly 150 Wh/kg. Considering which alternatives are on the market the value of their Specific Energy is within a range of 100-265 Wh/kg, that makes the Battery Pack ranking slightly under average (180 Wh/kg).

The layout of the Pack (*Figure33*) is T-shaped with 2 cells placed under Passengers Cabin in longitudinal direction and 8 cells in transversal direction forming two rectangles one above the other. Usually in a BEV (Battery Electric Vehicle) the Batteries are expected to be placed all under the cabin in order to lower the CoG of the car as much as possible, this is not the case: possibly due to a series of trade-offs the original design moved towards a less conventional choice. In order to reduce costs, time and avoid any kind of collateral problem the original Battery Pack has been maintained in its layout, thus along with its frame it works as a space constraint for the Rear Frame.

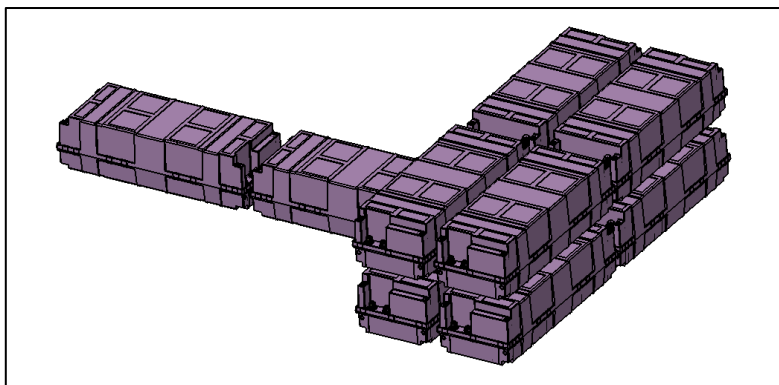


Figure 33. Battery Pack layout in CATIA.

Unlike a reservoir of fuel the performance of the Battery Pack is never linear or constant, its main parameters such as Open Circuit Voltage (OCV) or Specific Power are varying in first place with the

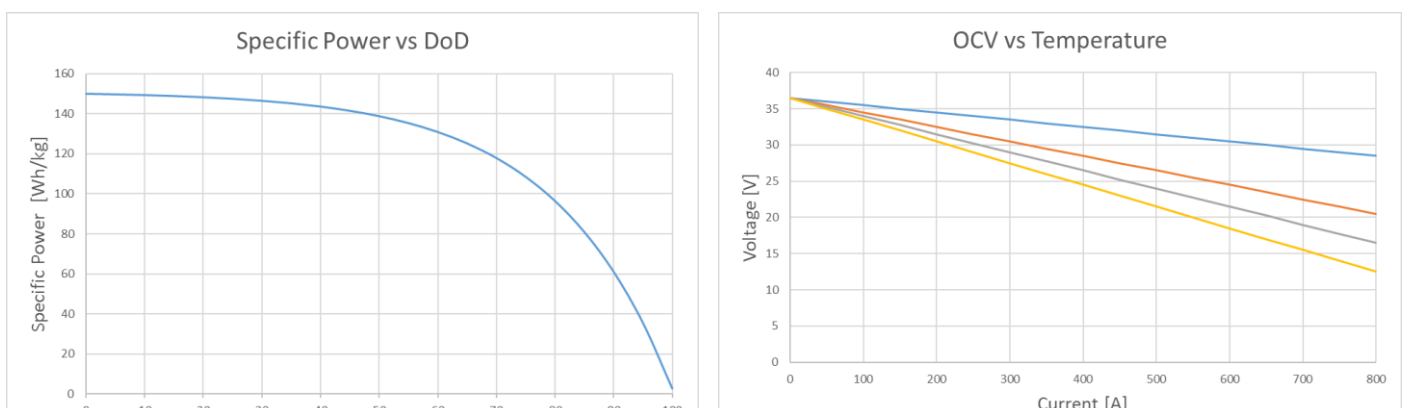


Figure 34. Qualitative reference for change in Batteries Performance.

State of Charge (SoC) of the cells, moreover they are also changing with the Temperature. Additionally it is useful to underline that it is impossible to design a battery to have simultaneously high Power and Energy Efficiency, due to this it is required a dedicated control system, the Battery Management System.

The main tasks performed by a BMS are in first place to keep the Battery Pack at optimal functioning Temperature, which implies a dedicated water cooling/heating circuit that adds weight to the vehicle, and then it has to manage the Energy and Power path from and to the cells in order to meet requested Efficiencies established during the design. To sum up the BMS is rather a circuit than a bulk sized component and it is integrated within the cells, but in any case at least a single box for the main control unit needs to be placed into the control volume in analysis: hence the BMS will be placed exactly in its original place over the battery pack and so it is not linked to the Rear Frame.



*Figure 35. BMS Central Unit placed over the Battery Pack.*

#### **2.3.4 DC/DC Converter**

Since on the vehicle there are electric circuits working at different values of Voltage it comes the need for a device that allows to manage Power at different voltages. Such device is called a DC/DC Converter, usually it is used to adapt voltage between an Energy or Power source and various components such as: another Battery Pack or a Fuel Cell System, another Power Converter or the vehicle auxiliaries.

A DC/DC Converter is mainly based on two technologies: the Diode and the Transistor. A Diode is a device that allows the Current to flow only in one direction, called Direct Polarization, and ideally at 0 V. In a real Diode the actual voltage during conduction will be slightly higher than 0 and a reverse voltage is sustained by the device only until a value named Breakdown Voltage at which the Diode is broken.



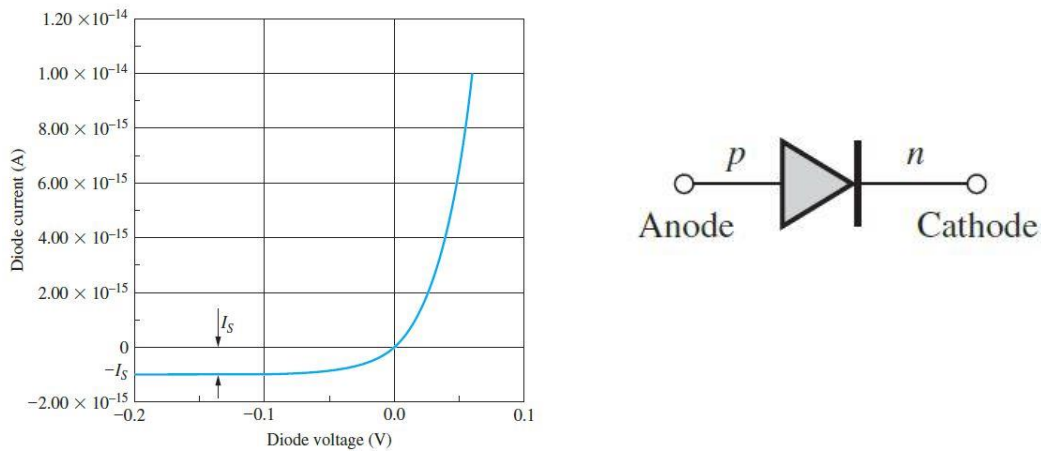


Figure 36. Diode behavior and symbol.

A Transistor is a High Frequency Switch that has 3 terminals, usually called Gates, 2 of them are Power gates while the third is a control-signal gate. By means of the control-signal the switch is turned ON and OFF with frequencies going from 20-30 kHz to hundreds of kHz. In automotive field the main devices adopted are MOSFET (Metal Oxide Semiconductor Field Effect Transistor) and IGBT (Insulated Gate Bipolar Transistor), the first values of voltages lower than 60 V, the other for hundreds of Volts.

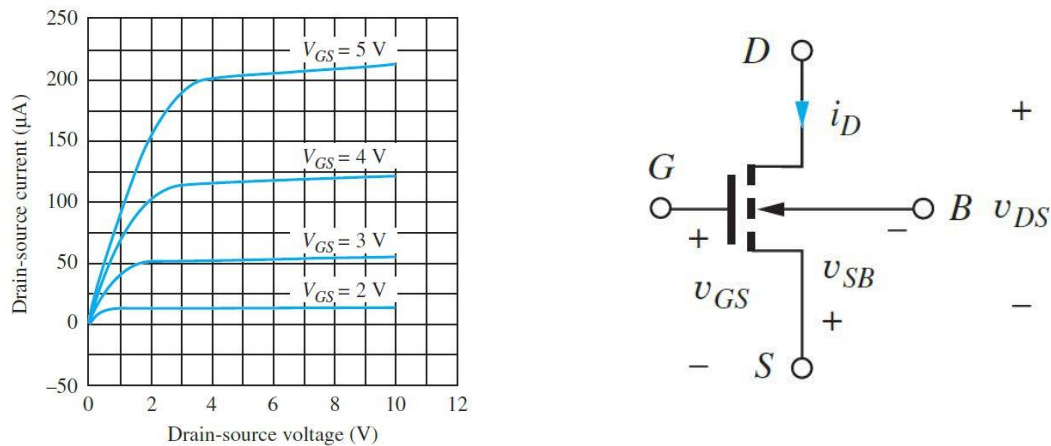


Figure 37. MOSFET behavior and circuit representation.

The converter is then built in different ways if it has to act as a Step-Up or Step-Down Converter, on the vehicle are installed two different Step-Down DC/DC Converters (Figure 38). They can be placed one next to the other but they are performing conversion between different voltages. The first DC/DC Converter works amidst 750 Vdc and 365 Vdc, the values are not casual: 365 V is the voltage supplied by the Battery Pack while 750 Vdc is the DC Fast-charge line voltage. The other DC/DC Converter is employed in order to carry power to the vehicle auxiliaries, that run at 12 V, so it works from 365 V to 12 V.

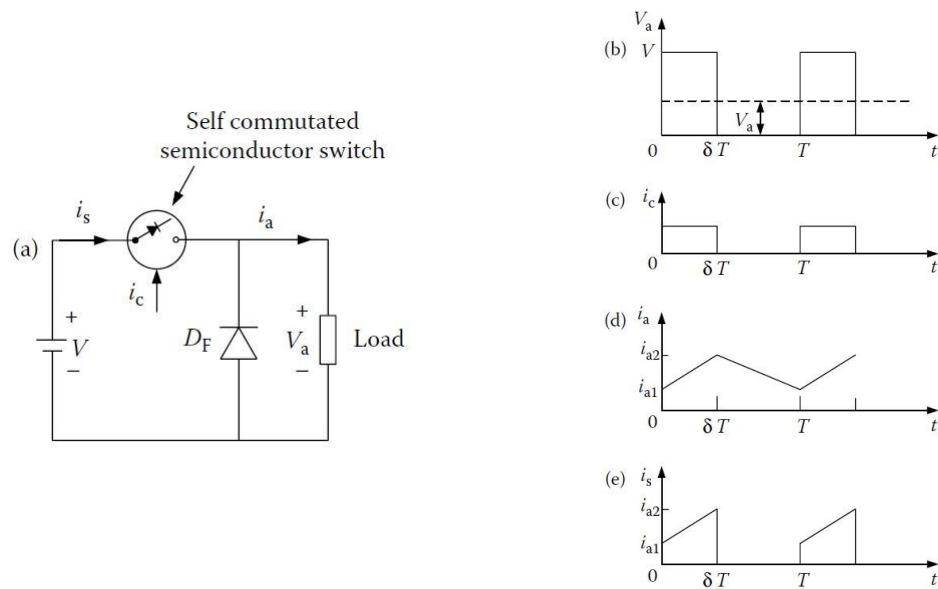


Figure 38. DC/DC Converter scheme (a) and waveforms: load Voltage (b), control current(C), load current (d) and current through switch (e).

As shown in *Figure38.a* by action of the Switch and the Diode the input voltage  $V$  is reduced to a voltage  $V_a$ , function of the input voltage and the ON Duty cycle of the Switch:  $V_a = \delta * V$ ; with  $\delta$  being the ratio between the time the Switch is ON and the total Period, varying between 0 and 1.

Physically the two DC/DC Converters are two metal boxes on the outside, in fact small compared to the other components of the Electric Power System so relatively easy to mount on the vehicle. Originally, they were fixed to the frame by means of bolts, so they present pass-through holes on a flanged sheet component integrated in the box.

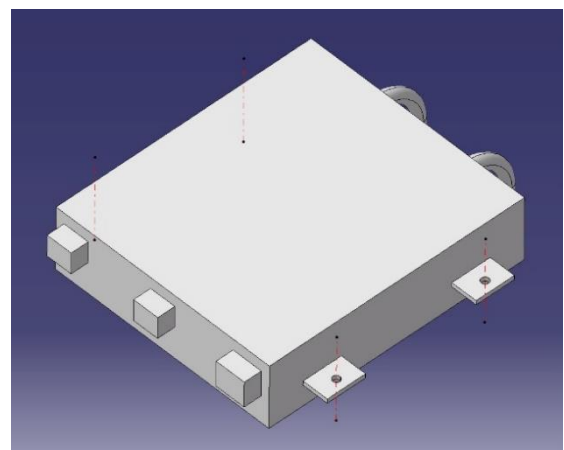
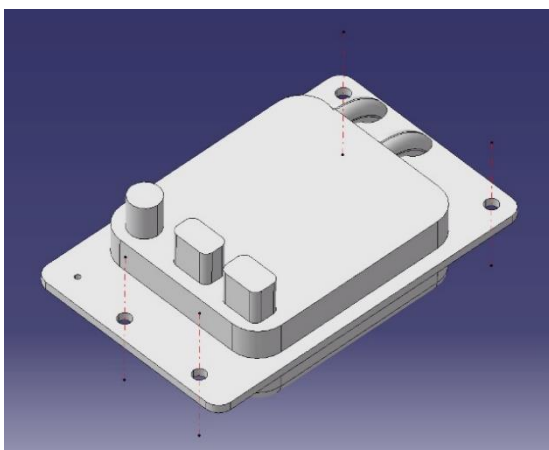


Figure 39. Components size and holes axes. Left: DC/DC Converter 12V; Right: DC/DC Converter 365V.



Figure 40. Installed DC/DC Converters.

So the design of the Rear Frame will include a third element between Frame and DC/DC Converters in order to link them, its design will start from the already existent holes and will reach and couple with the tubes frame, as further described.

### 2.3.5 Inverter

The Inverter, also named DC/AC Converter in an Electric Machine involved in Power management as the DC/DC Converter. The Inverter is responsible for converting a DC Voltage, output of an Energy Storage, into a 3-phased Alternating Current suitable to supply a 3-phased Electric Motor. Notably, all Energy supplies delivers a DC Voltage, so the Inverter is a machine needed in all type of vehicle with Electric Drive. An AC/DC Converter is based on the same devices previously described, the Diode and the Transistor, what changes from a DC/DC is the total amount of the components and their position in the circuit.

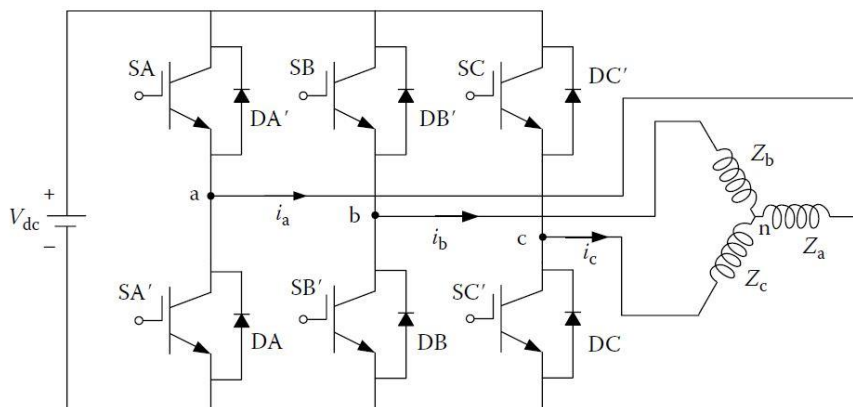


Figure 41. Common 3-phased DC/AC Converter circuit.

In a 3-phased Inverter there are 6 Switches and 6 Diodes, 2 of them for each Phase, one in ON and one in OFF condition. The control on the Phases ON-OFF state is the key point of the Inverter, and in total there are 7 of them. The control is performed with techniques called Pulse Width Modulation (PWM), a simple example of it can be the analog Sinus-Triangle Modulation: the

Reference sinus wave of each phase is compared to a Triangular Wave, determining if the Phase is ON (>) or OFF (<). Starting from a DC Voltage is obtained a 3-phased alternating current given that the switching frequency is high.

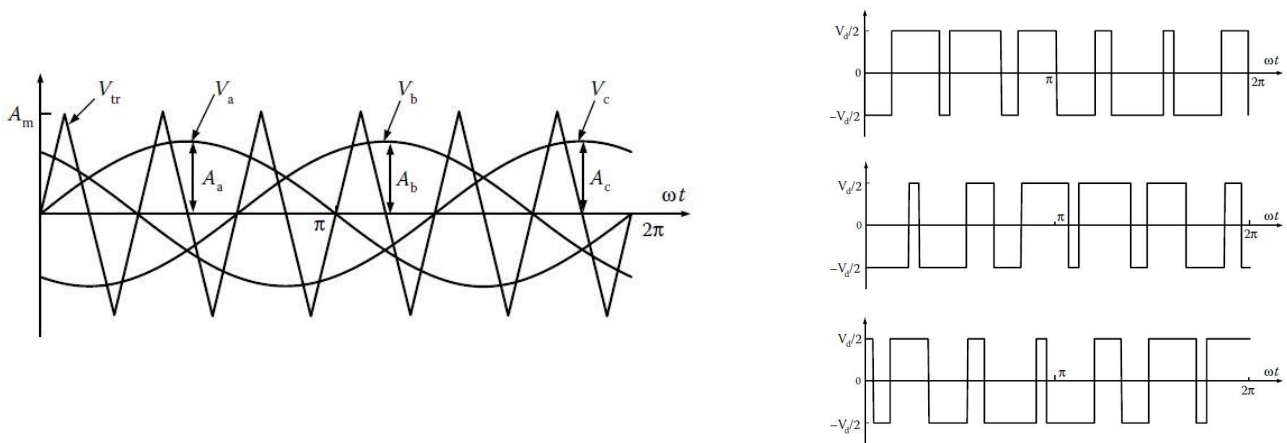


Figure 42. PWM. Left: Comparison between Waves; Right: Voltage of each Phase.

The Inverter to install on the vehicle is again a metal box roughly occupying  $310 \times 360 \times 135 \text{ mm}^3$  that makes it larger than both DC/DC Converters. On the two sides of the device there are already 4 protrusion made to mount the Inverter in its previous position: this means that the component to be added on the Rear Frame in order to carry the DC/DC Converters will be extended to carry also the Inverter, matching the holes for the pass-through fastening screws.

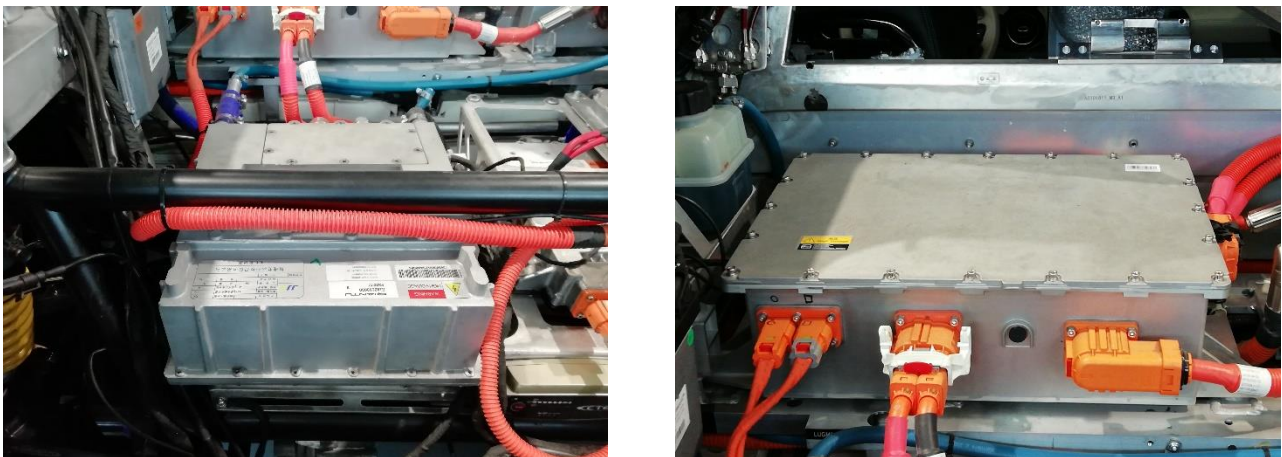


Figure 43. Left: Inverter installed on vehicle; Right: Charger above the Battery Pack.



### 3.2.6 Charger Unit

The Charger Unit is complex system with key role in the Energy management of the vehicle. Even if it is an electric system more than a single device there is in any case a metal box in which are contained its main components, that must be fitted in the Rear of the car as for the rest of the Electric Power System. Since formerly it was placed over the Battery Pack along with the BMS central unit for the same reason the choice has been to maintain it in the same spot.

The tasks of the Charger are all involved with an Energy flow from an external Power supply to the batteries, and they vary based on which type of recharge is being performed. The vehicle can be recharged with a 220 V AC current line, passing through the management of the Charger and once it is converted into a 365 V DC current it is employed to charge the Batteries. It is also possible to charge the car in Fast Charge mode: it is needed a 750 V DC current that is scaled down to 365 V by the DC/DC Converter and then reaches the Battery Pack through the Charger.

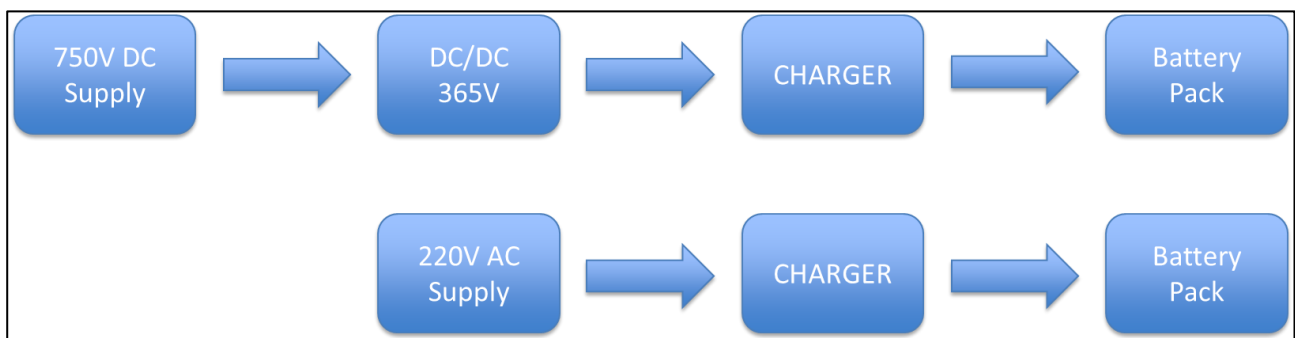


Figure 44. Recharging Power Paths.



Figure 45. Final layout of the Power Electric Circuit.

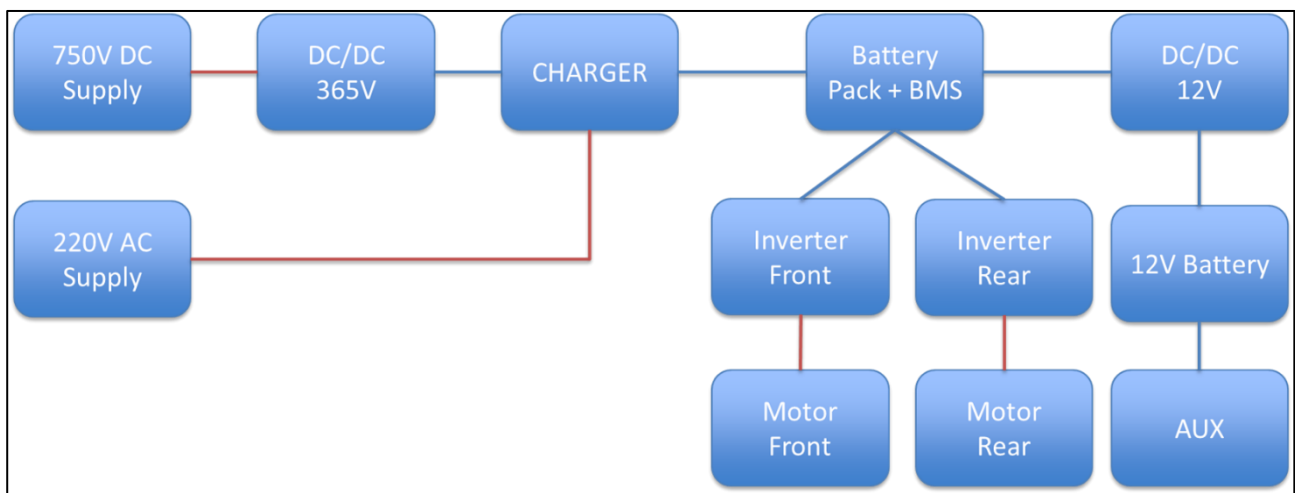


Figure 46. Scheme of the Electric Power System.

Finally, in *Figure45* is represented the overall layout of all the components discussed that are within the volume defined in the rear of the car.

In *Figure46* is drawn a scheme of the Electric Power System, in which are outlined the different lines for AC (Red) and DC (Blue) wiring and the possible Paths for the current to flow. A side note must be added for the BMS: all the possible paths from and to the Battery Pack are indeed managed by the BMS, so the battery cells will be charged differently one from the other accordingly to several parameters starting from the SoC of each and so it does not depend on the Charger control; even when power is needed for traction or auxiliaries is duty of the BMS to direct the Energy from the cells to the supply line.

### 3.2.7 Rear Wing System

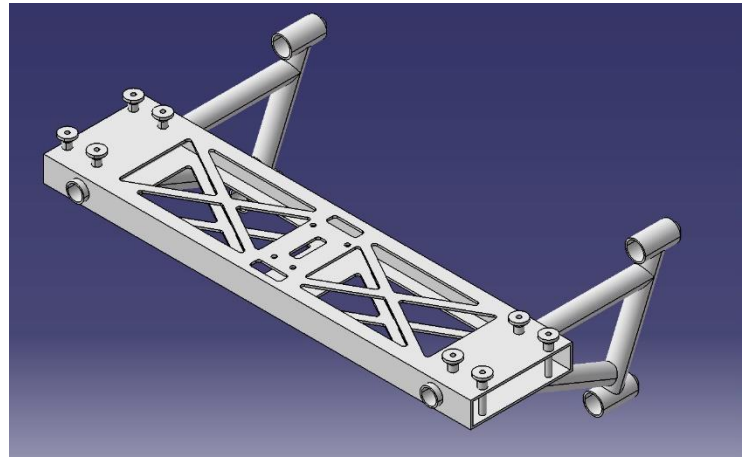


Figure 47. Left: Rear End of the car; Right: Rear End in CATIA.

Briefly, the last system lying in the back of the car is the Electronics and the Hydraulics Systems employed to move the Rear Wing. The System is not directly involved with the Rear Frame design, but with the Rear End, a subframe mounted on the back of the Rear Frame and included in a series of tasks: support of the 12V Battery, Rear Wing Control Unit, Solenoid-valves group and still parts of the Hydraulics system. On top of this, the Rear End is fastened with the Aluminum part of the Rear Bumper, since both are coupled with the Hydraulic system, hence given that the Bumper is itself mounted on two longitudinal beams coming from the Central Cell the result is an overall increase of the stiffness of the vehicle, even if the contribution of the Rear End can be considered smaller than the stiffness of the Rear Frame.

In conclusion, the Rear End in fact increases the stiffness of the Chassis but for sake of simplicity the Rear Frame can be analyzed without taking it into account, as a result the Frame will face a higher load. Once that the structural analysis is performed and the Rear Frame is valued as good it can be of interest to repeat it adding to the model also the Rear End.



### 3. CHAPTER 3 – REAR FRAME

#### 3.1 Rear Frame Structure

Given that the starting point of the design of the vehicle chassis is the central Cell in aluminum, it comes the need to add a Front and a Rear Frame on top of the COP component, one of the easiest way to do so is to design 2 new frames compliant with all the requirements and fastening them on the Cell: this means that possibly some interface elements will be put between the Cell and the Frames.

##### 3.1.1 Material: 25CD4 Steel Alloy

The most common choices for the Frames material are mainly 2: Aluminum as for the Cell or Steel alloys. The main advantages of choosing 2 aluminum chassis are all linked with the weight budget, since the prototype is a BEV the weight of the Battery Pack is an issue to be faced and reducing the weight of chassis employing aluminum is a solution. Potentially a drawback could be that the resulting stiffness of the car would be not high enough, leading to poor performance in handling. The other choice is then to use a Steel Alloy for the new frames, which basically has opposite characteristics with respect to the Aluminum, it weights almost 3 times more and would bring the chassis to be much more rigid. Once this is settled it follows that necessarily the choice will be a Trade-off between Stiffness and Weight, since Costs and materials availability are less relevant. In conclusion, the new chassis will be made of Steel in order to give to the vehicle higher stiffness possible, considering that the weight of the Steel would not be much of a problem if considered during the design.

Steel 25CD4		
Density	$\rho$	7.8 kg/dm <sup>3</sup>
Young Modulus	E	210 GPa
Ultimate Tensile Strength	UTS	800-950 MPa
Yielding Stress	R <sub>P0,2</sub>	600 MPa
Elongation	--	14%

Table 13. 25CD4 Mechanical Properties.

Name	C	Cr	Mo	Mn	Si	S	P	Fe
25CD4	0.22-0.29%	0.9-1.2%	0.15-0.3%	0.6-0.9%	Max 0.4%	Max 0.035%	Max 0.025%	Remaining

Table 14. 25CD4 Chemical Composition.

The 25CD4 Steel is a low carbon steel available in both tubes and billets, making it suitable for a wide set of applications. The main alloyed elements are Chromium and Molybdenum, common for steel alloys: the Chromium has the property to increase the material hardness by formation of stable Carbides and aids the creation of thin grain structure following the thermal treatments; the Molybdenum belongs to the same Chemical Group of the Chromium, it forms complex and hard Carbides, increases even more the Hardenability of the material and acts in order to stabilize the

Martensitic structure. Therefore the 25CD4 is a material that comes quenched and tempered and usually it is adopted for mechanical construction in fields like Aeronautics, Motorsport and Automotive in general: its good weldability makes it suitable for building any kind of chassis, so it is commonly employed for Rollcages and Frames, but since it is available even in billets it is possible to design milled structural components such as the Control Arms for Suspension, like the LCA on this vehicle. Usually it is not used for components involved in Power transmission, e.g. Halfshafts or Gears, that may require further thermal and thermo-chemical treatments.

### 3.1.2 Geometric Structure

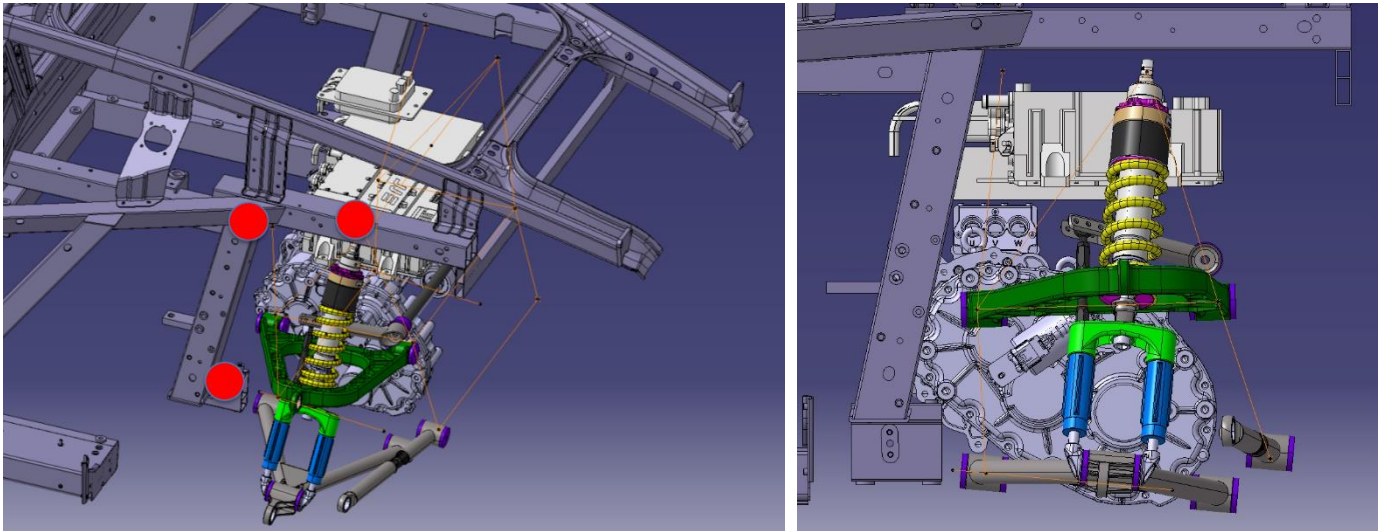


Figure 48. Left: Geometric Structure of the Rear Frame; Right: Side view.

Considering all that has been discussed it is possible to draw a scheme such as in *Figure 48*, where are displayed the main components mentioned but the Bodywork and what is not linked directly to the Frame. To start building the Geometry of the frame it is needed to add the points where the Frame will attach to the Cell: shown as the 3 Red dots.

*Nota bene*, the choice of the attach points is fundamental to create a Chassis capable of sustaining the maximum performance of the Vehicle, and it is advised by L.M. Gianetti designing experience: one point should be close to the Top Mount of the Damper and other good points are those in which there is a node on the CoP Chassis. It is possible to use one existing Chassis node and to exploit the interface of another one that has been cut off and then substituted by a new one.

Once that all the requirements are set it is possible to discuss the actual geometry of the frame. Since it has to satisfy several tasks common sense suggests that it is impossible to consider a frame made only with tubes, hence it will include other components as well. A first idea could be to consider several joints built with welded metal sheets which has a series of advantages: it is low in costs, easy to manufacture and easy to assembly. The main problem, and cause for their discard, is that such joint will be too weak to face loads coming from the car dynamics, through the suspensions towards the central cell, the quantity of material is not enough to avoid high stress and moreover due to their shape most of the load would be applied locally and the frame would perform badly from a structural point of view. Thus the best choice is to create a group of milled Nodes then welded



together with the tubes, all in Steel 25CD4, with each of them specifically designed to couple with the surroundings.

On top of this, during the analysis of the devices mounted in the back the car it was stated the need for an additional element to link the frame to the Inverter and the two DC/DC Converters: such element can be a metal sheet in steel or aluminum with holes pairing with those already on the devices, and sort of appendices to reach the tubes of the nodes of the frame to be fastened to it.

Now the Wireframe of the Rear Chassis can be determined: it will consist in lines representing the axis of the tubes and points which will be more or less the center of each node, in practice the Nodes will have a complex shape so their center will move around the reference. The number of Nodes will be determined as follow, there should be one of them for each Hardpoint involved, so they are 2 for the LCA, 2 for the UCA and 1 each for the Top Mount (considering only one side of the car, due to symmetry). Looking at *Figure 48* (Right) it can be noticed that the node for the front pivot of the LCA and the one for the Top mount are close to the point chosen to fix the chassis on the cell, this will lead to a more complex form of the nodes that will perform both tasks. Since the third joint (Red dots) is missing a direct link to the frame it is needed a dedicated node to reach it and a piece of tube to join it to the frame. This makes the total amount of nodes 6 per side, 12 in total.

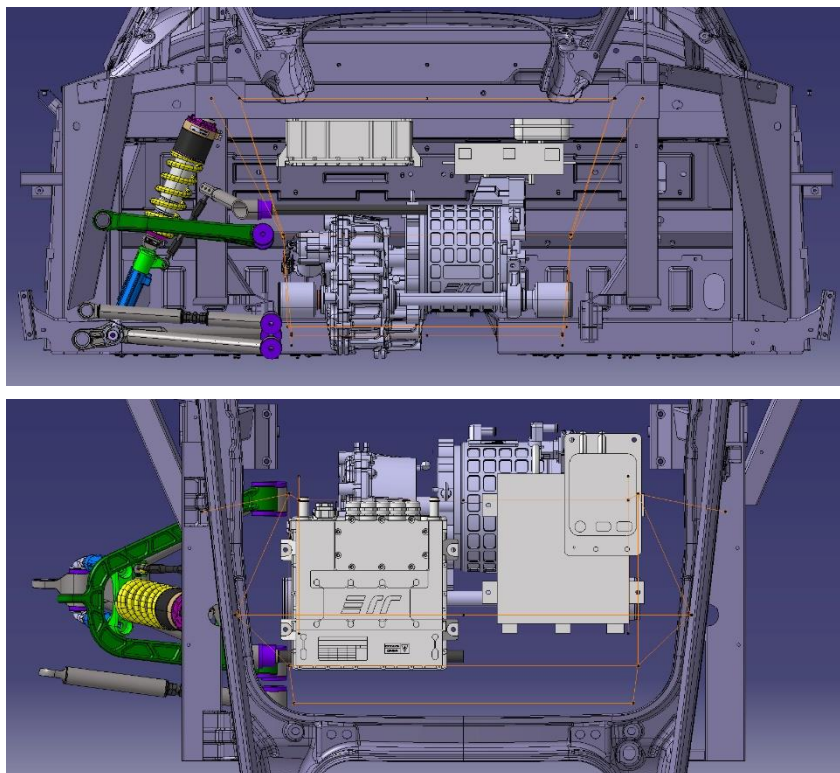


*Figure 49. Rear and Top view of the Wireframe.*

Considering Side view it is clear that the Wireframe matches the position of the Hardpoints, forming a sort of square in the bottom with a triangle on top of it plus a leg to reach the Central cell, this shape is repeated on the other side so the missing parts of the Wireframe are only the links between

the two sides, which will be made by straight tubes. The final position of the nodes is based on the constraint made by the Cell so they will hang at a distance of about 30 mm from it.

Looking at the Rear and Top view (*Figure49*) it can be noticed that the Wireframe is not only built to meet the Hardpoints but it is also developed around the Powertrain, in fact in the front part it misses the transversal tube linking the two sides because it would be impossible to fit it. The Wireframe will be narrower than the Suspension Points by roughly 50 mm, that is a trade-off granting enough space to build a node and keep the frame far from the Powertrain. Moreover it can be seen the empty space in the top part of the frame, it becomes easy to see why the Inverter and the DC/DC Converter have been placed there, not only there is plenty of empty space to exploit but that position is also the best to bolt down the devices on a metal sheet then mounted on the frame: notice that in any case the Inverter should be as close as possible to the motor, in fact the thickest wiring is placed between those two components due to the huge amount of Power transmitted, therefore to reduce overall costs and energy losses the two devices must be as close as possible.

## 3.2 Rear Frame Components

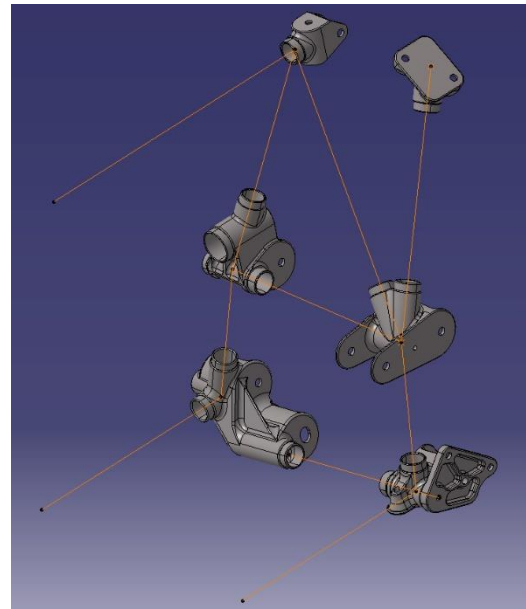
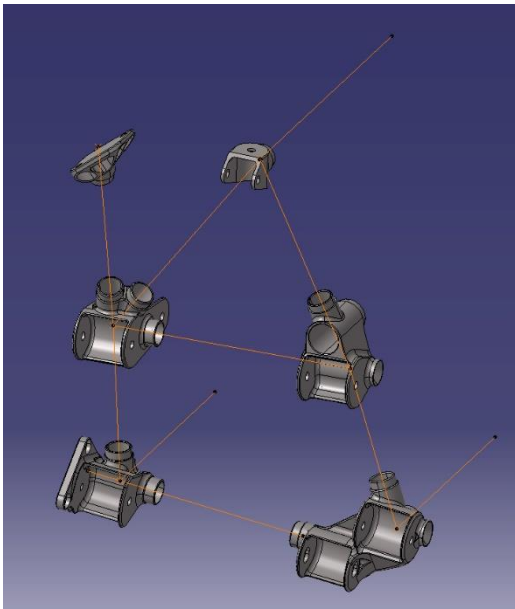


Figure 50. Half Wireframe with the Nodes.

Will now follow the description of all the components of the chassis, starting from the Nodes that have the most complex design, top to bottom, then the Tubes that will connect them.

### 3.2.1 Upper Node

The Upper Node is the node dedicated to add a fastening point between the Rear Frame and the Central Cell. Since it has only this purpose the component is rather simple, with respect to the other nodes. It is designed starting from a plane, that will be the major contact surface of the joint, on which is considered a rectangle 70x90 mm so that 2 out of 3 of the raw material dimensions are set. The third is obtained considering that the Node is coupling with a tube, so it is needed a protrusion in order to match the tube and allow the welding of the components. Once that the 70x90x40 mm



raw is defined the piece is finished by eliminating all the material in excess, shaping the interface for the tube and adding two holes to allow the screws through.

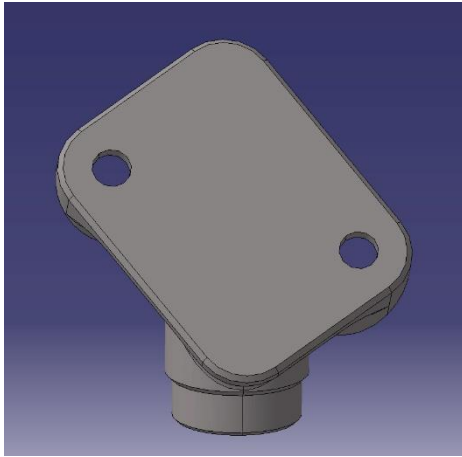


Figure 51. Left: Upper Node in CATIA; Right: Machined Upper Node.

The coupling interface with the tube (*Figure 52*) is almost the same for all the tubes in the frame, it may change only depending on the diameter and thickness of the tube so that in any case it would be different in dimensions but not in shape. On the node there is a cylinder leaning outward from the bulk with a diameter equal to the inner diameter of the tube, in this case that is  $\varnothing 36\text{mm}$ . On the cylinder there is a collar with greater diameter, equal to the outer diameter of the tube  $\varnothing 40\text{mm}$ , which provides the contact surface between Node and Tube. Furthermore it is important to chamfer this collar in order to get a better welding.

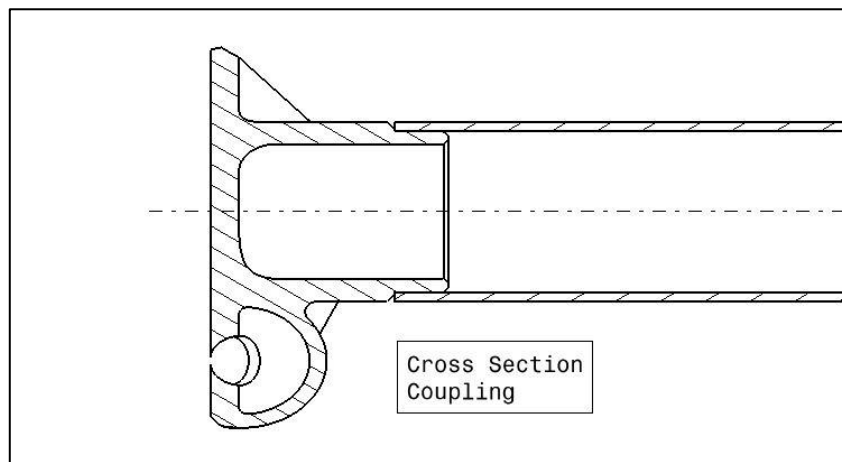


Figure 52. Detail of the coupling between Node and Tube.

Looking at the Drawings (see Annex at the end of the document) it is possible to underline the parameters required by the design. First of all the raw material needed is a 25CD4 prism roughly  $100 \times 80 \times 50\text{mm}$ , than in order to have correct mounting the main quotes are: right bias between the centers of the counterbored holes; slope of the cylinder with respect to the contact surface; contact surface maximum deviation of  $0.05\text{mm}$  from the reference plane; allowance of  $-0.1/-0.2\text{mm}$  on the diameter  $\varnothing 36$  where the tubes is mounted, dimension of the chamfer for welding  $1.5 \times 45^\circ$ . Finally it is important that the bore of the holes is as small as possible considering a M10 screw, that will be

Ø10.1mm: this is due to the assembly process, since a certain amount of distortion is expected following the welding the holes will not match with the counterpart, the best idea is to keep more material than needed on the hole so that it is possible to recover the error drilling away the material where needed.

### 3.2.2 Top Mount

The Top Mount Node is another simple component of the frame, but it performs two different tasks: coupling of the frame with the Central Cell and attach of the top part of the Damper. It is designed starting from a 50x55x90mm prism of 25CD4 and it is formed by 3 main elements: on the outboard side it is shaped like a fork in order to couple with the ball joint of the damper through positioning bushings which lock the ball with a screw passing through the fork; in the inboard side it presents the protrusion already described to match with a tube of the frame, even in this case the diameter of the cylinder is Ø36mm and again there is the chamfered collar where they will be welded together; on the top it is needed a flat surface in order to make the contact with the Central Cell Interface Component and a pass-through hole is added in order to fix the screw.



Figure 53. Finished Top Mount.

Considering the Drawings (Annex) it can be noticed the already stated raw material dimensions, and further the main parameter of the design: the reference is set to be the collar where the tube is centered for the welding, starting from it is defined the position of all the holes, with a tolerance of  $\pm 0.05\text{mm}$ ; then to couple with the screw, the ball joint and the bushings there is an allowance of  $+0.1/+0.2\text{mm}$  on the width of the fork and  $0/+0.5\text{mm}$  on the Ø12mm hole for the screw passage; finally it is repeated the interface for the tube welding, the Ø36mm cylinder has the allowance of  $-0.1/-0.2\text{mm}$  and there is a  $1\text{mm} \times 45^\circ$  chamfer on the collar.

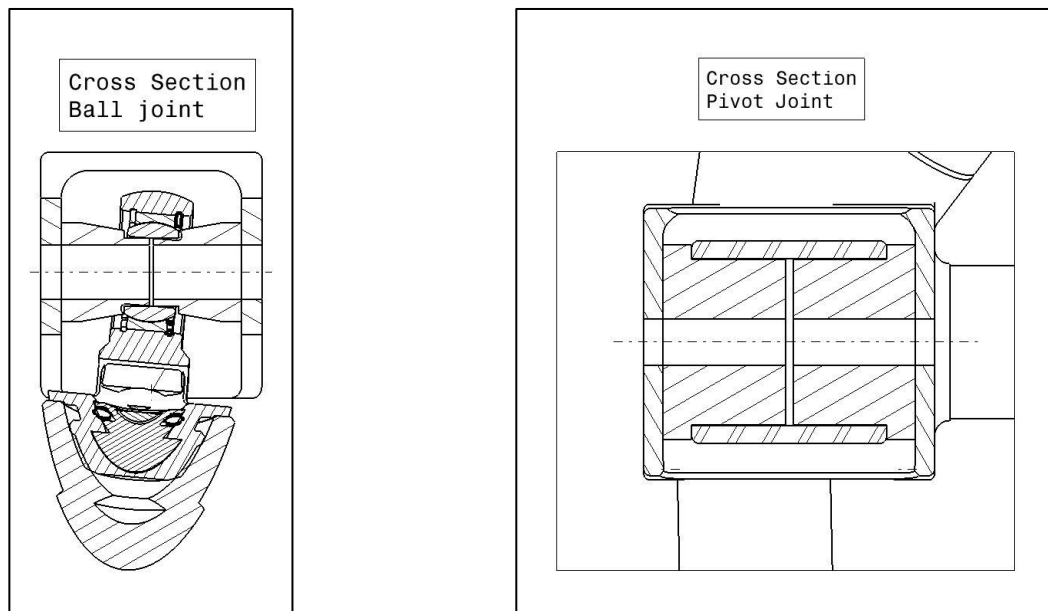


Figure 54. Left: Detail of the coupling of Top Mount and Damper; Right: Cross section of the Pivot Joint.

### 3.2.3 Upper Control Arm Front Node

The Upper Control Arm of the double wishbone suspension described needs two pivot joints on the chassis side, thus on the chassis there will be two Nodes designed primarily to hold the still part of the joint: one for the front leg of the UCA and one for the rear. The UCA Front Node is the first of the more complex nodes, its shape is the best compromise considering the group of tasks that it must perform.

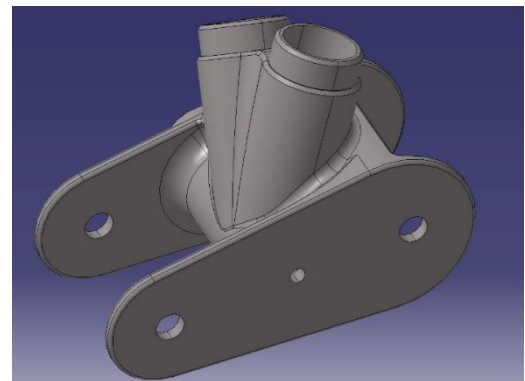
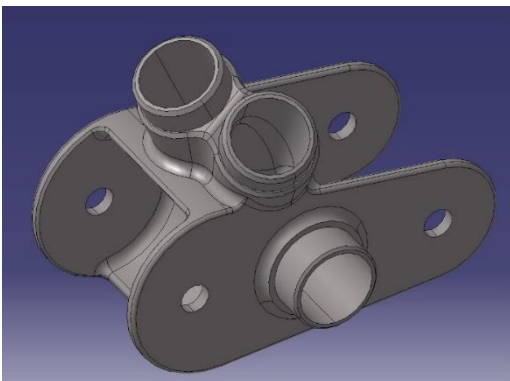
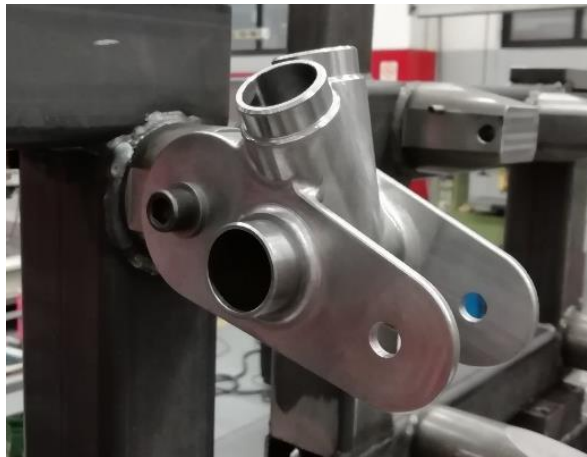


Figure 55. UCA Front Node in CATIA.

On the outboard side it presents the interface for the pivot joint, that is a fork designed to be screwed with the *Powerflex* and the metal bushing inside of it (*Figure 54*). The two sides of the fork are linked together in the inner part by a sort of half sleeve, machined with a diameter bigger than the one of the UCA bushing so that it is free to move around the pivot axis. In the inboard side of the Nodes there are two flaps protruding forming another fork, also in this case they work in order to pair with a *Powerflex* by means of a bolt that lock them close. The joint is one of the attaches needed to mount the powertrain group, in particular this is linked to its left side, to the Reducer.

In *Figure 50* is shown how the Nodes is connected with the rest of the frame, in total there are 3 tubes reaching for it: one link the UCA Front and Rear Nodes, one is the connection from this Nodes to the Upper Node, the last is coming from the Top Mount and the number of protrusions matching the tubes is set. It must be underlined the presence of an extra hole in the front part of the nodes, opposite to the joint towards the UCA Rear Node. This hole is made to overcome a problem occurring during the welding process: due to the high heat flow of the process the air inside the tubes is going under pressure and this rises a series of problems such the risk for the welding seam to break or in any case a residual stress in frame. The hole assures that the inside of the tube does not become a closed volume during the process, so the air is free to flow out and it does not increase in pressure.



*Figure 56. Finished UCA Front Node on the Welding Tool.*

From the Drawing (Annex) it is possible to get the size of the raw material needed to mill the component, 160x120x60mm. There plenty of important quotes to observe: the holes for the passing through screws are quoted with respect to the axis of the horizontal tube linking the two UCA nodes. The same axis is used in order to locate the axis of the other two protrusions and the height of the collar, on which is added a tolerance equal to  $\pm 0.05\text{mm}$ : in such a way all the pairing components will match with the smaller error possible. Other remarkable tolerances are put on the width of the forks, in particular there must be an allowance in order to guarantee the mounting of the *Powerflex*, so the tolerance on the quote will be  $+0.1/+0.2\text{mm}$ . On the holes for the screws is added another tolerance of  $0/+0.05\text{mm}$  that has the purpose to keep the pivot axis as close as possible to the ideal one. Finally, as for all the other couplings with the tubes the  $\varnothing 36\text{mm}$  diameters are provided with allowance  $-0.1/-0.2\text{mm}$ .

### **3.2.4 Upper Control Arm Rear Node**

The other UCA node, sited in the rear of the chassis, is another elaborated milled component, optimized for different purposes, to proceed with the description it is useful to consider it as divided in an upper and a lower part.

In the bottom part, outer side, it couples with the UCA through pivot joint already described in *Figure 54*: Right, hence its shape will recall the one seen in the UCA Front Node, a fork with holed

flaps linked together by a half sleeve with cylindrical form that will pair with the *Powerflex* Universal Joint. The Front side of the node presents the same kind of protrusion created to meet the second side the tubes coming from the other UCA Node: geometrically it is equal to the one already seen. In the Rear side the Node is modelled with sort of conical seat overhanging out of the Node, with a threaded M10x1.25 hole in the center: this element is needed in order to attach the Rear End on the Rear Frame. On the inner side it may be noticed a simple cylindrical surface that will help to weld a vertical tube arriving at the UCA Rear Node from the LCA Rear Node.

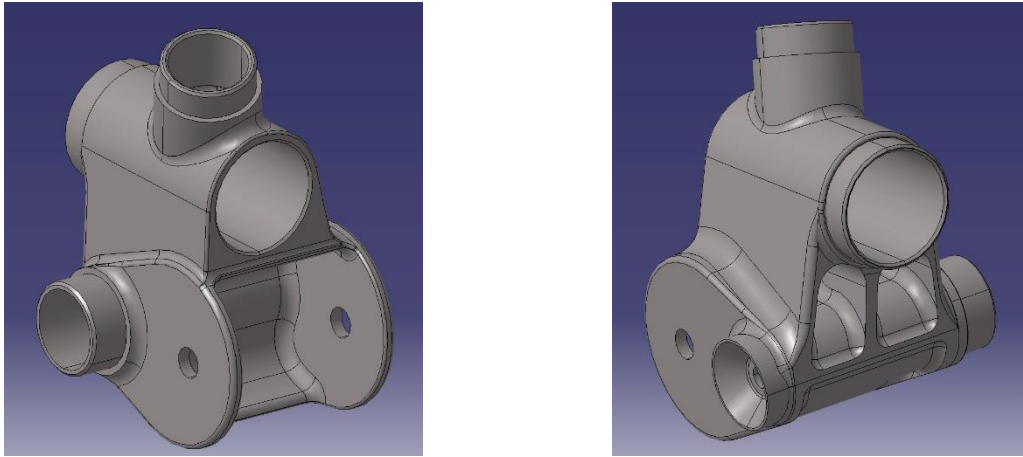


Figure 57. UCA Rear Node in CATIA.

In the Upper part of the node it is located the interface to install the Anti-Roll bar, mainly it is formed by two elements. On the outboard side over the fork there is a large hole with bore  $\varnothing 43.5\text{mm}$  in which will be put a Universal joint, always by *Powerflex*, that in the inside is paired with the side Bushing of the Anti-Roll bar, a rubber joint of this kind is employed in order to make the bar silent. On the inboard side the Node has a protrusion with the same shape of the ones needed to center the tubes, but it has a larger diameter  $\varnothing 48$  since it couples with transversal tube  $\varnothing 50 \times 1$ . The Anti-Roll bar will pass through this tube therefore the *Powerflex* on each side will keep the bar from moving inside the larger tube.

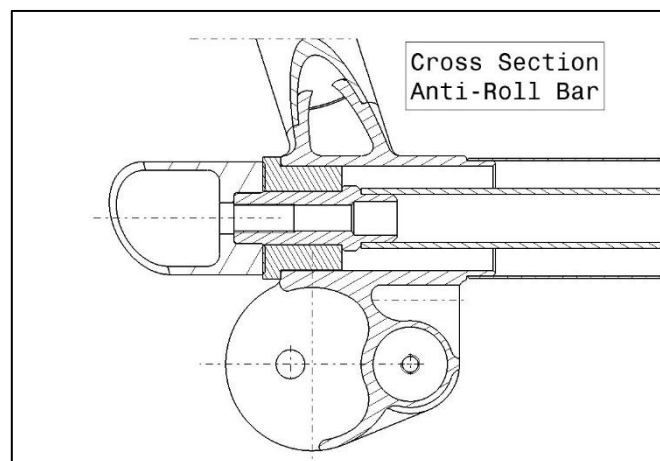


Figure 58. Cross section of the Node-Antiroll Bar mounting.

In conclusion on the Top of the Node is present another cylindrical extrusion that will center with the tube coming from the Top Mount to the UCA Rear Node.



*Figure 59. Finished UCA Rear Node on the Welding Tool.*

In Drawing attached at the end of the document are indicated the main production parameters, starting with the raw material dimensions, 160x120x110mm. The point chosen to be the central reference is the Hardpoint of the UCA Rear pivot, in the middle of the fork, starting from it the surface pairing with the horizontal tube is located with tolerance of  $\pm 0.05\text{mm}$ . The fork has the same tolerances already seen in the other Drawings: the width must be within  $+0.1/+0.2\text{mm}$  in order to maintain an allowance to mount the pivot joint, while the holes have tolerance  $0/+0.05\text{mm}$  on the diameter to keep the UCA Rear Hardpoint on spot. Finally, the 3 cylindrical protrusions  $\varnothing 48\text{mm}$  and  $\varnothing 36\text{mm}$  pairing with the tubes have a tolerance of  $-0.1/-0.2\text{mm}$  as for they counterparts on the previous drawings analyzed, all the other quotes are needed in order to get the geometrical shape requested for the mounting of the frame.

### **3.2.5 Lower Control Arm Front Node**

The Lower Control Arm Node is placed on the lower layer of the Rear Frame towards the Central Cell. In the Front part it has a flanged body with 4 holes in total and a plane surface to couple with the Central Cell itself: two holes are pass-through  $\varnothing 10.2\text{mm}$  and are paired with two threaded holes on the Cell to fix the lower point of the chassis with screws; one hole is designed in the opposite way so that the pass-through hole is on the cell and the Node has a threaded M10 hole; the last hole is threaded M12 and it is made to pair with the screw locking the Pivot joint of the LCA. Hence, on the outer side of the Node there is the interface for the Pivot Joint the usual fork with the sleeve present in all the Control Arm Nodes.

In the Rear area of the Node comes a tube from the other LCA Node, therefore it is repeated in the design the cylindrical extrusion with the collar to weld all together.

On the inside face of the Node must be distinguished an upper and a lower part. The upper part has a protrusion to center the Node with the tube going up towards the UCA Front Node. The lower part



has a more complex shape due to the need to create a conical notch to pair with a bushing welded on a transversal tube. This solution is adapted in order to allow the disassembly of this tube: since the chassis is enveloped around the powertrain it is needed at least one removable transversal tube in order to put it on or off of the vehicle, may it be during the assembly or for maintenance. Finally, in the upper face of the notch there is a threaded hole M10x1.25 to fix the removable tube.

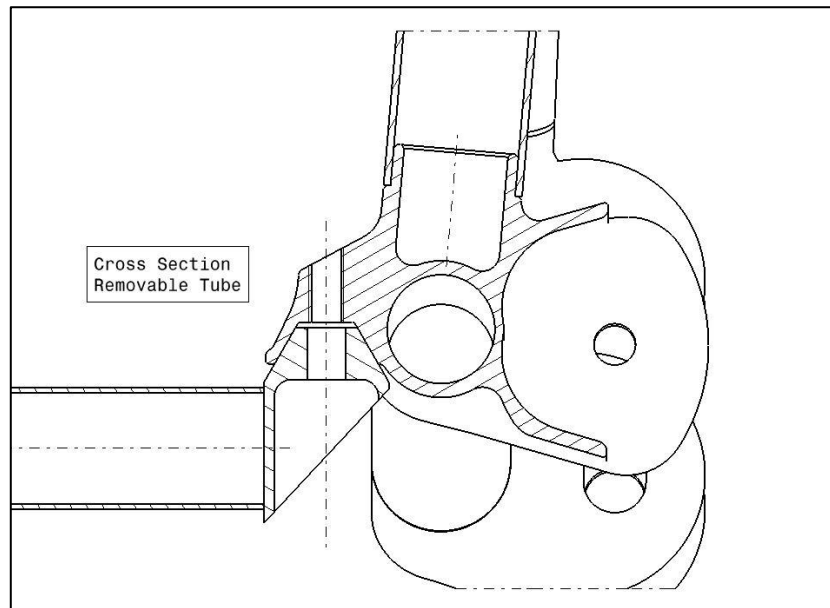


Figure 60. Cross Section of the Removable Tube mounting.

In *Figure 60* can be noticed how the positioning of the bushing on the node is made by means of the conical surface and not the surface on the top of the notch.



Figure 61. Finished LCA Front Node.

The main design parameters of this component are summarized as follow (from Drawing in Annex), starting from the material needed to machine the Node, that is 110x120x160mm. Again, for the main reasons already clarified, are repeated the quotes on the  $\varnothing 36\text{mm}$  (-0.1/-0.2mm) cylinders coupling with tubes of the chassis, the width of the fork (+0.1/+0.2), the passing-through hole (0/+0.05mm) for pairing with the pivot joint and the position of the tube coupling contact surfaces

( $\pm 0.05\text{mm}$ ). Since all the element on the Node are based on inclined axis it is important to define the reference for them, so the slope of the upper protrusion and the centering cone for the removable tube is set with respect to the horizontal axis of the tube linking the two LCA Nodes. Then, considering them on the same plane, the axis of the cone is located relative to the protrusion axis. Even the axis of the hole for the pivot joint is appointed from the horizontal axis and, finally, also the slope of the flange.

### 3.2.6 Lower Control Arm Rear Node

The last node, the Lower Control Arm Rear Node, is the most complex component of all the Rear Frame, due to the several tasks that it must perform. First, in practice the Hardpoints for the LCAr and the ITR are really close to each other, too much to think as a good solution to weld together two different components along with the surrounding tubes: the result would indeed be a weak spot on the Rear Frame considering the rather high number of welding seams that would be needed. Hence, since all the nodes are already obtained by machining from solid, the increase in cost or time due to the complexity of this component will not affect too much the overall production of the vehicle.

Starting the description from the outboard side of the Node the main elements are two forks with similar design to the ones seen previously, two flaps with holes for the screws connected with a “C-shaped” sleeve. In the frontal part is put a cylindrical protrusion to couple with the side of the tube coming from the LCA Front Node, while in the back of the node a conical notch with a threaded hole in the center is carved into a cylindrical extrusion in order to create another point to fix the Rear End, as already seen on the UCA Rear Node. On the top and inner side of the node there another two cylinder hanging out to be welded with respectively the vertical tube going from the node to the UCA Rear Node and the horizontal tube linking the two side of the Rear Frame, in particular the latter will be welded on the mirrored LCA Rear Node. It is important to notice that a design as already depicted would be extremely weak to any kind of bending or torsional moment: for this reason the component must be strengthened with several ribs between the two forks, the main bodies of the node, one on the upper area and 3 on the bottom.

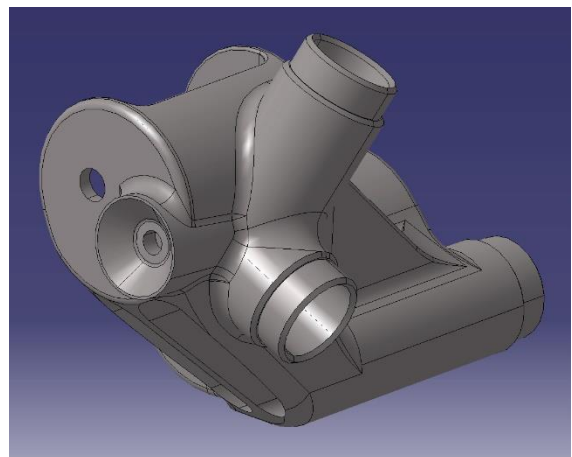
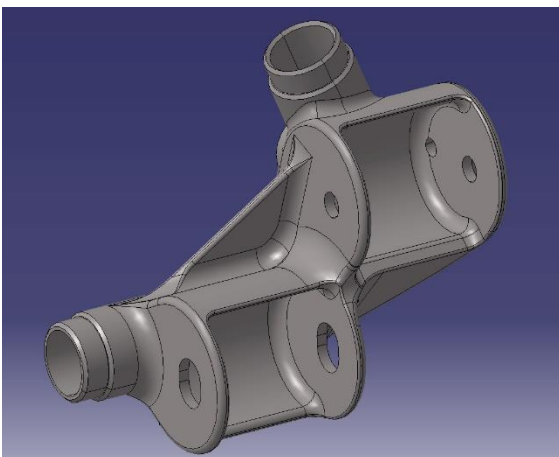


Figure 62. LCA Rear Node in CATIA.



Due to the complexity of the component it is implied that the production process will be based mainly on the 3D CAD file, but in any case a Drawing has been created, and in general are contained this principal parameters: the 3 cylinders coupling with the tubes ( $\varnothing 36$ ,  $-0.1/-0.2$  mm) and the width of the forks ( $+0.1/+0.2$ mm) must guarantee allowance in order to assembly the frame on the welding tool; the position of the collars acting as end stops for the tubes must be within 0.05mm; the position of the pivot axes and the bore of the holes for the pass-through screw must be close to nominal value in order to obtain real Hardpoint close to the ideal ones. In conclusion, the other quotes are aimed to define the inclination of all the elements protruding from the main body of the node with respect to the vertical, horizontal and pivot axes.

### 3.2.7 Tubes

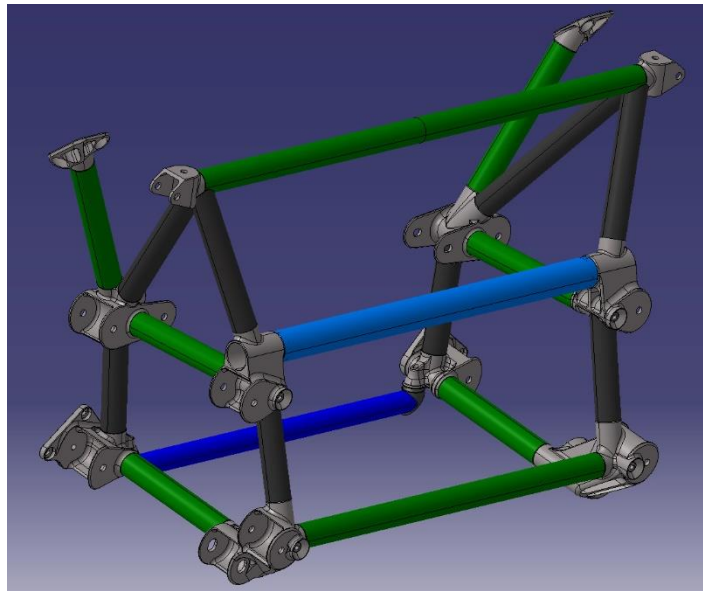


Figure 63. Rear Frame: Nodes and Tubes.

The tubes are the second category of components needed to build the Frame and since the junction points are almost all done by means of the nodes their shape is rather simple with respect to the tubes that usually are employed in other works e.g. a Rollcage.

With reference to the colors in *Figure63* the description of the tubes is in fact quite short:

- Tubes in Green (qty 8): these are tubes with cross section  $\varnothing 40 \times 2$ mm, they present on both ends a straight cut with respect to their axis, so they are the simplest possible type of tube. They are easily obtained by means of a circular saw;
- Tube in Light Blue (qty 1): this tube has cross section of  $\varnothing 50 \times 1$ mm, it also has a straight cut on both ends;
- Tube in Dark Blue (qty 1): this is the removable tube with cross section  $\varnothing 35 \times 1.5$ mm. At both ends it presents a hole if diameter  $\varnothing 36$ mm perpendicular to its axis, since the shape of the cut is a circle it is possible to make it by means of a dedicated machine that works with a roller adjustable in diameter;

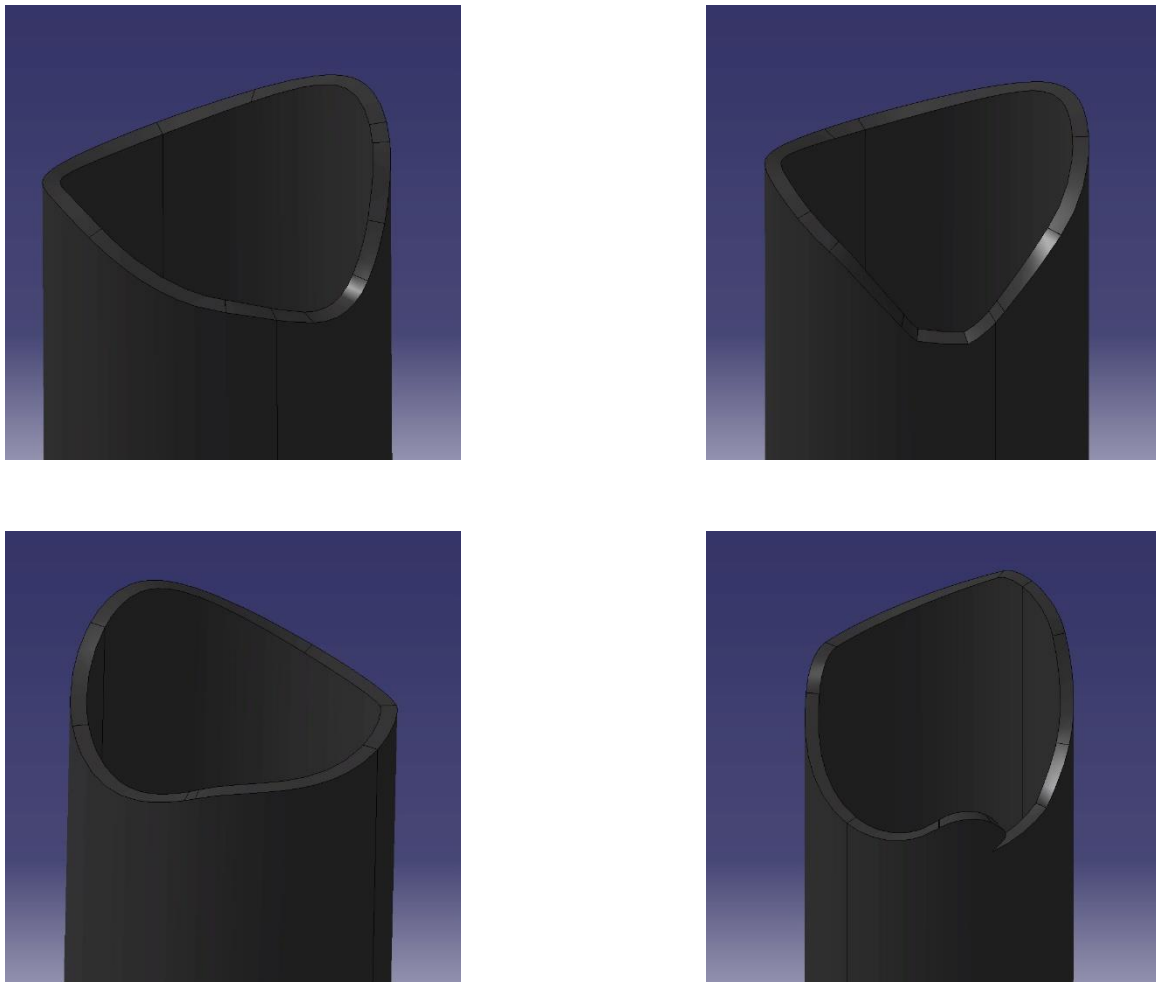


Figure 64. Detail of the Laser Cutting Shapes.

- Tubes in Dark Grey (qty 8): these tubes have a straight cut on one end, pairing with a cylinder on the corresponding node, while on the other end they get a complex shape given by form of the element on which they are going to be welded. Due to complexity of the cut the best solution is to produce them with a Laser Cutting Machine.

Side note: as for the nodes, a part for the transversal tubes the tube on one side of the frame are the mirrored copy of the ones on the other.

### 3.3 Frame Interface Components

The Frame Interface Components are elements added to the frame in order to satisfy all functional requirement as described in Chapter 2. They may divide into 2 categories: the components linking the Chassis to the Devices in the back of the vehicle, the ones connecting the Rear Frame to the Central Cell.

#### 3.3.1 Inverter and DC/DC Converters Interface

The main device to install in the rear motor bay is clearly the Inverter, not only for the task performed but essentially because its position is the one that most affects the Costs or any other issue about the Power Electric System. As already stated from the Inverter to the Motor there are three thick copper wires, one for each phase, that are the most expensive on the vehicle: so the Inverter must be compulsorily close to the Motor, ideally at maximum few tens of centimeters.

Since above the Rear chassis there is plenty of space it is easy to find a good site to install the Inverter and this will be slightly above the transversal tube wrapped around the Anti-Roll Bar, on the left side of the frame. The space available with this configuration allow to place another device alongside to the Inverter, the best idea is to put the second larger component, being the DC/DC Converter working with the higher voltage, 365V.

Considering the interface already existing on the said devices it is possible to place them on the same plane and therefore couple the plane with a thin metal sheet (3mm) with holes corresponding to the ones on the devices. A metal sheet offers several advantages: first it is light weighted, easy to design and produce, moreover it offers the opportunity to add other holes in a second time during the assembly if they are needed.

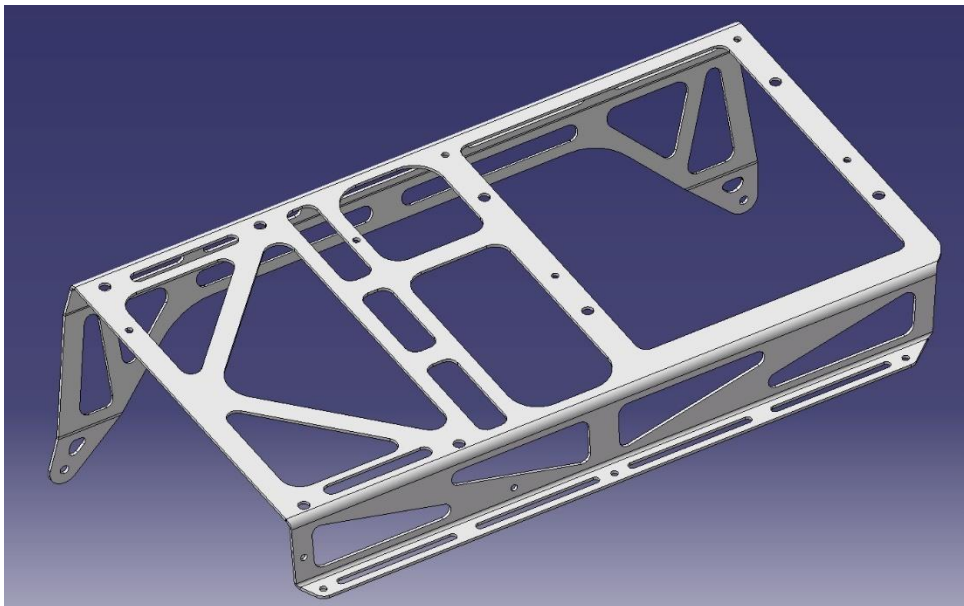


*Figure 65. Shape of the Inverter and DC/DC 365V Converter Support.*

In *Figure65* is seen the shape of the metal sheet: on the top it presents the plane on which the devices are fixed, the holes needed and the cuts to light the weight of the component and to allow

the passage for any kind of wiring needed or the Cooling and Electric Systems. In the Front side it presents to flap that are reaching for the UCA Front Nodes in order to screw the sheet. In the Rear the sheet is bended to form another plane parallel to the Anti-Roll Bar wrap around tube, on which during the assembly are welded 3 bushings with threaded holes to lock the support in position (Figure66).

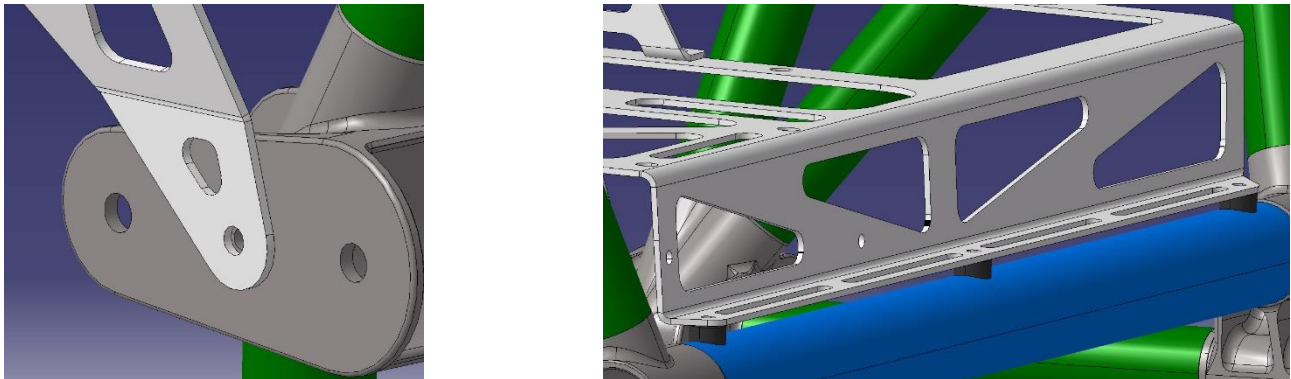


Figure 66. Left: Mounting of the Sheet flaps on the UCA Front Node; Right: Fixing of the Sheet on the Welded Bushings.

The material chosen for the Sheet is aluminum alloy ALU 5754. First, the aluminum is stiff enough to perform the task and moreover the stiffness of the component is increased after the fixing of the devices on it. Then this Aluminum-Magnesium alloy is very versatile: it is possible to bend the metal sheet, unlike for the ALU 6082, it is weldable is ever needed for an unseen necessity and serve the same purpose being soft allowing hand drilling on the assembly site.

ALU 5754		
Density	$\rho$	2.67 kg/dm <sup>3</sup>
Young Modulus	E	70 GPa
Ultimate Tensile Strength	UTS	190 MPa
Yielding Stress	R <sub>P0,2</sub>	80 MPa
Elongation	--	18%
Hardness	HB	20

Table 15. ALU 5754 Mechanical Properties.

Name	Mg	Cu	Zn	Si	Fe	Mn	Cr	Ti	Impurity	Al
ALU 5754	2.60-3.60%	0.1%	0.2%	0.4%	0.4%	0.5%	0.3%	0.15%	0.05-0.15%	Remaining

Table 16. ALU 5754 Chemical Composition.

The production process of the component is really simple, basically the component is developed using a CAD software in order to stretch it on a plane, then the given profile is passed on a Laser Cutting Machine. Once the component is cut it is then bended using as parameters the inner bending radius and the angle of the bend.

The same solution adopted for the Inverter and the first DC/DC Converter is then repeated for the other, due to the same reasons already discussed.

The DC/DC 12V Converter Support is a 3mm metal sheet in ALU 5754 compliant with a plane higher than the one previously seen, with holes corresponding to the ones on the original Converter. On both sides the metal sheet is bended onto to legs that further slit in 4 flaps, on each flap there is a hole made to fix the second metal sheet on the first by means of 4 screws, on the other components the holes are made on the thin ribs of material around the other DC/DC Converter. The central part of the sheet is completely cut away, since the weight to be supported is modest and once the stiffness of the DC/DC case will prevent the sheet from skewing.

On the original configuration there were two different 12V Converters, on the first proposal it was intended to use only one of the two, but it is wise to design the second metal sheet to have anyway two slots in case the choice is changed in future, as in the end has happened. This is to underline the importance of keeping the design of the components open to variation as much as possible, in order to solve issues occurring in late design or assembly with less effort.

Finally, the 12V DC/DC Support is mounted over the Inverter Sheet so that its sides are going down along the 365V DC/DC Converter, leaving the DC/DC Converters one on top of the other.

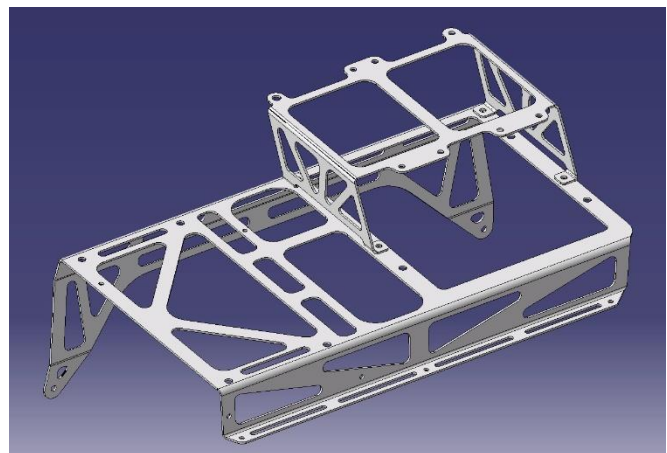
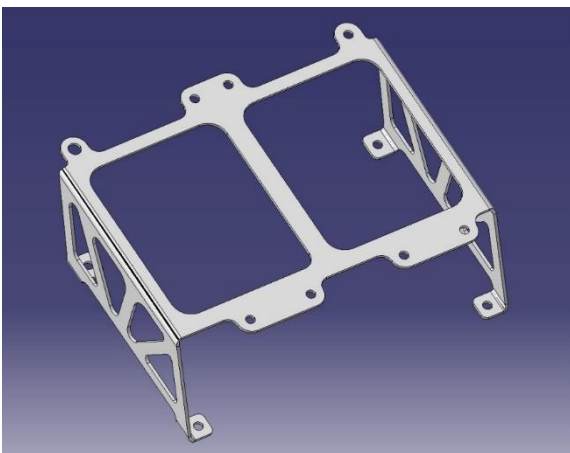


Figure 67 Left: 12V DC/DC Converter Support; Right: Mounting Position.

### 3.3.2 Motor Mounts

In order to install the Powertrain on the vehicle is good idea to consider what it is needed in theory to lock a body in a 3D space: a body would have a total of 6 degrees of freedom and would need 3 different constraints to be fixed in one position.

Said that, the layout of the Powertrain and their interface, i.e. the holes already designed on their cases to mount them, allow to set the constraints as follow: two mounts will be in the front, one on the left or Reducer side and one on the right or Motor side, with the main task to sustain the weight of the Powertrain and to define its position with reference to the chassis; one Mount in the rear, facing the inner side of the reducer, with the main task to prevent the group from swinging and to counteract to the Motor torque.

An important reminder: the design of all the three Mounts is based on the employment of the Universal Joint by *Powerflex* already widely adopted on the vehicle, it is important to recall the main advantage of such a component, being the adoption of a Polyurethane sleeve that separates the coupling bodies dampening the vibrations and recovering any small displacement with its elasticity. Due to the complexity of the Mount they are obviously designed in order to be produced from the solid by milling.

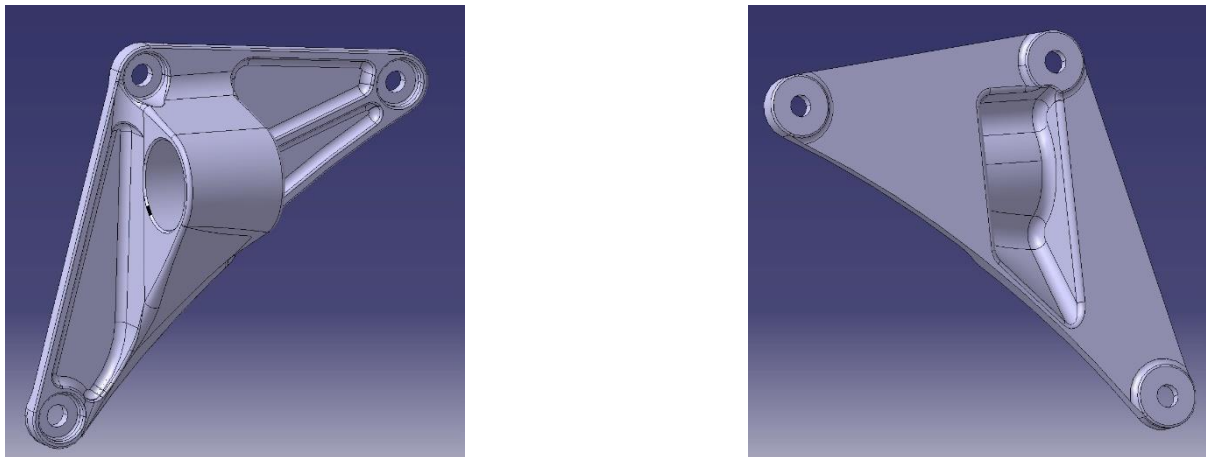


Figure 68. Motor Left Mount in CATIA.

All the 3 Powertrain Mounts are made of Aluminum alloy ALU7075 T6, which properties have already been described by means of the *Tables 9 and 10*, and the choice is mainly due to the Dynamic loads acting between the Chassis and the Powertrain: any Steel alloy would have been an appropriate material, but considering an Aluminum alloy it is requested the best mechanical properties possible, thereby the solution is pointing toward the ALU 7075.

Considering the *Figure68* is possible to start describing the first of the Mounts, the Motor Left Mount. The component is basically formed by two sub-elements: an eyelet with diameter  $\varnothing 43.2\text{mm}$  in which is positioned the *Powerflex* Universal Joint, surrounded by the minimum amount of material needed; a wide flange with 3 counterbored pass-through holes to fix the Mount on the holes already on the Reducer with three M10 screws.



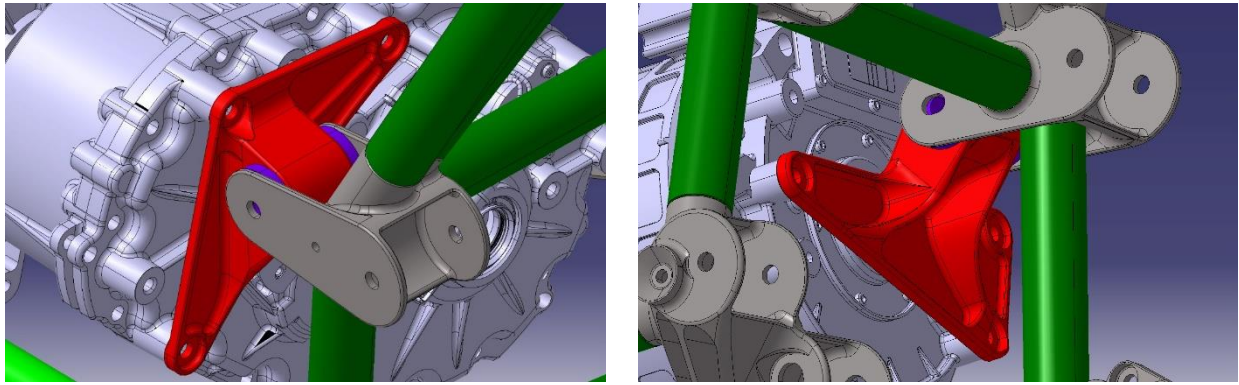


Figure 69. Assembly of the Left and Right Motor Mounts.

The main constraints for the design are clearly the position of the eyelet that must be close to the UCA Front Node, but since the space is quite narrow it might move only by a slight amount; the holes on the Reducer: for simplicity not all the holes are taken into account to build the Mount, those chosen are wide enough to get a fair distribution of the loads under working conditions.

The main production parameters are indicated on the Drawing (Annex) beginning with the raw material dimensions, roughly 75x170x220mm. The narrowest tolerances are put on the distances between the holes, in order to pair them with the holes on the Reducer, and on the distance between the axis of the eyelet and the contact surface between Mount and Reducer. Moreover to guarantee not to bend the Mount once it is screwed the contact surfaces with the Reducer must be within 0.05mm from the reference plane. The missing quotes are all defining the component in its geometry or indicating the bore of the holes (2 x  $\varnothing 11\text{mm}$  and 1 x  $\varnothing 10.5\text{mm}$ ) and the counterbore on the flange ( $\varnothing 23\text{mm}$ ) and the bore to install the Universal Joint  $\varnothing 43.2$ .

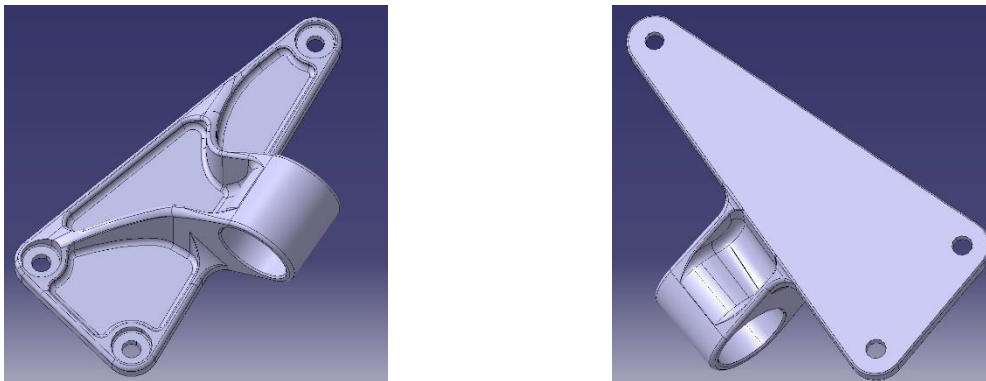


Figure 70. Motor Right Mount in CATIA.

The Motor Right Mount is designed with exactly the same guidelines of the Left one (Figure 69), it is formed by two parts: one flange with counterbored pass-through holes on the Motor side, with the holes matching with those already on the motor, in such a way that they are as wide as possible to distribute the loads in optimal way; an eyelet made to fix the Universal Joint in position to be coupled with its seat in the corresponding Node on the Frame. The two main parts are linked by means of 2 ribs of material that increase the overall stiffness of the component (Figure 70).

Concerning the Drawing for the production the main quotes are those defining the volume of material needed, being 235x135x90mm, the ones setting the position of the eyelet with respect to the flange plane and the one positioning the holes on the flange. The more strict tolerances are put on the plane of the flange, that must stay within 0.05 mm to its reference, that along with small tolerances on the holes distance guarantees correct coupling of the component; moreover narrow tolerances are needed on the bore (+0.2mm) and on the width (-0.1/-0.2mm) of the eyelet in order to fit it into its seat in the Frame Node.

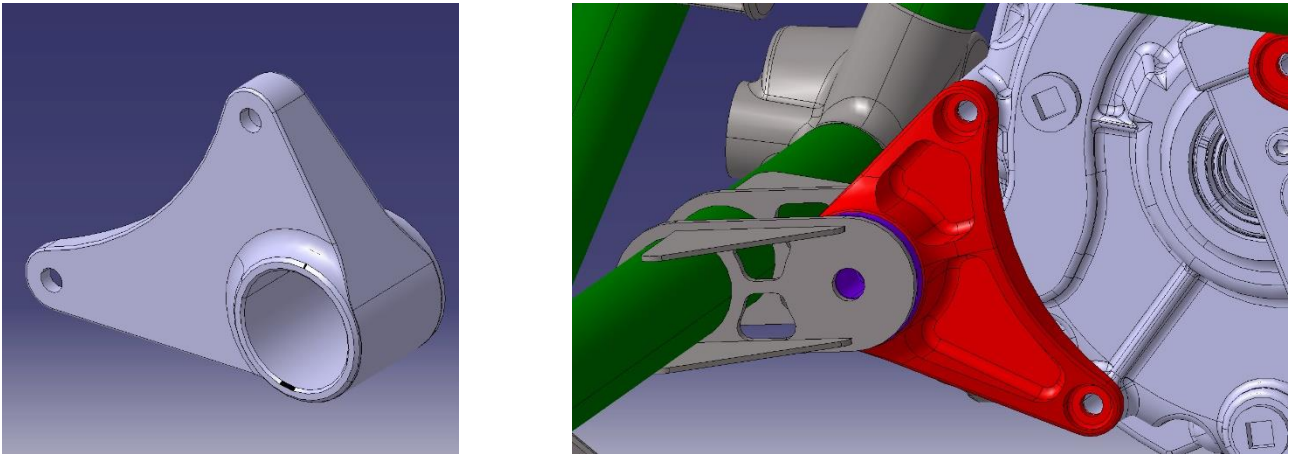


Figure 71. Left: Motor Rear Mount; Right: Fixed Motor Rear Mount.

The Motor Rear Mount is the third and last required constraint to lock the Motor and Reducer Group on the Rear Frame, as already mentioned its main role is to counteract the Torque provided by the Motor. In order to do so the Rear Mount is placed in the opposite longitudinal position with respect to the other two Mounts, and in such a way that the distance between them is as large as possible: this distance is the arm related to the Torque to be sustained by the Frame, the bigger the arm the smaller the Forces transmitted to the Frame.

The shape is rather simple: one flat surface to be coupled on the inner side of the Reducer, by means of two already existing threaded holes, plus an eyelet to house the *Powerflex* joint. The volume obtained is then notched in order to reduce the weight, leaving three ribs of material to keep the component stiff.

In *Figure 71 (Right)* is shown the coupling between the Mount and the Frame, since it is a simple solution in fact it can't be considered as a proper component, so it is described here. The Mount is kept in position by 2 metal sheets in Steel 25CD4 placed on the sides of the eyelet, on the sheet there are 2 main holes: one to allow the fastening of the Joint with a Bolt M12, one to mount the sheets on the lower transversal tube of the Rear Frame. Then other holes are made to reduce the weight and other 4 triangular metal sheets are to be welded in order to increase the stiffness and therefore the strength of the Mount seat.

The raw material needed for this part is roughly 135x105x55mm, and as for the other Mounts the main tolerances regards the flat surface, the eyelet and the holes center distances.



### 3.3.3 Central Cell Interface

As already discussed and shown in *Figure 48* there are 3 points (per side, 6 in total) chosen to link the Rear Frame to the Central Cell: one near the Top Mount of the Suspension, two in the front side of the Rear Frame, one on the top and one at the bottom.

It is not possible to take into account to weld the Rear Frame with the Cell, in fact they are made of two different materials, therefore one of the best solutions is to create an intermediate component between the 2 parts of the Chassis, specifically one for each point defined earlier. These parts will be made by milling from solid, the material chosen is Aluminum alloy, AL6082: this alloy is good for welding and has good mechanical properties being Aluminum, slightly better than other alloys such as ALU 5083.

The choice of the material comes from the decision to weld the interface components on the Central Cell, which is in Aluminum boxed tubes usually made of Aluminum alloy of the Series 6000, then fasten the Rear Frame on the Interface Components by means of screws.

ALU 6082		
Density	$\rho$	2.71 kg/dm <sup>3</sup>
Young Modulus	E	70 GPa
Ultimate Tensile Strength	UTS	295 MPa
Yielding Stress	R <sub>p0,2</sub>	240 MPa
Elongation	--	7%
Hardness	HB	90

Table 17. ALU 6082 Mechanical Properties.

Name	Mg	Cu	Zn	Si	Fe	Mn	Cr	Ti	Impurity	Al
ALU 6082	0.6-1.2%	0.1%	0.2%	0.7-1.3%	0.5%	0.4-1%	0.25%	0.1%	0.05-0.15%	Remaining

Table 18. ALU 6082 Chemical Composition.

The first Interface component is placed at the Top Mount Node of the Rear Frame, it is the simpler between the 3: it is basically just a bushing made on Lathe with main diameter  $\varnothing 44$ mm and a collar  $\varnothing 48$ mm at the lower end, with total length of 73mm. The bushing has a pass-through hole  $\varnothing 10$ mm, that on the side coupling with the Frame has a Thread M14x1.5 used as seat for an Insert *Keensert* KNM10x1.5\_IN.

The *Keensert* is a type of insert which consist in a bushing with thread on both inner and outer sides, made of steel. It is employed in order to fix a screw which is made of hard steel with a component made of Aluminum or Plastics, that won't be a good choice given the difference in Hardness of the two materials. The Insert is mounted in the component through the outer thread and it presents 4 protrusions (Kees) that are hammered into the thread made of soft material and locks the insert into the hole of the component.

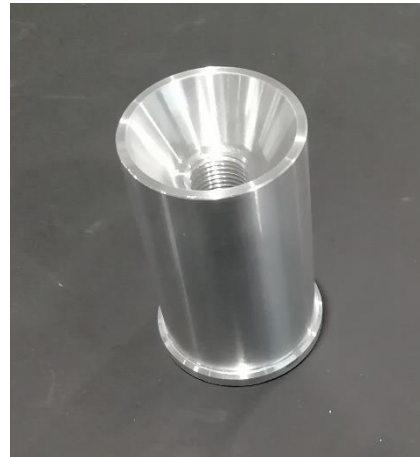
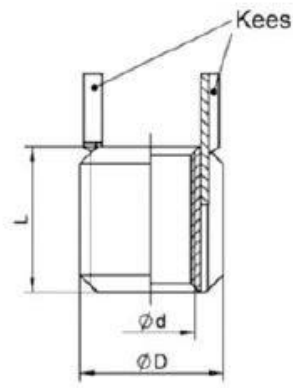


Figure 72. Left: Keensert Cross Section; Right: Top Mount Welded Cell Mount.

Since the Mount is simple there are not strict production parameters to comply with, but it can be noted that also the other end of the pass-through hole is threaded M16x1.5 and it presents a conical surface as those employed to coupling in other components: since the Top of this part will face the inner side of the Rear Engine bay it is wise to design the part in this way so that the surface and the thread can be exploited in case of need during the assembly of the vehicle.

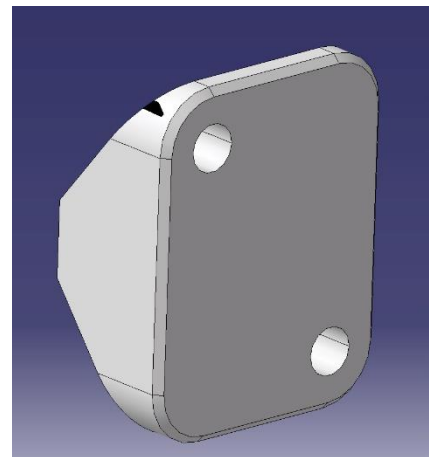
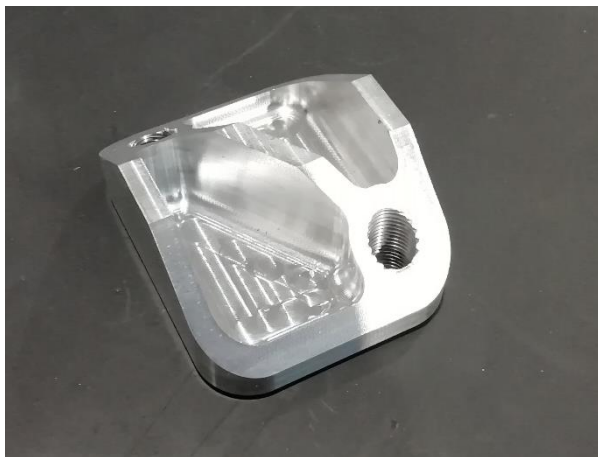


Figure 73. Higher Welded Cell Mount.

The next Interface Component is the Higher Cell Mount (*Figure73*) another simple part obtained by milling: it is formed by a flat surface that will couple with the corresponding Node of the Frame and another 2 slanted surfaces that are following the shape of the Central Cell at interface point. On the front of the part are bored two threaded holes M14x1.5 to seat the *Keensert* and on the rear the solid is notched to reduce the weight where material is not needed. In order to have a better welding of the component a chamfer 2mmx45° is added on the front surface.

The raw material for this part must have a volume of at least 90x70x40mm and the smallest tolerances are put on the holes centers distances and on the flat surface to secure correct coupling with the Frame Node at interface.

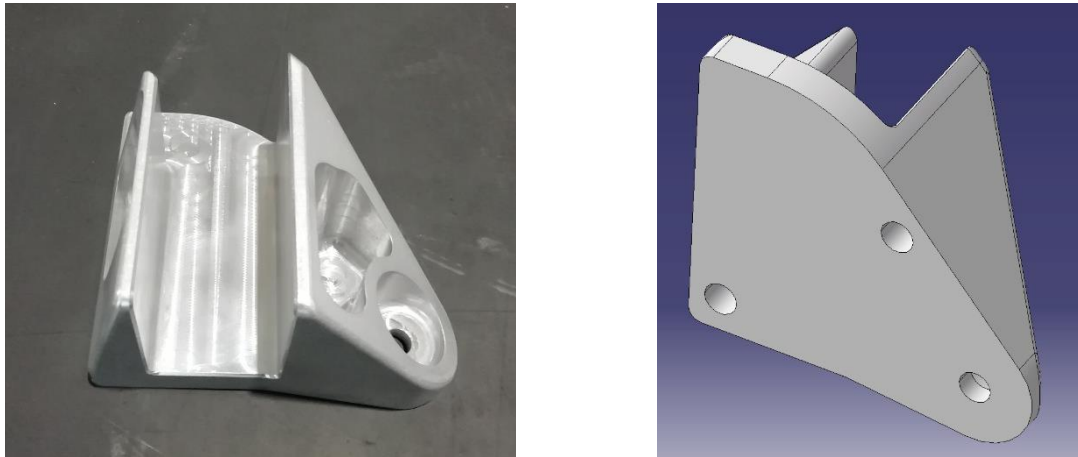


Figure 74. Lower Welded Cell Mount.

The last of the interface components is represented in *Figure 74*, it is designed starting from a flat surface coupling with the corresponding Node on the Frame, on which are bored 3 pass-through holes: 2 are threaded holes M14x1.5 to seat an insert, the other is a  $\varnothing 10.5\text{mm}$  hole made to allow a third screw to work. On the other side the Part is modelled around an existing part of the Chassis, so it is a full volume with a square section notch passing through it, on top of that there is still material enough so a cut is added to reduce weight.

In order to produce the component the milling starts from a raw material of 135x125x75mm, as for the other components the important tolerances to meet are on the flat surface and on the holes positions.



## 4. CHAPTER 4 – PRODUCTION PROCESS

### 4.1 Welding

#### 4.1.1 TIG Welding

Welding is a production process that consist in joining two or more different components in a continuous and permanent way by using a huge heat transfer to cause the local fusion of the material. Considering a general scheme of two welded components (*Figure75*) it is possible to define: the pieces of Base Material (*lembo*), the Chamfer on the interface between the two pieces (*cianfrino*), the Heat Affected Zone (*ZTA*) and the Welding Seam.

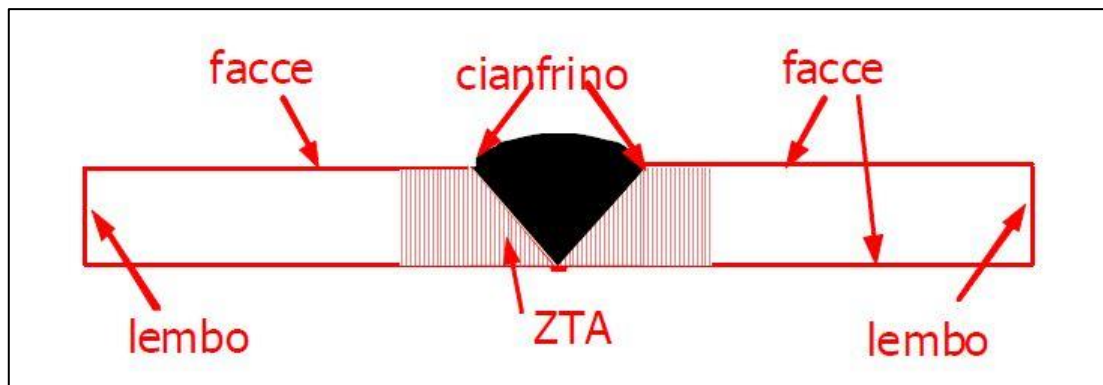


Figure 75. Welding Scheme.

The welding seam is a key element of the welding since it is formed by the base and the additional material cooled down after the fusion, the quality of the welding depends on the Seam that must have mechanical properties as close as possible to the base material and must not include slags, debris or holes. Around the seam it is defined the Heat Affected Zone, that is another important element to focus on: during the process due to the high heat flow all the material involved undergoes expansion or in any case distortion, the distortion stands and might be amplified during the cooling down, therefore it might introduce residual tensions and error in the geometry.

In L.M. Gianetti workshop is possible to perform 3 different types of welding: MIG (Metal Inert Gas) for Steel, TIG (Tungsten Inert Gas) for Steel and Aluminum and TIG for Titanium. When it is needed to weld a frame for automotive application, a front or rear frame as the case in this Thesis, a Rollcage or a Crossmember, the only method taken into account is the Tungsten Inert Gas Welding, or TIG.

TIG Welding (*Figure76*) is a method of welding that exploits the Heat generate by an Electric Arc between the Welding Torch and the Component. In this particular case of Arc Welding the Electrode in the Torch does not undergo fusion and the arc is surrounded by an inert gas, Argon. The main advantages in adopting TIG Welding can be summarized as follow:

- The Welding Beam is clean: after the operation it is not needed additional cleaning actions;
- Very small Heat Affected Zone;
- The fused material is not projected around causing defects;
- It is possible to perform the welding in every position;

- Presence of slag in the Beam is dramatically reduced;
- TIG can weld a wide range of materials: Steel, Aluminum, Magnesium, Titanium.

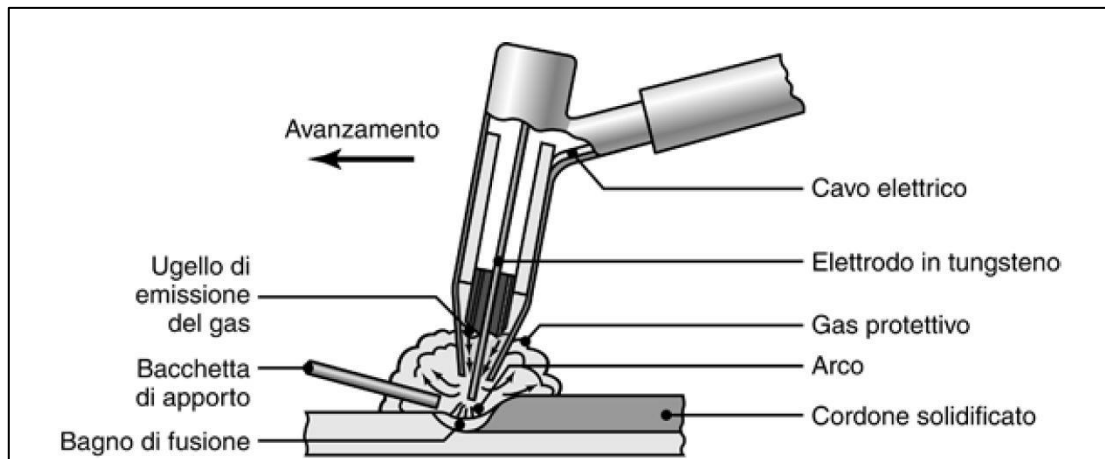


Figure 76. TIG Welding Scheme.

The main drawback of the TIG Welding is the overall cost: cost of the Tools, the Tungsten Electrode and the Inert Gas supply. On top of that it requires a high trained operator to be performed: the Electrode must be kept close to the parts, at few millimeters, but it must never touch the materials to be welded; the additional material in form of a thin bar must be kept under the arc and the gas flow and it must be provided manually, at least in manual operations.

The result is that the TIG Welding guarantees a high level of quality, but it comes with high costs and it is slower than the other Welding methods. As a general rule it can be assumed that the Penetration of the Welding is proportional to the Current passing through the Torch and inverse proportional to the Speed at which the Welding is performed.

Additional consideration must be made about the material to be welded, in this case Steel Alloy 25CD4, which is a low carbon low alloy steel. Therefore it comes that the choice of Argon as inert gas is good and the last element to be decided is the Additional Material. Due to the nature of the 25CD4 it is not possible to use common TIG Bars, with code *SG1*, usually adopted for Structural Steel which is really low alloyed and mainly with Manganese. Neither it is possible to employ *TIG Bars 316L* that contains Chromium as the 25CD4 but are used in case of Stainless Steel which has a really high content of Chromium. The best solution is to choose dedicated TIG Bars contain both Chromium and Molybdenum and therefore are as close as possible to the 25CD4 itself. A good example of TIG Bars that can be used are the *TIG CrMo1*, which have roughly the same amount of Cr and Mo of the 25CD4 and satisfactory mechanical properties.

TIG CrMo1		
Ultimate Tensile Strength	UTS	580 MPa
Yielding Stress	R <sub>p0,2</sub>	470 MPa
Elongation	--	23%

Table 19. TIG CrMo1 Mechanical Properties.

Name	C	Mn	Si	Mo	Cr	Impurity
TIG CrMo1	0.08%	0.6%	0.6%	0.5%	1.3%	0.5%

Table 20. TIG CrMo1 Chemical Composition.

In order to define all the parameters needed for the Welding Process it is of interest evaluate the weldability of the material in analysis. This can be done computing the *Equivalent Carbon* Content: each alloyed metal is scaled with a parameter and summed to the percentage Carbon content, the Equivalent Carbon is obtained by means of a formula given by manuals and its value is then compared to a Table in order to define the Weldability. Afterwards always by means of Tables is possible to decide the pre-heat temperature and cool down time if required.

The 25CD4 Chemical Composition has already been declared in Table14, then it is possible to compute Equivalent Carbon as:

$$C_{eq} = C + \frac{Mn}{6} + \frac{Cr+Mo+V}{5} + \frac{Ni+Cu}{15} = 0.74$$

Considering a maximum content for each element: C=0.29, Mn=0.9, Cr=1.2, Mo=0.3. Finally, the Equivalent Carbon is in fact high, the tables would suggest to pre-heat before welding, referring to a mean value of thickness of 20mm. In the case in analysis, as for the most seen in L.M. Gianetti the thickness of the components to weld is usually less than 1/10 of this value, therefore the welding is performed without pre-heating and the results obtained are in any case compliant with the quality requirements.

#### 4.1.2 Defects Detection

The welding process is not perfect for several reasons: the Heat is transferred locally to the piece, then it raises a difference of Temperature on the component that is unavoidably deformed; the main task of the Heat Transfer is to induce the melting of the Additional and Base Material, therefore the Microstructure of the materials at the end of the process will be must different from initial conditions, moreover, the change of the material phase is sudden so it will be easy to found any kind of defect into the Welding Seam. Finally, the creation of the Welding Seam itself will lead to a sensible contraction of the component that is not negligible and must be involved in the Design Process.

The main defects occurring in Welding Process may be:

- *Pores*: they are basically inclusion of gases, possibly steam coming from air or materials, or Argon from the arc, that leaves one or several holes into the Bead. Due to pores it is not possible to assure the expected Mechanical properties, the Bead will be weak.
- *Slags*: the inclusion of slags coming from the Base or the Additional Material has an effect similar to the pores, the chemical composition and microstructure of the Bead is altered and so are the Mechanical properties.



- *Incomplete Fusion*: if the Welding is too fast or the Current not high enough the Base material will not undergo fusion and the Bead will be incomplete, therefore the junction is not formed, the component will easily break.
- *Cracks*: they are a dangerous defect since it may be caused by a large group of factors, they may happen at high or low Temperature, due to arc interruption. They may form in all the materials involved in the Welding, not only in the Bead and moreover they could be interior and not detectable at first sight.
- *Residual Stress*: even if it may not create a fracture residual stress is harmful for the life of the components, therefore in some cases it is appropriate to perform additional operation before and after the Welding, usually pre-heat and slow cool down.

Identify defects is a key element of the Production since it allows to set the right Welding Parameters, to detect failed components and repair them is possible or otherwise exclude them from the process. At L.M. Gianetti Plant is not possible to perform in-depth tests capable of revealing defects in Welding, but when explicitly requested by the customers the tests are performed by external suppliers, therefore it is a service not directly offered but easily performed on demand. The 3 main tests are *Dye Penetrant Inspection*, *Industrial Radiography* and *Industrial Computed Tomography*.

*Nota bene*: for the Chassis currently under analysis in this Thesis the customer, i.e. *GFG Style by Giorgetto and Fabrizio Giugiaro*, has not requested any of this Test, therefore they have not been conducted. I personally consider important to address how this Tests are performed and what kind of result they lead to, at least at a very basic level, because they are in any case related to my experience in L.M. Gianetti since they have been performed on different Projects assigned by other Customers.

Briefly, the Dye Penetrant Inspection (*Figure 77*) is a Test performed on welded component that has the aim to detect any crack in the welding bead. First (2), a specific fluid is sprayed on the Chassis and by means of capillary action it penetrates in cracks or cavities. The excess of liquid is cleaned off (3) and a second liquid is sprayed on the Chassis (4): it has the property to change color while reacting with the first liquid sprayed, therefore it is possible to see by eye or using a visible light or UV lamp the flow of liquid coming off the crevices or crack, if any of them are present. The main advantage of this test is to be non-destructive, easy to be performed almost everywhere and relatively low cost, the main drawbacks are that the test can only be performed on non-porous materials and can detect only surface defect. Moreover the shape of the welding bead may require a highly trained operator in order to evaluate the result of the test.

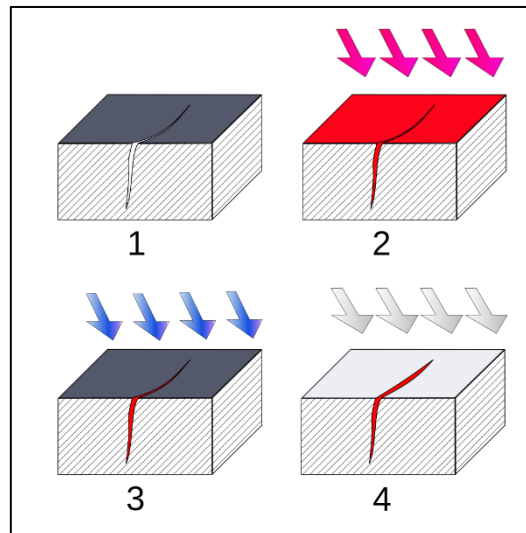


Figure 77. Dye Penetrant Inspection test phases.

#### 4.1.3 Industrial Radiography

The Industrial Radiography is non-destructive test performed on welded components exploiting X-Rays technology such the one employed in medical applications. The sample is put into a dedicated machine capable of generating X-Rays and it is then crossed by the ray. Usually under the sample, in the machine, is put a detector which can be made of several materials (Silver halide, Phosphor) that is able to capture the negative of the projection of the sample, highlighting the difference in density between air and the sample.

The Test consists on the creation of 3 Images relative to different cross sections of the sample, each at 120° from the other, so the welding can be analyzed in such sections.

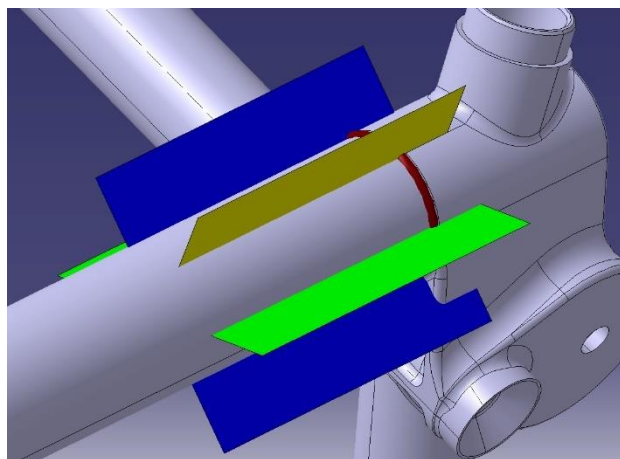


Figure 78. Scheme of the Industrial Radiography.

Looking at *Figure 78* is possible to understand which sections of the sample are considered, being the Welding Bead in Red and the 3 planes of the cross sections in Green, Blue and Yellow. After that the Radiography is completed the images are available to be analyzed in search for pores, crevices, incomplete Bead or cracks. Will now follow a series of Images aimed to describe possible results of the test.

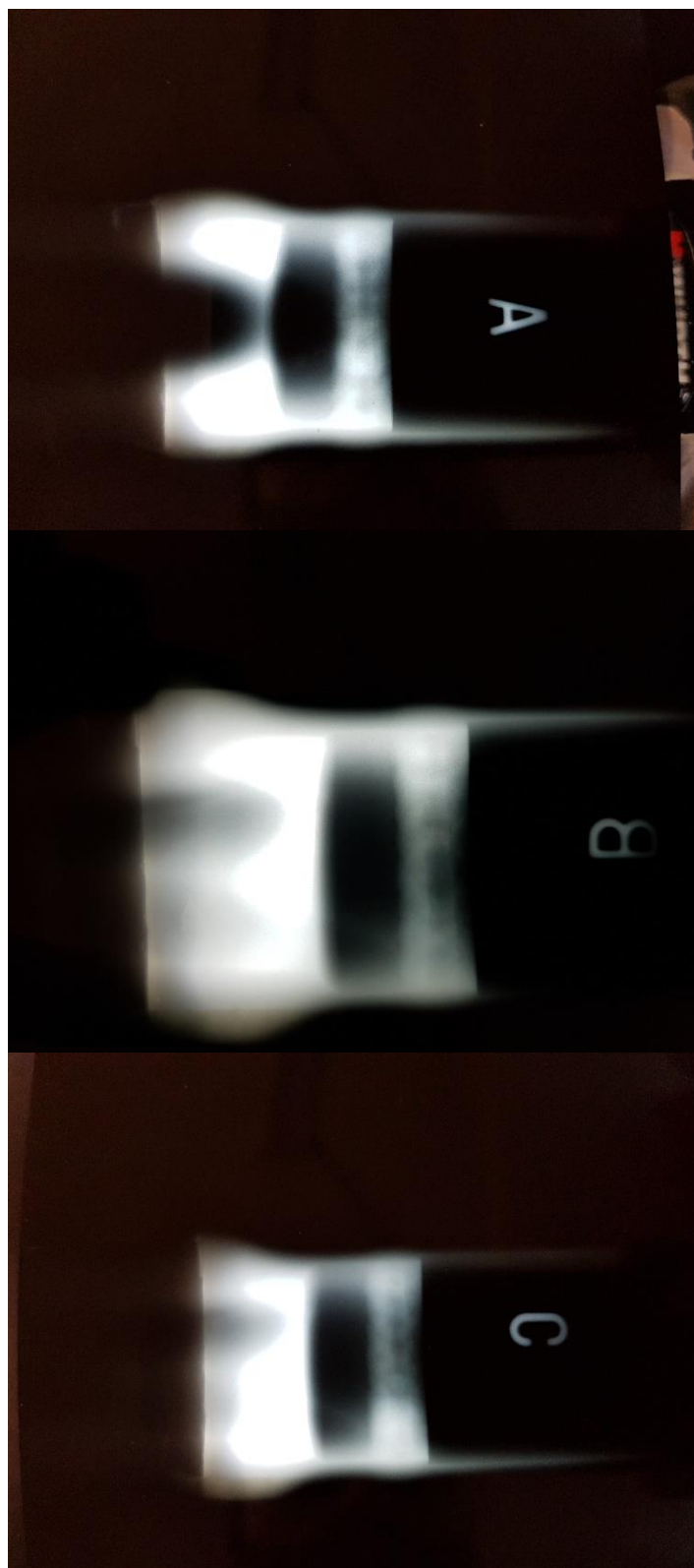


Figure 79. Industrial Radiography: Sample OK.

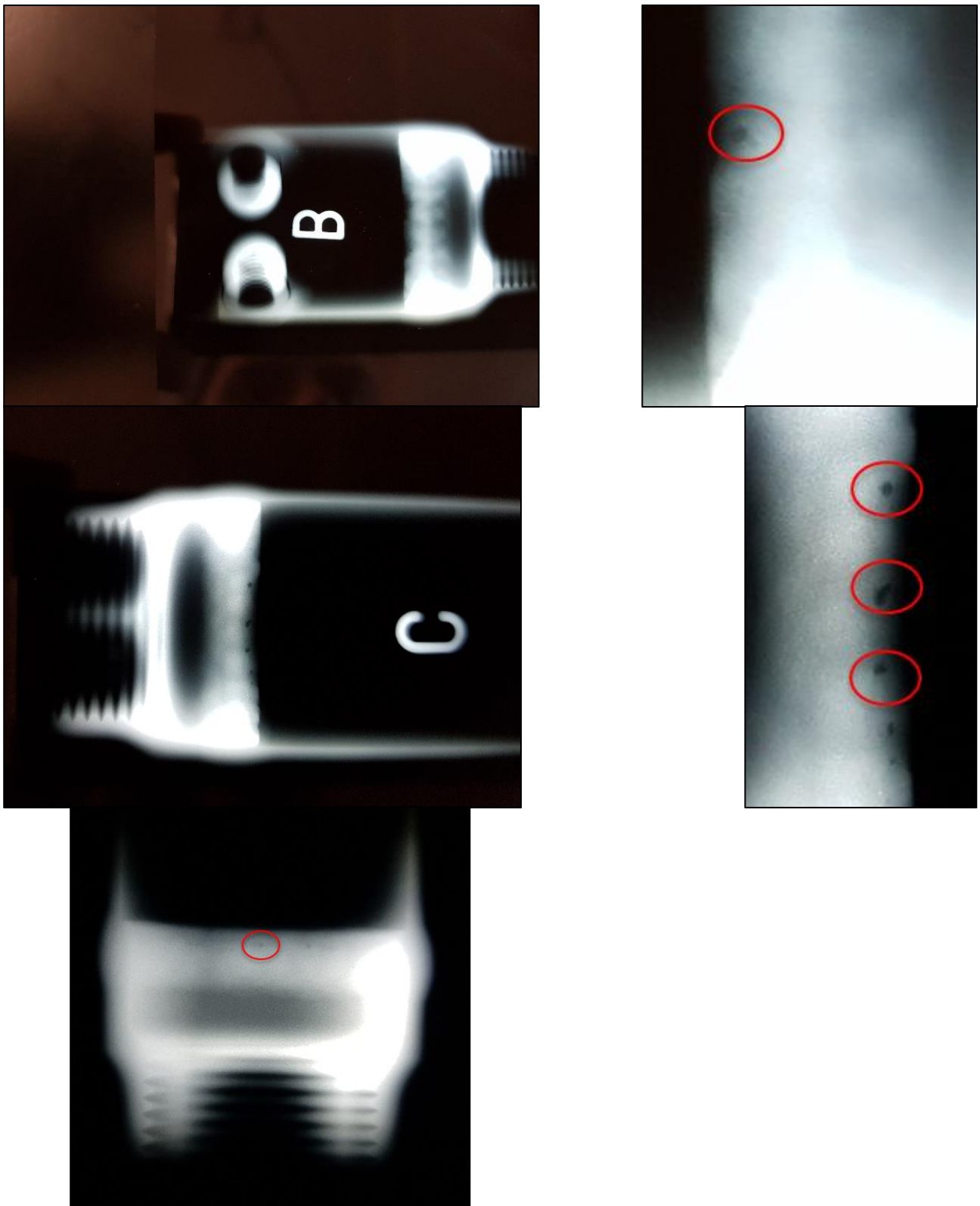


Figure 80. Industrial Radiography: Different Sample with Defects.

Considering *Figure79* is possible to observe 3 Section of a Sample without any major defect, the Welding Bead is in fact one full piece and at the sides there not significant porosities or cracks. In the following *Figure80* are reported examples of defects coming from different samples, in the Top

Images is illustrated a Porosity evaluated of roughly 0.4mm, in the middle the value is about 0.6mm and in the Bottom Image it is smaller, 0.2mm. All 3 the samples have been declared *Acceptable* therefore the components have not been rejected, mainly because not only they are small in size but they are also concentrate on the outer side of the Bead, the core is solid as it should be and the Mechanical Properties of the part are as expected.

#### 4.1.4 Industrial Computed Tomography

A further application of the Industrial Radiography technology is the Industrial Computed Tomography. Also for this test X-Rays are exploited but the scan is aided with a computer that with the rays is capable of defining a 3-dimensional representation of the exterior and especially of the interior of the sample.

The 3D Representation can be evaluated after the scan in search for any kind of defect, in particular internal cracks, inclusions and porosities. Will now follow some examples of Industrial Computed Tomography. Starting with *Figure81*, which is an example of a welding without major defects.

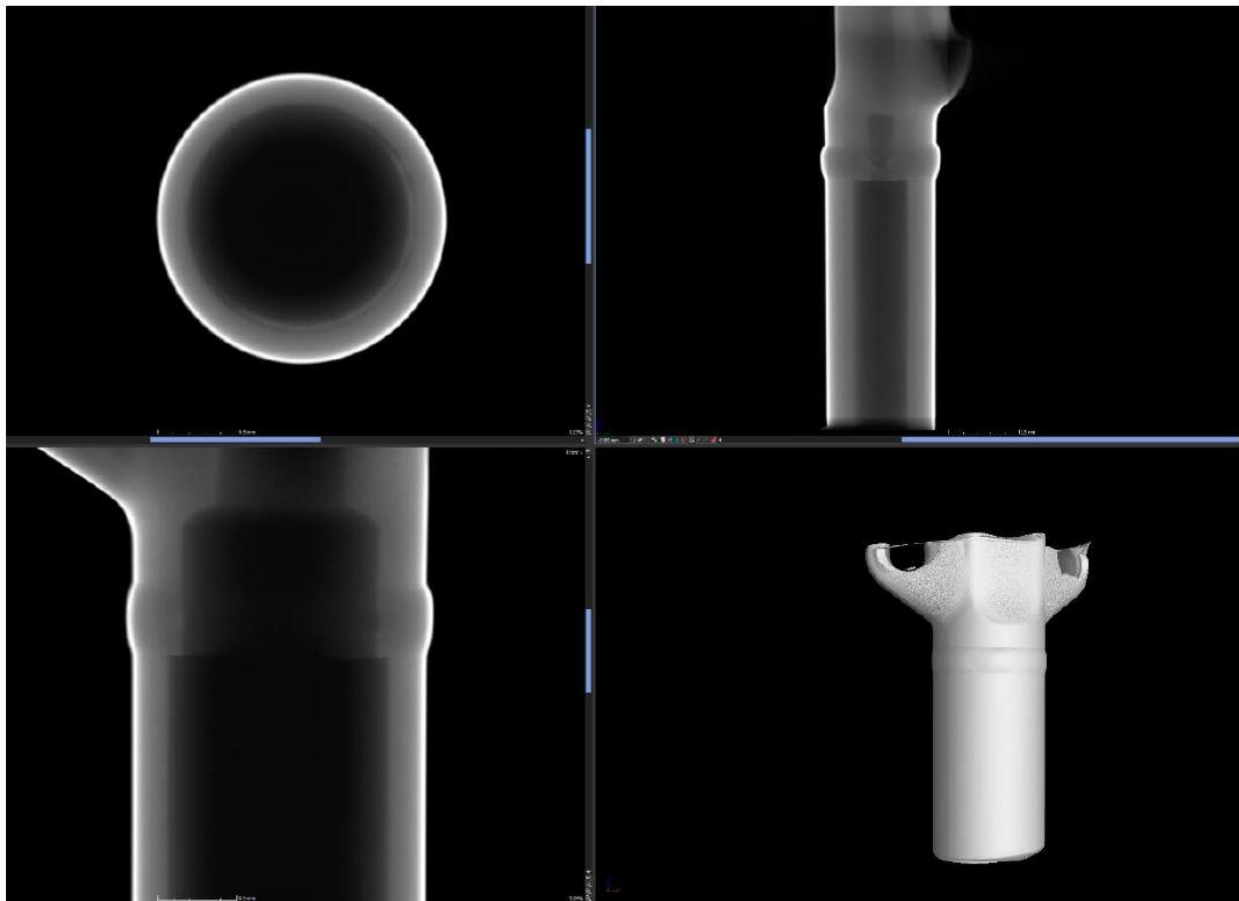


Figure 81. Tomography, Sample 1, Welding 1.

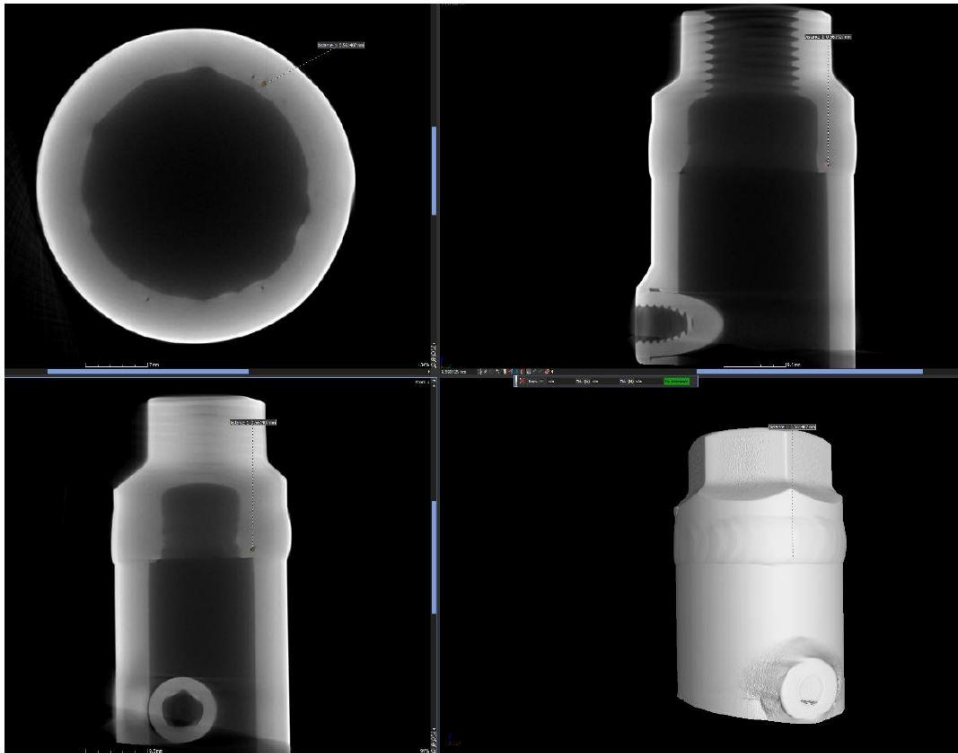


Figure 82. Tomography: Sample 1, Welding 2.

Figure82 represents a welding with an outlined porosity of roughly 0.33mm.



Figure 83. Tomography: Sample 2, Welding 1.

Figure83 represents a welding with poor quality, highlighting some inclusions with size 1.3mm.

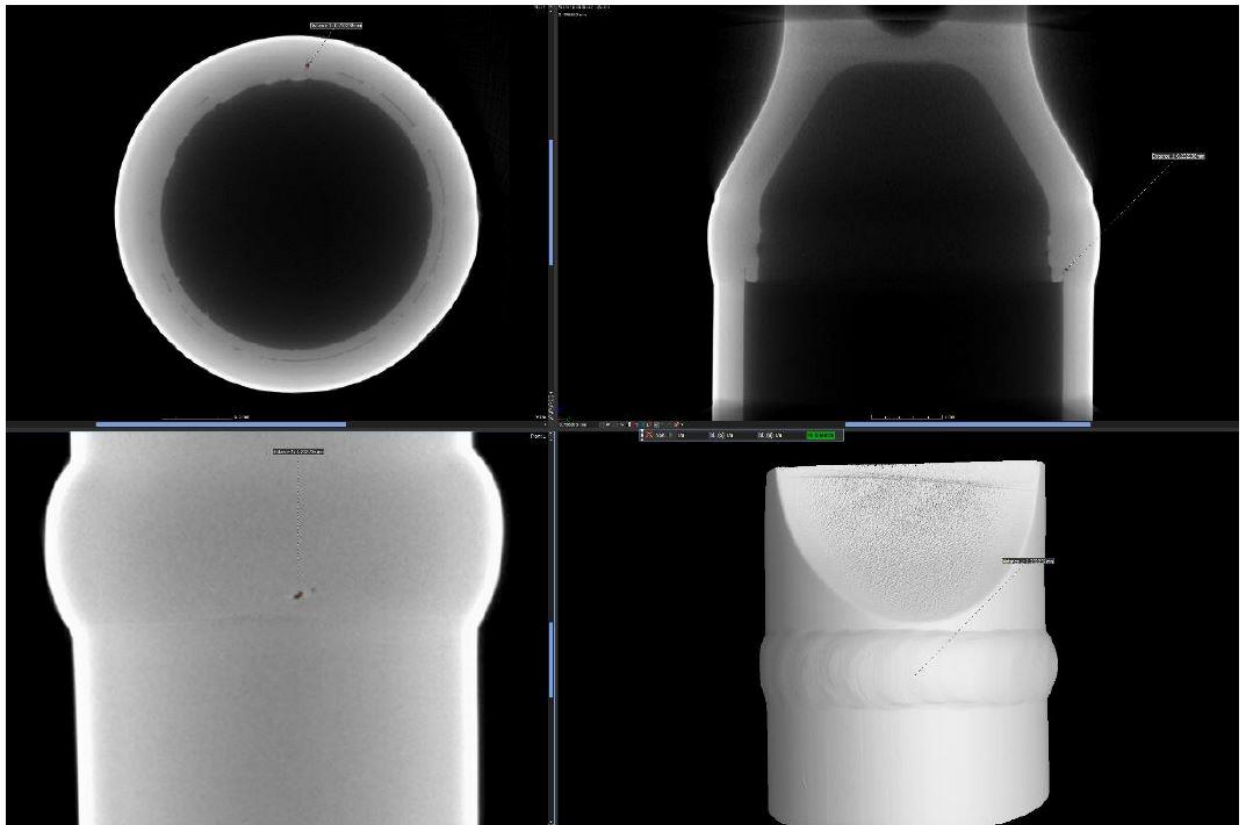


Figure 84. Tomography: Sample 2, Welding 2.

Figure 84 represents a sample with a single porosity of size 0.23mm.

In conclusion, the Tomography is a deep analysis tool that gives a response about the overall quality of the Welding, it has high costs therefore must be completed only if explicitly requested and needed. For a quick response about the Welding it may be employed a Dye Penetrant Inspection that allows to recover from a gross mistake in setting the Welding Parameters, while for addressing problems within the Welding Bead at least an Industrial Radiography Test must be performed.



## 4.2 Welding Tools

Even if a Welding is free from major defects there are still issues to be resolved. In fact any Welding will imply a macro distortion/deformation of the component, in particular the Part will result contracted due to the nature of the Process, involving high Heat transfer, melting and solidification of the material. If a dedicated solution is not taken into account the final component will result shorter with respect to the expected dimensions or distorted if it is of a more complex geometry. In the field of Engineering there are companies selling Software capable of predicting the shrinkage of the components, but they may not be the best solution to the problem, the main issues are that they still have a certain amount of error on the computed shrinkage and they are expensive for small companies. The best idea is to deal with the problem with the experience of the personnel, along with the fact that before starting with the serial production of component is possible to build several pre-production prototypes, allowing to set all the needed parameters and production steps. For the Chassis under analysis, that is a *One-off* prototype there is not the possibility for a pre-production prototypes therefore the interaction between the Design Process and the personnel experience is even higher.

When dealing with the shrinkage of the welded component the best solution to keep the Parts within tolerance is to build a dedicated Welding Tool around the component and only then perform the welding. The main purposes of the Welding tool are: keep all the components in position during the process, provide additional stiffness to the structure in order to resist to the tension that leads to the shrinkage and allows to verify if all the parts are assembling correctly before the operation.

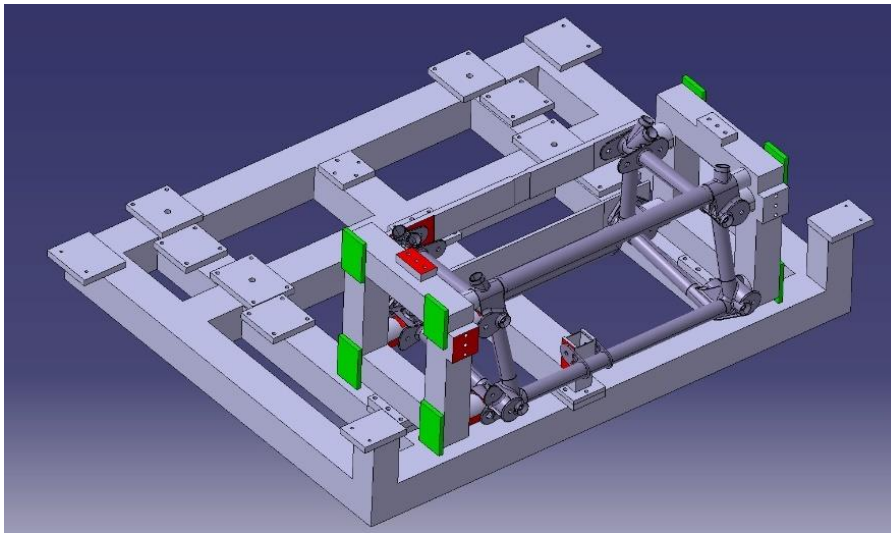


Figure 85. Overview of the Welding Tools.

The welding tool for the Rear Frame may appear complex: this is due to the fact that it is formed by a base and a dedicated tool for each of the Frame present in the vehicle, therefore one for the Front Frame and one for the Rear Frame, only the latter will be described.

The main characteristics required for a welding tool are that it must be cheap, stiff, weldable and possibly light. The first choice for the material is always Steel, it absolutely should not be alloyed

and with small Carbon Content, even if in some application also aluminum can be considered, but not for a Frame as large as the one involved. The steel chosen is almost always construction steel S235 a steel low in Carbon and considerable content of Manganese.

Steel S235		
Density	$\rho$	7.8 kg/dm <sup>3</sup>
Young Modulus	E	210 GPa
Ultimate Tensile Strength	UTS	380-670 MPa
Yielding Stress	R <sub>P0,2</sub>	235 MPa
Elongation	--	10%
Hardness	HB	110-200

Table 21. S235 Mechanical Properties.

Name	C	Mn	Cu	P	S	N	Impurity	Fe
Steel S235	0.19%	1.5%	0.4%	0.03-0.04%	0.03-0.04%	0.01%	0.05-0.15%	Remaining

Table 22. S235 Chemical Composition.

The structure of the Welding Toll can be described as follow, starting from the Base. The base is a plane frame made with boxed steel S235 with cross section 100x100mm and wall thickness of 5mm. The principle of the design is to Steel Plates where needed and to build a frame that links all of them together. As already stated, the Base is used to mount both the Front and the Rear Frame Tools in different moments during the production process of the vehicle, so of the total 17 Steel Plates only 3 are needed to assembly the Rear Frame: the 3 Steel Plates colored in Green (*Figure86*).

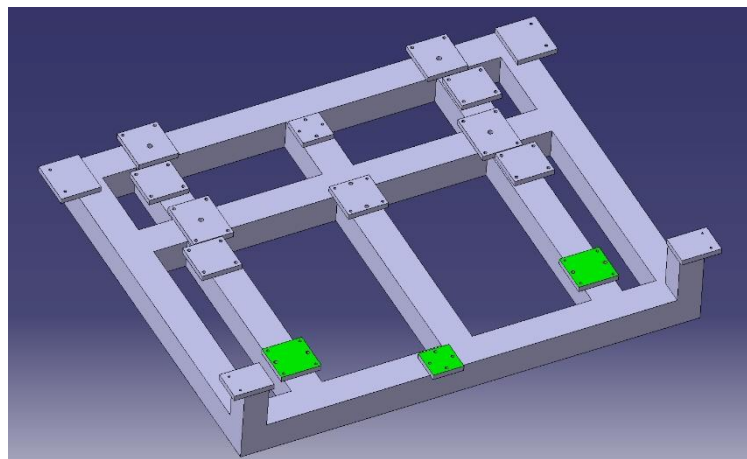


Figure 86. Welding Tools: Base.

The 2 Plates on the sides are used to mount the Rear Frame Tool, by means of 4 Screws M10 each, and to keep the two Tools in position on the Plates are bored 2  $\varnothing 12H7$  holes that will house a Centering Pin. The Plate in the middle is smaller, therefore only 2 Screws are enough to fix a Turret, centered with 2  $\varnothing 10$  Pins. The Turret, later described, is used in order to fix the Rear Motor Mount. The assembly is guaranteed in first place by the precision of the CNC Machinery, but is exploited

even more with the following method: all the Steel Plates are more thick with respect to the desired thickness, after they are welded on the Base Frame the Frame is put into a CNC Machine and milled to obtain the desired final geometry. The CNC milling guarantees a precision of about 0.5mm even for frames of considerable dimensions such as the Base, which is 1230x1500mm.

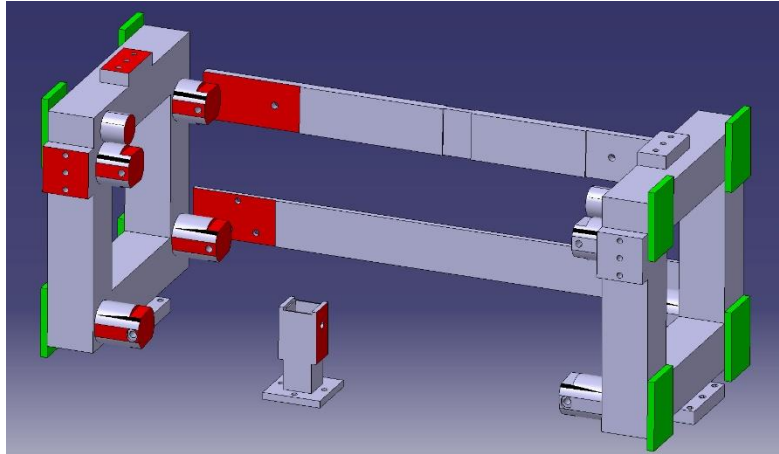


Figure 87. Welding Tools: Rear Frame Tool.

On top of the Base Tool is mounted the Rear Frame Tool, on which in fact the Rear Frame is assembled. It is formed by 2 symmetrical parts, since the Frame is symmetric, linked with 2 Steel Strips plus an isolated Turret apart. The Strips are obtained from two different sizes: the higher one from a 20mm thick 80mm wide strip, the lower one from a strip 10mm thick. The higher strip is milled in order to be coupled with the two UCA Front Nodes, so the Red surface (*Figure 87*) are obtained to match the flat side of the Node, and 2 holes  $\varnothing 12.2\text{mm}$  are added in order to fix the Strip and the Node with 2 Bolts M12, and the same is repeated on the other side. The lower Strip will be mounted on the LCA Front Nodes with the same principle, so for each Node are needed 4 holes.

The Turret in the middle has the function of positioning the Rear Motor Mount, it is made with a Steel Plate fixed on the Base on top of which is welded a boxed steel tube 50x50mm with two Steel Plates. The Mount will be fastened by means of a passing through bolt M12.

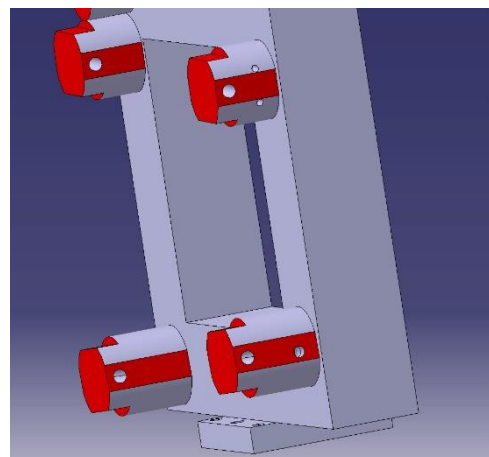
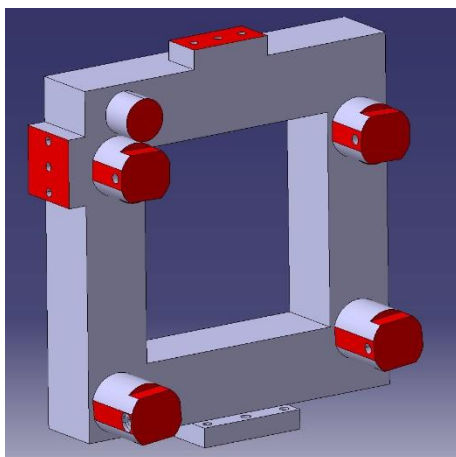


Figure 88. Welding Tools: Rear Frame Toll, details.

Finally, the main body of the Rear Frame Tool (*Figure88*) is symmetric for the two sides and it is formed by a boxed steel square 410x410mm on top of which are welded a series of elements. On the Top and Rear sides are welded 2 Steel Plates with a M10 and 2  $\varnothing 10H7$  holes each, they are put in order to be exploited in case of necessity to add other parts to the Tool. On the bottom side is welded a Plate with holes matching with those on the Base in order to assembly the Welding Tool. The inner side of the Tool is the most important, on in are directly mounted the Nodes of the Rear Frame. On the Tool are welded one Steel Block  $\varnothing 70$ mm for each Node of the Frame, apart for the UCA Rear Node for which it is required a second Block: the second block is used in order to guarantee the right position of the Rear Anti-Roll Bar interface.

The principle of the design of the blocks may appear complex but it is simple as follows (watching the Block from the inner side of the Tool):

- 2 planes are milled in almost vertical direction (with a slight slope) on the Left and Right side, on them in centered the Fork that is built on the Node in order to couple with the Universal Joint of the Suspensions;
- 2 planes are milled in almost horizontal direction, on top and bottom of the block: once that the Fork is in position it is free to rotate and move along the plane previously defined. So on these other 2 planes is centered the inner of the C-shaped sleeve that link the two parts of the fork;
- The Front plane is milled in order to remove the additional material of the block and allow the mounting of the Node on the Tool;
- A passing-through hole  $\varnothing 12$  is drilled according to the direction of the Pivot Joint in order to fix the Node on the Block with a bolt M12.

Looking at *Figure88, Left*, they must be noticed 2 additional Holes on the UCA Front Block: during the design of the welding tools the Node seemed to still be capable of rotating due to its external shape, hence 2  $\varnothing 6$  holes have been added in order to house 2  $\varnothing 6$  pins.

In conclusion it can be addressed that each Node is in fact locked with 3 constraint, as the theory suggests, they are needed to lock a 3D Body in the space. In order to fully understand how the assembly is performed it is useful to analyze the Production Process, in which it is explained why only the lower part of the Rear Frame is fixed on the Welding Tool.

### 4.3 Production Process

The building of the Welding Tool and the Welding of the Rear Frame are just 2 of the many steps of the Production Process. In order to address all the issues of interest about the Rear Frame it is useful to describe, in a very simple and schematic way, the overall process that leads to the making of the Frame.

1. *Preparation of the Central Cell:* in first place the existing Chassis has to be modified, the Front and Rear Frames are cut off the Cell according to the Trim lines defined during the Design of the vehicle.



Figure 89. COP Chassis before and after the Trim.

2. *Production of the Components:* after the end of the Design Process all the components of the vehicle are immediately queued for production, each subsystem of the car was assigned with an index of priority in order to organize the production schedule. The main issue is the Milling of the Nodes which requires a considerable amount of time, for this reason 3 out of 4 Nodes has been assigned to external suppliers to reduce queue time. The Tubes and the Metal Sheet, on the other hand, are indeed fast to be created thanks to the Laser Cutting machines and were available just after a couple of days (compared to the 2 weeks needed for the Milling);
3. *Production of the Welding Tool:* the Welding Tool should be ready before the Nodes are finished, therefore it has been processed along with the Components of the Frame, since the material is common the Tools are welded with MIG Welding (Metal-Arc Inert Gas) which exploits a Continuous Wire additional material source, that makes the welding much faster with respect to TIG Welding but with lower Welding quality (in any case acceptable for this application). The Milling of the Tools is way faster than the milling of the nodes, since on the tools are required only flat surfaces and a limited number of holes. To be clear in fact the Welding Tools were ready way before the Rear Frame Components: the Tool was needed in order to build the Front Frame that has been welded before the Rear Frame.



4. *Rear Frame Welding on the Tools:* when the Welding Tools and the Components are ready it is possible to begin the actual production step, all the Tube and Nodes are assembled on the Welding Tool and the TIG Welding can be performed. Only the lower part of the Rear Frame is involved in this process, due to an issue coming from the next step.



Figure 90. Assembly of the Rear Frame on the Welding Tools.

5. *Welding of the Central Cell Mounts:* when the first part of the Rear Frame is welded it is needed to prepare the central Cell in order to fix the Rear Frame on it, hence the 3 interface components in Aluminum are welded on the Cell. The issue with this Production step is that not only Aluminum add a sensible amount of uncertainty on the overall shrinkage of the Welding, but not for all the 3 components is possible to prepare a Welding Tool to fix their position with respect to the existing Cell. For this reason the Interface is welded on the Cell employing a Surface Gauge introducing some error in the position that is recovered in the next Step. In conclusion, the Top Mount Interface is welded adopting a simple welding tool formed by a boxed steel tube, while the other 2 Interface components are positioned by means of the Surface Gauge and the coordinates obtained in CAD Software;



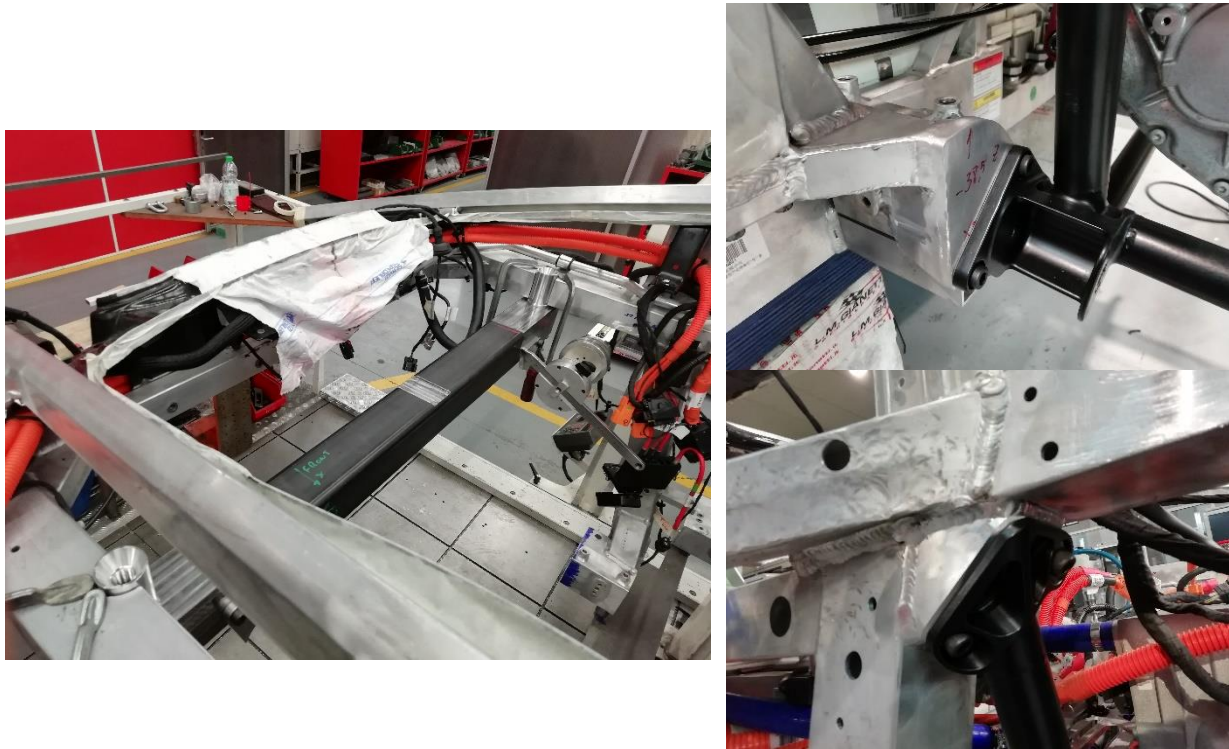


Figure 91. Welding of the Cell Interface.

6. *Welding of the Rear Frame on the Cell:* when the Interface is ready it is possible to end the Welding of the Rear Frame. The Frame is fastened on the Central Cell by means of the Surface Gauge to be set in the right position, and since the Top part of the Rear Frame is free to move it adapts to error introduced by the Welding of the Aluminum components. Finally, the Cell is stiff enough to act as welding Tool for the Welding of the Rear Frame and the Frame is completed.

7. *Final step:* when the Frame is ready it is disassembled from the Cell and sent to be painted, the Black paint will protect the Frame from corrosion and other damage as well as serve for aesthetic requirements. After the painting the Frame is assembled on the Cell for the last time and all the other components can be mounted on it.



Figure 92. Left: Rear Frame with some Electric System Components; Right: Rear Frame with Powertrain and part of the Rear End.

### 4.4 Rear Frame Weight

The weight of the Rear Frame, in fact, has not been taken too much into account during the Design Process, apart for the end of the process, in which it has been evaluated in CAD environment to get an idea on the order of magnitude and consider if a cut of weight was needed. The final result is a very light Rear Frame of roughly 28 kg, the value may seem too low if compared with the weight of the vehicle (around 2200kg) but it is the result of keeping a part of the existing Rear Frame due to the position of the Battery Pack.

The biggest part is played by the Milled Nodes (Steel 25CD4) that are responsible for 16.8 kg, more than half of the total weight, while the rest consist mainly of the weight of the tubes. Finally, the weight of the Aluminum components is small as expected, the Inverter and DC/DC Converter Supports (ALU5754) are just 1.5 kg, while in total the Motor Mounts (ALU7075) are slightly more than 1 kg, outlining how convenient is to employ Aluminum Alloy when allowed by Loads and Costs.

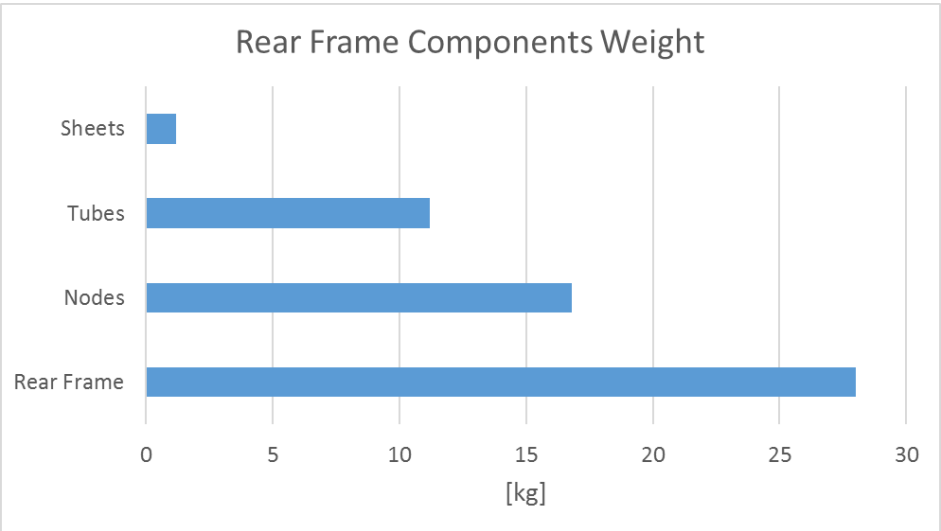


Figure 93. Rear Frame Components Weight

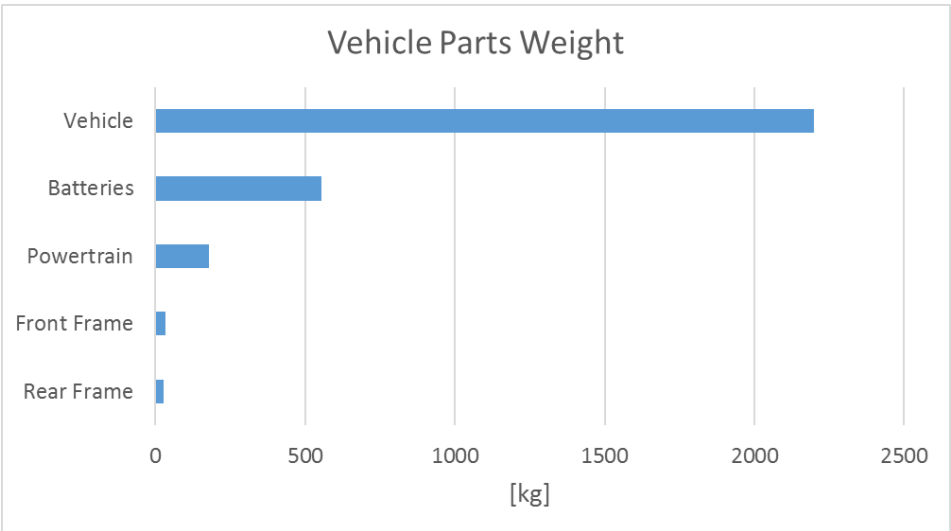


Figure 94. Vehicle Parts Weight



## 5. CHAPTER 5 – TEST REFERENCE

After the definition of the main geometry of the Rear Frame it is mandatory to verify if the Component is capable of facing loads that may be applied on the Chassis, or at least to verify if all the considerations done during the Design are leading to a satisfactory Frame. In order to do so different Dynamics conditions are taken under analysis, given by L.M. Gianetti design experience, so that Dynamics Loads can be computed and then applied as input for a Finite Element Method Analysis (from now on called FEM Analysis).

Vehicle Data			
Vehicle Weight	<b>W</b>	2200	kg
Wheelbase	<b>w<sub>b</sub></b>	2830	mm
CoG Front Distance	<b>a</b>	1415	mm
CoG Rear Distance	<b>b</b>	1415	mm
Track	<b>t</b>	1751	mm
CoG Height	<b>h<sub>G</sub></b>	250	mm
Front Axle Weight Distribution	<b>W<sub>f</sub></b>	0,5	--
Rear Axle Weight Distribution	<b>W<sub>r</sub></b>	0,5	--
Wheel Diameter	<b>d<sub>w</sub></b>	806,3	mm
Maximum Tyre Friction Coefficient X	<b>μ<sub>x,max</sub></b>	1	--
Maximum Tyre Friction Coefficient Y	<b>μ<sub>y,max</sub></b>	0,8	--

Table 23. Vehicle Data for computing Loadcases.

### 5.1 Dynamics Behavior

The first category of Dynamics Cases comes from actual Dynamics conditions that may arise if the vehicle was brought on the Track to test its maximum performance and limits. Hence, the cases will regard maximum drive and braking acceleration along with lateral acceleration affecting the vehicle while confronting corners.

#### 5.1.1 Longitudinal Acceleration 1.2g

The first Loadcase deals about a Longitudinal Acceleration of 1.2g, being 'g' the Gravitational Acceleration, with no lateral acceleration involved. Looking at *Figure95* is possible to define which Forces are acting on the Vehicle. First of all there is the Weight of the Car distributed on both Axles, since the Weight Distribution is close to 50% Front - 50% Rear is correct to assume half of the weight acting on the Front Axle and half on the Rear. The Longitudinal Acceleration generates a Weight Transfer from the Front Axle towards the Rear Axle which changes the values of the Forces acting on vertical (Z) direction, hence the load will be higher on the Rear Axle. Finally, on each Axle there is Longitudinal Force proportional the vertical load on the Axle and the friction coefficient of the Tyres.



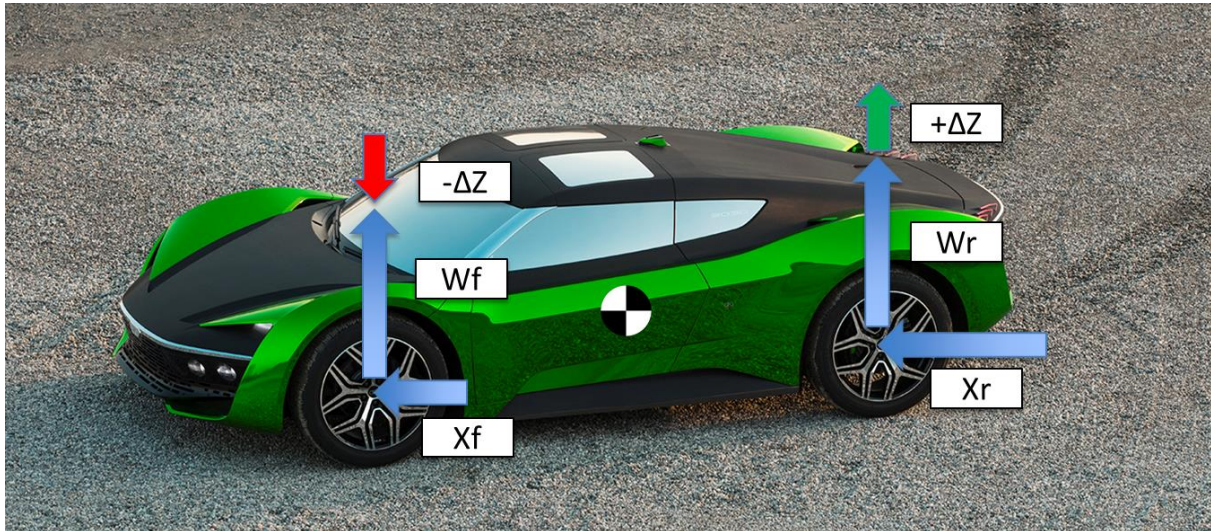


Figure 95. Loadcase: Acceleration 1.5g.

It is possible to compute the Loads as follows, starting from the weight of the vehicle  $W$  the weight on each Axle at resting conditions is computed as:

$$W_f = \frac{W \cdot g \cdot b}{W_b} = 10791 \text{ N} \quad \text{and} \quad W_r = \frac{W \cdot g \cdot a}{W_b} = 10791 \text{ N},$$

where  $a$  and  $b$  are the Distances of the CoG from Front and Rear Axles and  $W_b$  is the wheelbase. In order to get the real Force acting on each wheel the Weight Transfer must be determined:

$$\Delta Z = \frac{F_x \cdot h_G}{W_b} = 2288 \text{ N}, \text{ with Longitudinal Force } F_x = W \cdot 1.2 = 25898 \text{ N}.$$

So, on each wheel of the Rear Axle will act a vertical force  $Z$  equal to half of the sum of the vertical static Force  $W_r$  and the Weight Transfer, and a longitudinal Force equal to the maximum Force transmissible by the tyres ( $\mu_{x, \max} = 1$ ):

$$Z_r = \frac{W_r + \Delta Z}{2} = 6540 \text{ N} \quad , \quad X_r = Z_r \cdot \mu_{x, \max} = 6540 \text{ N}.$$

The Forces in  $Z$  and  $X$  direction obtained are then applied on each wheel of the Rear Axle during the analysis.

### 5.1.2 Braking 1.5g

The next Loadcase derives from a braking condition in which on the vehicle is applied a deceleration of 1.5g. This case is alike the previous one, on the Car are acting the following Forces (Figure 96): half of the vehicle weight on each axle, modified by the weight transfer caused by the Longitudinal deceleration and the Longitudinal Force due to braking action, in the case of maximum adherence between tyres and road.

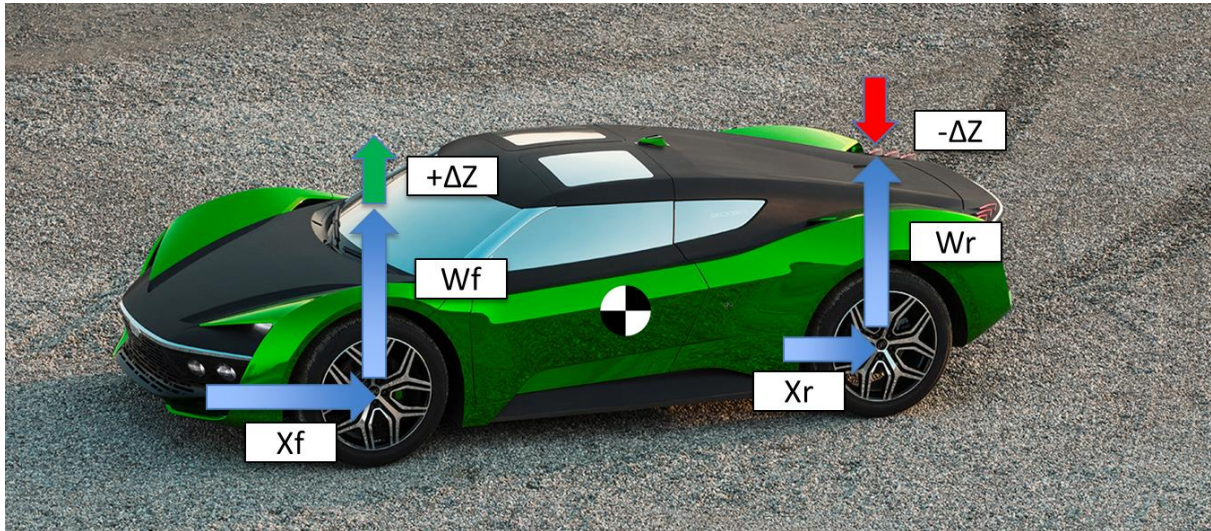


Figure 96. Loadcase: Braking 1.5g.

Considering the previous case is possible to repeat same calculations, starting from

$$W_f = 10791 \text{ N} \quad \text{and} \quad W_r = 10791 \text{ N}.$$

In order to get loads on a single wheel it is needed to evaluate the magnitude of the weight transfer:

$$\Delta Z = \frac{F_x \cdot h_G}{W_b} = 2860 \text{ N}, \text{ with Longitudinal Force } F_x = W \cdot 1.5 = 32373 \text{ N}.$$

In conclusion, also for the current Loadcase on each wheel of the Rear Axle will act a Vertical (Z) Force half of the difference between the Static Load and the weight transfer, plus a Longitudinal Force depending of the maximum friction coefficient of the tyres ( $\mu_{x, max} = 1$ ):

$$Z_r = \frac{W_r - \Delta Z}{2} = 3965 \text{ N} \quad , \quad X_r = Z_r \cdot \mu_{x, max} = 3965 \text{ N}.$$

As for the Acceleration case the Forces computed, Z and X, will be applied on each wheel hub to perform the analysis.

### 5.1.3 Cornering 1.5g

After the analysis of the loads in Longitudinal direction the last Dynamic case will focus on the Transversal orientation: it will be examined the case in which the Vehicle is traveling along a corner in such a way that on the Chassis is applied a Lateral Acceleration of 1.5g. Considering null the Longitudinal Acceleration of the Car the model will be divided between Right Hand (RH) and Left Hand (LH) sides, implying that half of the Car weight is on the RH side and half on the LH.

Observing *Figure97* it is possible to define the Loads on the vehicle: vertical load due to weight in static conditions on each side, plus or minus the module of the weight transfer induced by the Lateral Acceleration and the maximum transmissible lateral Force affected by both vertical load and friction coefficient. It must be addressed that to consider a more severe condition in taken into



account that the Car hits the curbs and therefore to the previous loads they must added two momentums in X direction.

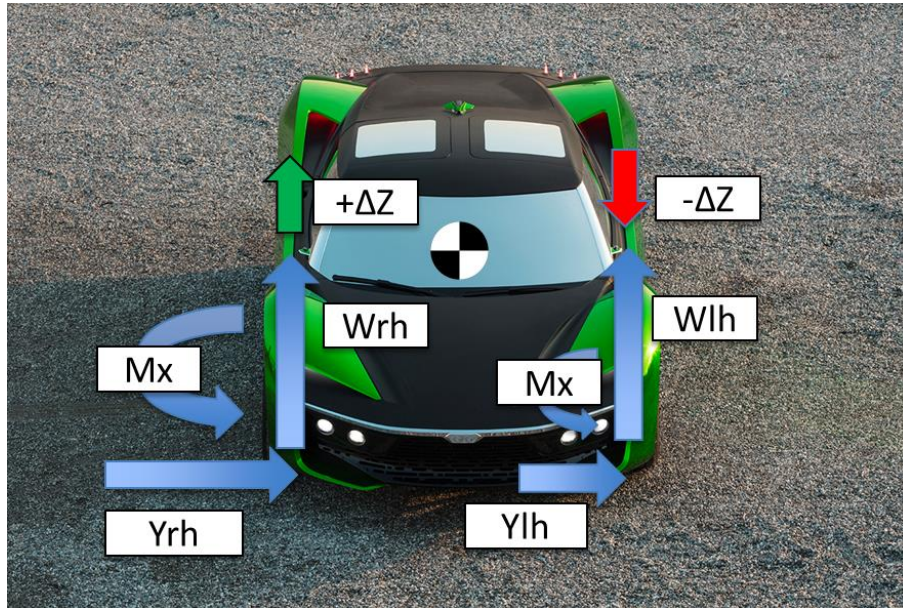


Figure 97. Loadcase: Cornering 1.5g.

Following a procedure similar to the other cases it is righteous to begin with the computation of the Static loads generated by the weight on both vehicle sides:

$$W_{RH} = \frac{W * g}{2} = 10791 \text{ N and } W_{LH} = \frac{W * g}{2} = 10791 \text{ N},$$

Obtaining the same results as before but observing a different path. Then, the next step is to calculate the magnitude of the lateral weight transfer, starting from the lateral load and the Track (t):

$$\Delta Z = \frac{F_y * h_G}{t} = 4622 \text{ N, with Lateral Force } F_y = W * 1.5 = 32373 \text{ N}.$$

It is now proper to divide the analysis between RH side and LH, starting from the latter which is less stressed. On the Rear LH wheel will act a vertical force Z equal to half the load on the LH side: the difference between static load and weight transfer. The Lateral load will depend on Z and on the maximum friction coefficient of the tyres ( $\mu_{y, max} = 0.8$ ), and will define the module of the applied Torque:

$$Z_{LH} = \frac{W_{LH} - \Delta Z}{2} = 3085 \text{ N, } Y_{LH} = Z_{LH} * \mu_{y, max} = 2468 \text{ N}.$$

The Torque will be calculated as the Lateral Force applied on an arm equal to the wheel radius:

$$M_{x, LH} = \frac{Y_{LH} * d_w}{2} = 994800 \text{ Nmm}.$$



Repeating the consideration above also for the RH side it is possible to complete the analysis, on this side the vertical load will be equal to the sum of Static load and weight transfer, varying the magnitude of the other loads:

$$Z_{RH} = \frac{W_{RH} + \Delta Z}{2} = 7705 \text{ N}, \quad Y_{RH} = Z_{RH} * \mu_{y, max} = 6165 \text{ N},$$

$$M_{x, RH} = \frac{Y_{RH} * d_w}{2} = 2485510 \text{ Nmm}.$$

Notice that the Torque are expressed as Nmm instead of Nm, this is due to the need for obtaining MPa as unit for the Tensions after the simulation, being the geometry in mm and the Forces in N it comes that the Torques must be applied in Nmm.

## 5.2 Impact Behavior

The following Loadcases are simpler with respect to the Cases derived from the Dynamics, in fact now the focus is on the behavior of the Rear Frame in case of the Vehicle might hit some obstacles.

The first case is considering the vehicle traveling and hitting a bump on the road, in such a way that the vertical acceleration applied on the Chassis would be 4g.

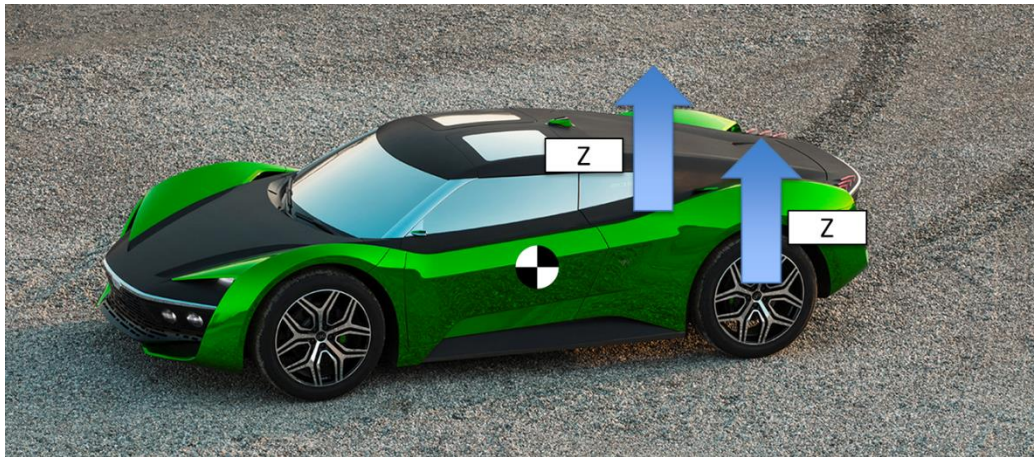


Figure 98. Loadcase: Bump 4g.

In order to get the load acting on the Rear wheels it considered that the Bump is equally divided on the 4 wheels, so it gives:

$$F_z = W * 4 = 86328 \text{ N},$$

and therefore:

$$Z_{RH} = \frac{F_z}{4} = 21582 \text{ N} \quad \text{and} \quad Z_{LH} = \frac{F_z}{4} = 21582 \text{ N}.$$

On the analysis model the loads will be thereby applied one on each wheel hub center.

The next Impact Load is even easier, it considers the vehicle hitting some obstacle on the lateral side, the load would be absorbed by both Front and Rear Frames, but since the interest is to verify the structure in the most stressing condition it is assumed that all the load is applied on the Rear Frame (the opposite would have been made in case of analysis of the Front Frame).



Figure 99. Loadcase: Lateral Impact.

With the purpose of getting a numerical value for Lateral Load the experience suggests to consider 4 times the maximum load on the Axle,

$$Y = 4 * W_r = 43165 \text{ N}, \text{ being } W_r = 10791 \text{ N}.$$

The Lateral Force Y obtained will be applied on a singular wheel hub, which one between RH or LH will not change the results.

The last Loadcase considered concerns the behavior of the structure if the Car is hitting a barrier in longitudinal direction, in this case with the Rear End of the Vehicle.



Figure 100. Loadcase: Longitudinal Impact.



---

The evaluation of the Load module even in this case refers to the experience recommendation, i.e. to apply a load equal to 2 times the weight of the Vehicle:

$$X = 2 * W = 43165 \text{ N}, \text{ with } W = 21582 \text{ N}.$$

The result is numerically equal to the Lateral Impact but this time the load will not be applied to the wheels hubs, the load will be transmitted from the Car Rear End through the Rear End Interface on the Rear Frame.



## 6. CHAPTER 6 – FEM ANALYSIS

### 6.1 Rear Frame Analysis

#### 6.1.1 Model and Loadcases

The aim of this Finite Element Method Analysis is to verify that the structure obtained at the end of the design process has a response as function of the loads described in the prior chapter within acceptance limits. The first requirement for the analysis is to build a geometric model that can be imported into the FEM analysis software *Altair Hypermesh*, thus the components are assembled and jointed together in CAD environment using *Dassault System CATIA* software in order to get a single part.

The model geometry is then cleaned from defect that would complicate the meshing process, by means of the in-built tools in the software. After the cleaning of the surfaces on the geometry is built a 2D Mesh with mixed QUAD and TRIA elements, that will work as a guideline for the 3D Mesh. The target mesh density is related to a mean element size of about 4mm, with possible values varying from 0.5mm to 5mm: in such a way it is possible to cover large regular surfaces like those of the tubes with fewer elements, while precision in complex local points is assured by the possibility to create smaller elements. It follows a correction of the 2D mesh in order to avoid collapsed 3D elements and then the 3D Mesh is generated using TETRA elements.

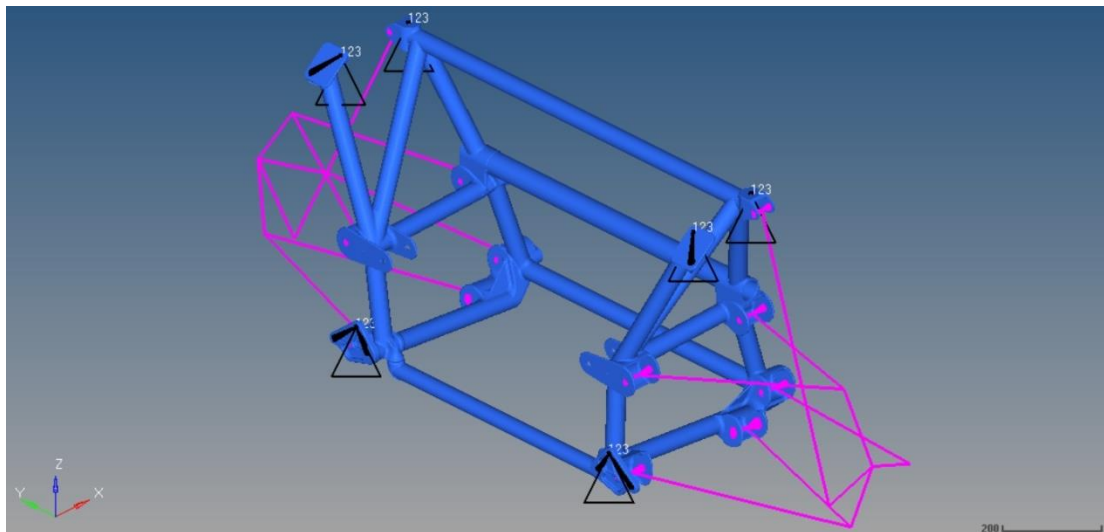


Figure 101. FEM Model with Suspensions interface.

After the mesh (*Figure101*, Blue) is defined the next step is to add any interface needed to transmit loads and put constraints on the Frame in the best way possible. The first group of created is that of the rigid elements RBE2 (*Figure101*, Purple) used to represent the suspensions geometry in the FEM environment. It is proper to address that the suspension geometry is linked to the Frame through a structure made of rigid elements named “spider element” (*Figure102*, Left) exploiting the holes that allows to fix the LCA and the UCA with bolts.

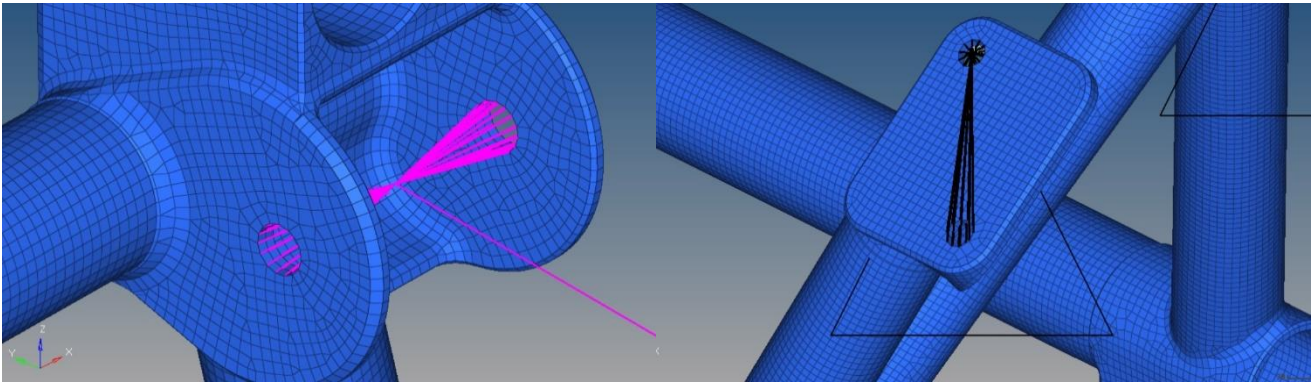


Figure 102. Left: Detail of Suspension rigids spider; Right: Detail of SPC rigids spider.

In order to assign the Single Point Constraints (SPC) it is necessary to create another rigids group (Black), generating a point in the center of one of the holes for the Screws and making a spider element with that point as a center, the SPC will be applied on the such center.

The model as it is now is ready to be used to analyses all the Loadcases in which the Forces/Torques are acting to the wheels hubs, so all the Loadcases apart for the Longitudinal Impact that will be applied on a different model. Such a model has not need for the suspensions to be involved but needs a proper rigids group that will allow to transfer the Force in X direction to the Rear End interface (Figure103).

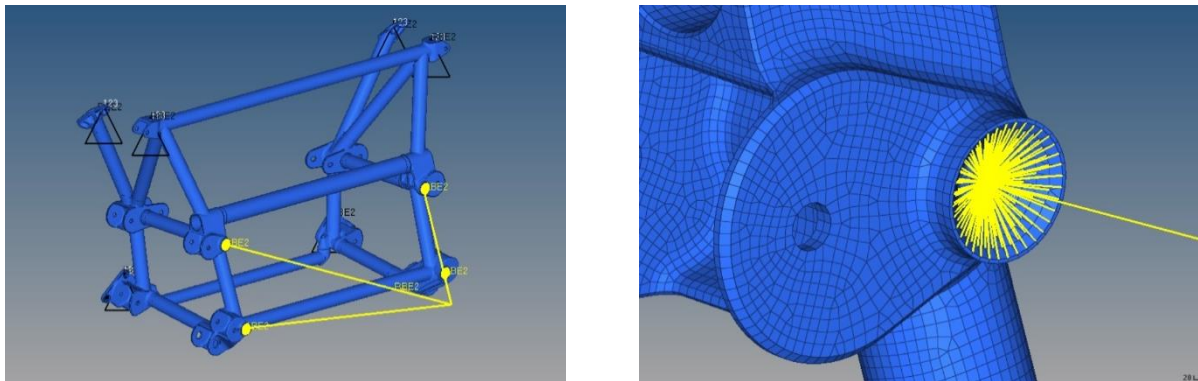


Figure 103. Left: Longitudinal Impact Model; Right: Detail of Rear End rigids spider.

The model is then completed by setting the right material properties to the meshed elements, in this case is quite simple since there is only one material involved. The reference values for the 25CD4 are contained into the Table13 and can be summarized as: Young Modulus  $E=210$  GPa; Poisson Ratio  $\nu = 0.3$ ; Density=  $7.8 \text{ kg/dm}^3$ ; UTS=800-950 MPa; Yielding Stress  $R_{p0.2}=600$  MPa.

The Loadcases applied to the Frame have already been described in the prior chapter and as a remark it can be said that the Forces/torques are all applied to the wheels hubs (the most outward points of the Suspensions rigids group) apart for the Longitudinal Impact. Now it follows a recap of the loads in modules and directions.

Loadcases						
	Left Wheel			Right Wheel		
Test	X [N or Nmm]	Y [N]	Z [N]	X [N or Nmm]	Y [N]	Z [N]
Acceleration 1,2g	6540 N	0	6540 N	6540 N	0	6540 N
Braking 1,5g	3965 N	0	3965 N	3965 N	0	3965 N
Cornering 1,5g	994800 Nmm	2467 N	3085 N	2485510 Nmm	6165 N	7705 N
Bump 4g	0	0	21582 N	0	0	21582 N
Lateral Impact	0	43164 N	0	0	0	0
Longitudinal Impact	43164 N	\\	\\	\\	\\	\\

Table 24. Loadcases Resume.

The SPC are easy to apply, they are put on the Interface Nodes employing the holes that allow the Rear Frame to be fastened on top of the CoP Cell, on the holes cylindrical surface, limiting the Degrees of Freedom (DoF) 1, 2 and 3 which corresponds to translation in x, y and z directions. The structure obtained will be Hyperstatic because in total the SPCs are acting on 6 different point, but it is close to what happens in reality and the choice of the constrained DoF is coming from a trade-off between describing in the proper way the fastening action and not overestimate the stiffness of the Rear Frame.

*Nota bene*, it is important to address all the assumption and hypothesis on which the model has been built, in no particular order:

- CoP Cell infinitively stiff: the data about the Central Cell are unknown and it is not possible to model it in FEM environment due to needed computer processor power, time and costs. Therefore the SPC are set in order to ignore the what happens on the rest of the vehicle and the loads are all applied to the Rear Frame, defining an analysis with conservative approach;
- Suspensions infinitively stiff: hypothesis needed in order to transmit the loads directly to the rear frame neglecting the deformation happening in the suspension components;
- Neglected Powertrain: in real conditions the Powertrain and Power Electronics Components are influencing the overall stiffness of the Frame, increasing it. The powertrain alone is primarily made of steel and weight around 90 kg, almost 3 times the weight of the Frame. This assumption moves the analysis further towards a conservative approach.
- Neglected Aluminum components: the stiffness is hardly influenced by the presence of the aluminum sheets, hence they are neglected to simplify the model without causing too much error.

Will now follow a list of results with a brief indication of the maximum displacement and stress of the frame, after that the analysis.



### 6.1.2 Acceleration Slip 1.2g

- Maximum Displacement:  $f = 0.073 \text{ mm}$ .

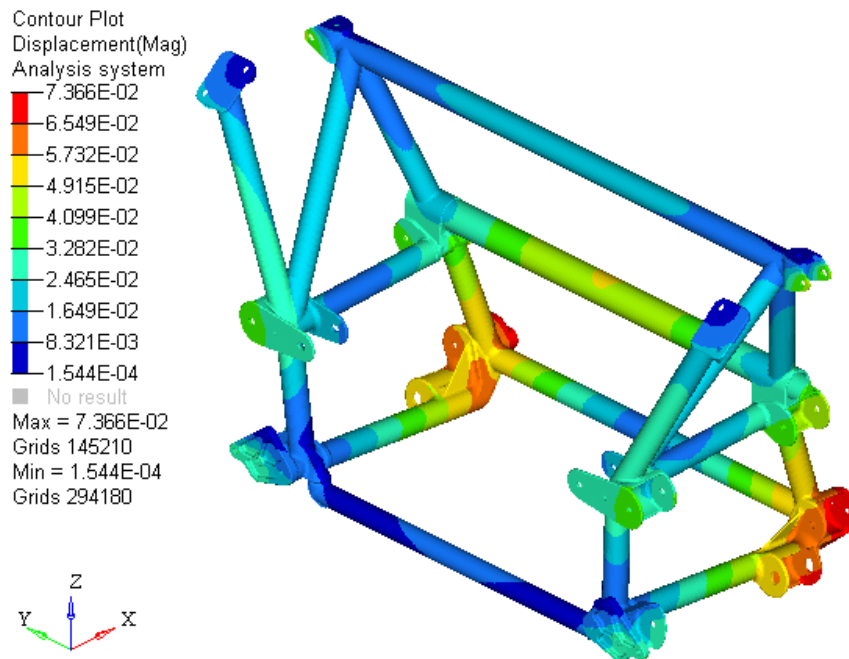


Figure 104: Acceleration 1.2g Displacements.

- Maximum Stress:  $\sigma_{MAX} = 164 \text{ MPa}$ .

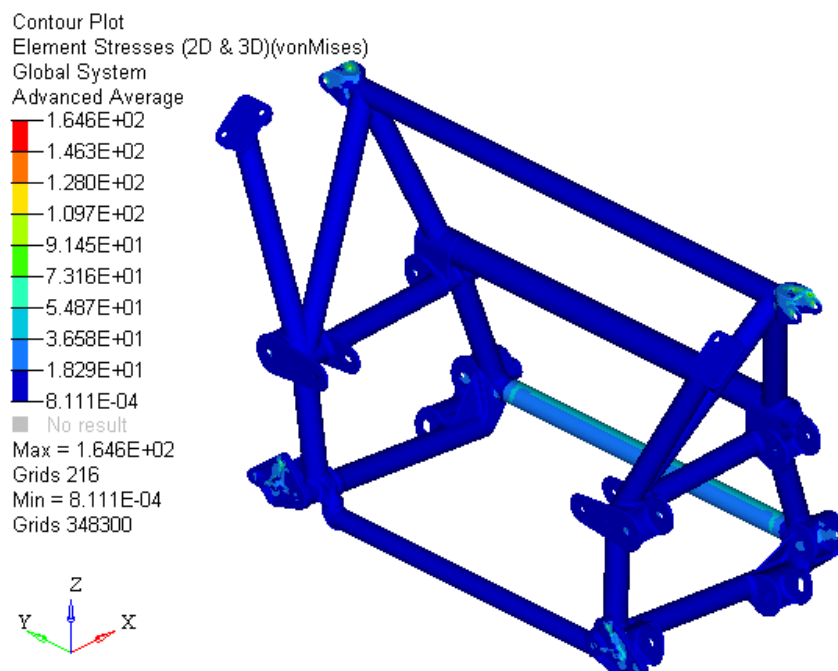


Figure 105. Acceleration 1.2g Stresses.

### 6.1.3 Braking 1.5g

- Maximum Displacement:  $f = 0.052$  mm.

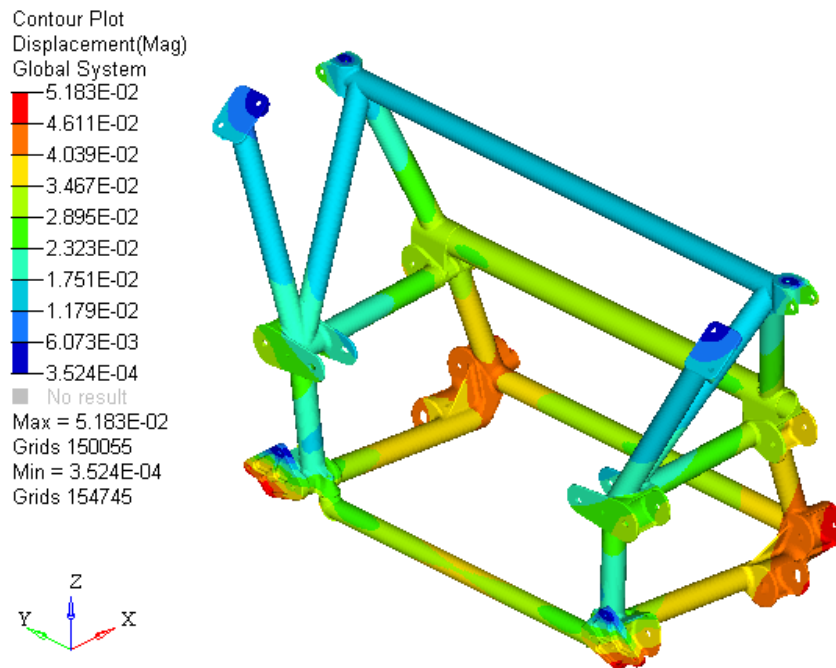


Figure 106. Braking 1.5g Displacements.

- Maximum Stress:  $\sigma_{MAX} = 127$  MPa.

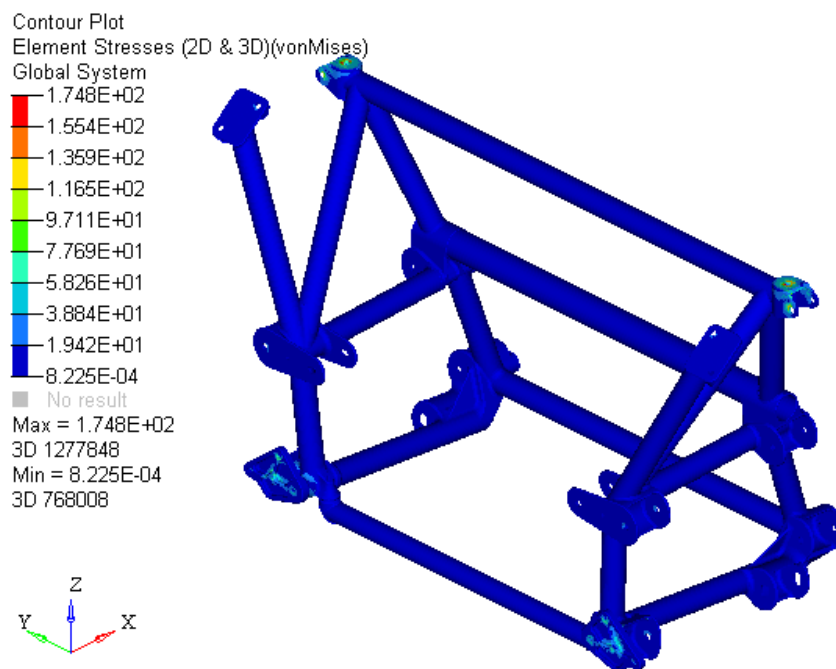


Figure 107: Braking 1.5g Stresses.

#### 6.1.4 Cornering 1.5g

- Maximum Displacement:  $f = 1.336 \text{ mm}$ .

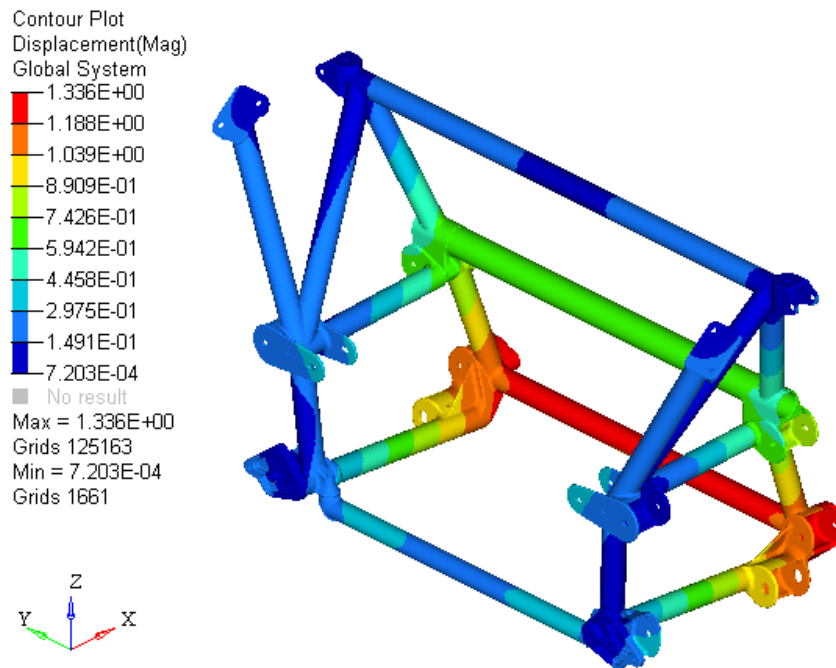


Figure 108: Cornering 1.5g Displacements.

- Maximum Stress:  $\sigma_{\text{MAX}} = 156 \text{ MPa}$ .

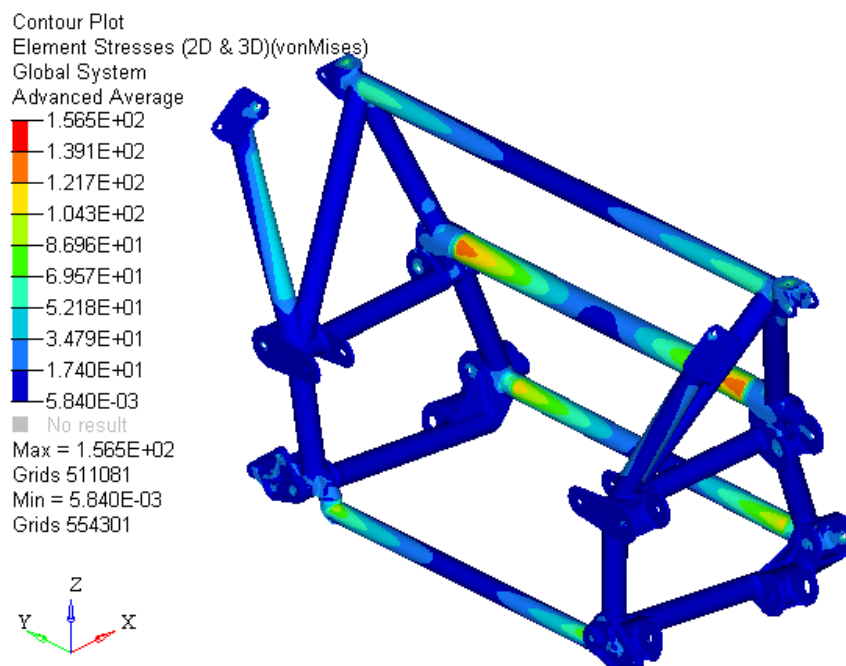


Figure 109: Cornering 1.5g Stresses.

### 6.1.5 Bump 4g

- Maximum Displacement:  $f = 0.11$  mm.

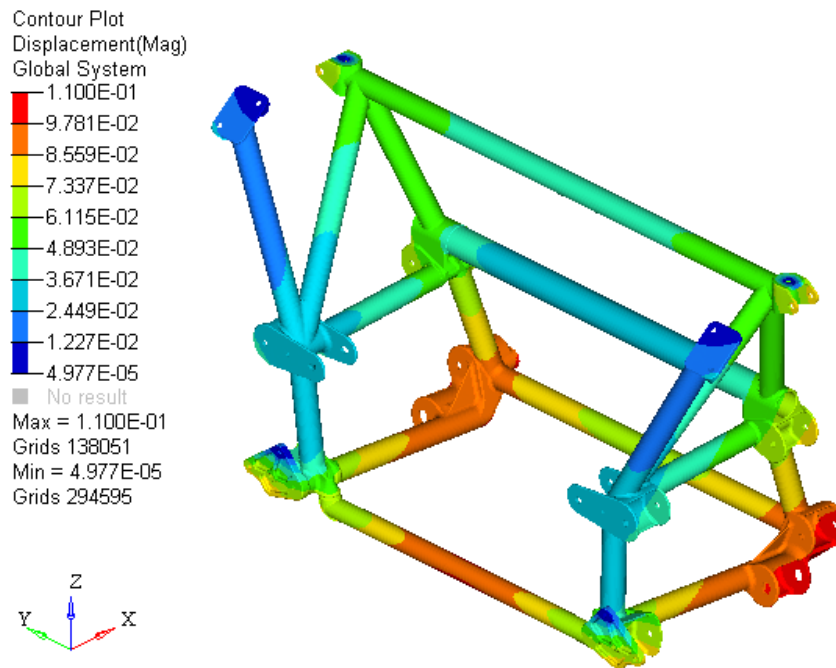


Figure 110: Bump 4g Displacements.

- Maximum Stress:  $\sigma_{MAX} = 396$  MPa.

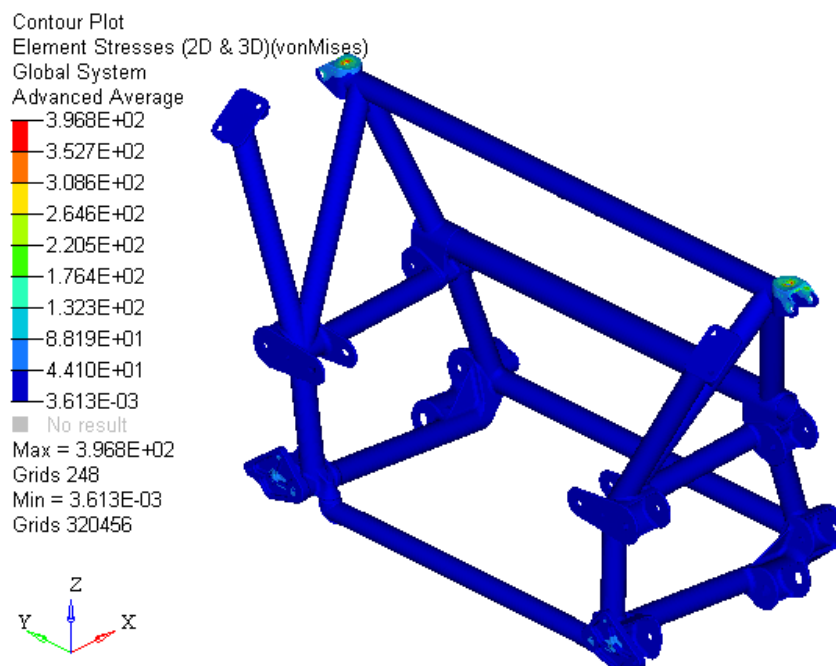


Figure 111: Bump 4g Stresses.

### 6.1.6 Lateral Impact

- Maximum Displacement:  $f = 4.556 \text{ mm}$ .

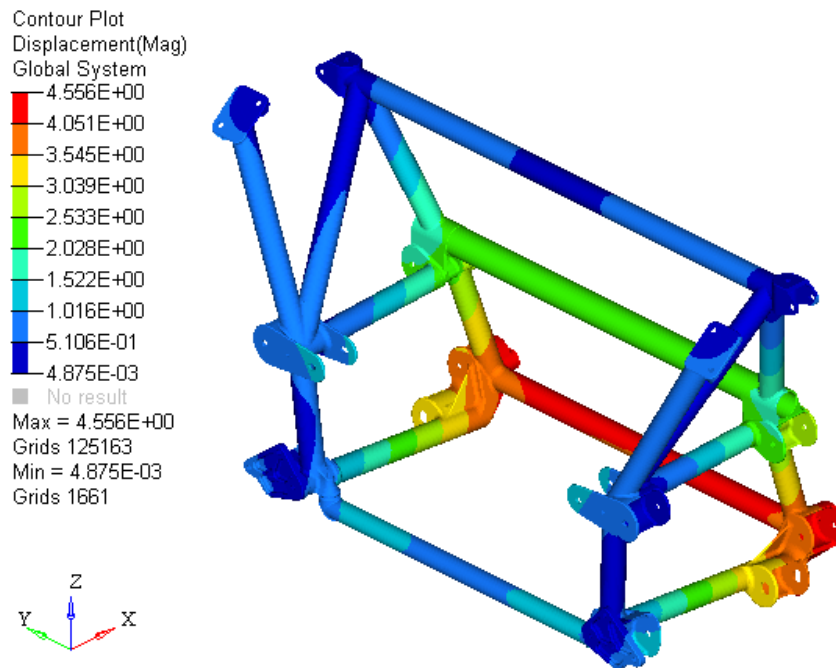


Figure 112: Lateral Impact Displacements.

- Maximum Stress:  $\sigma_{MAX} = 539 \text{ MPa}$ .

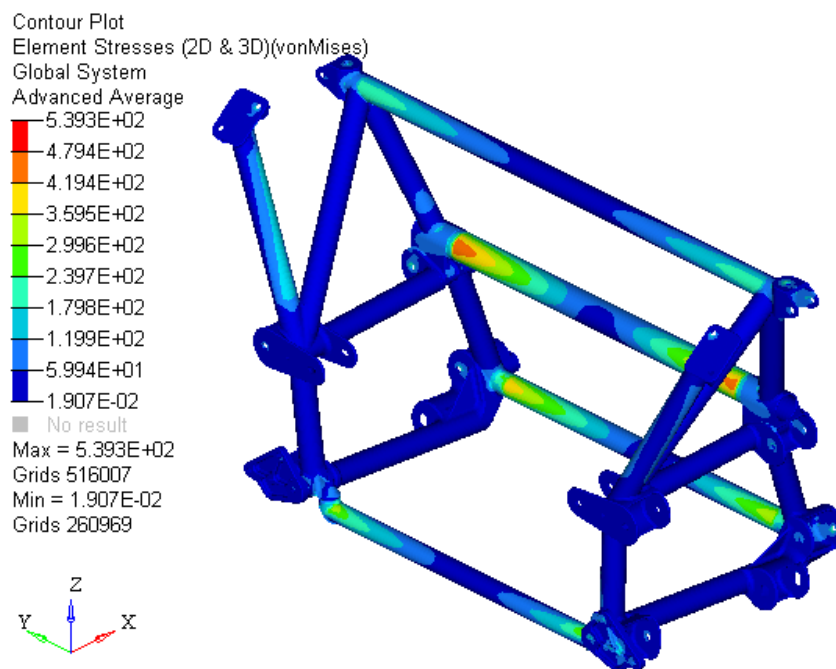


Figure 113: Lateral Impact Stresses.

### 6.1.7 Longitudinal Impact

- Maximum Displacement:  $f = 4.556$  mm.

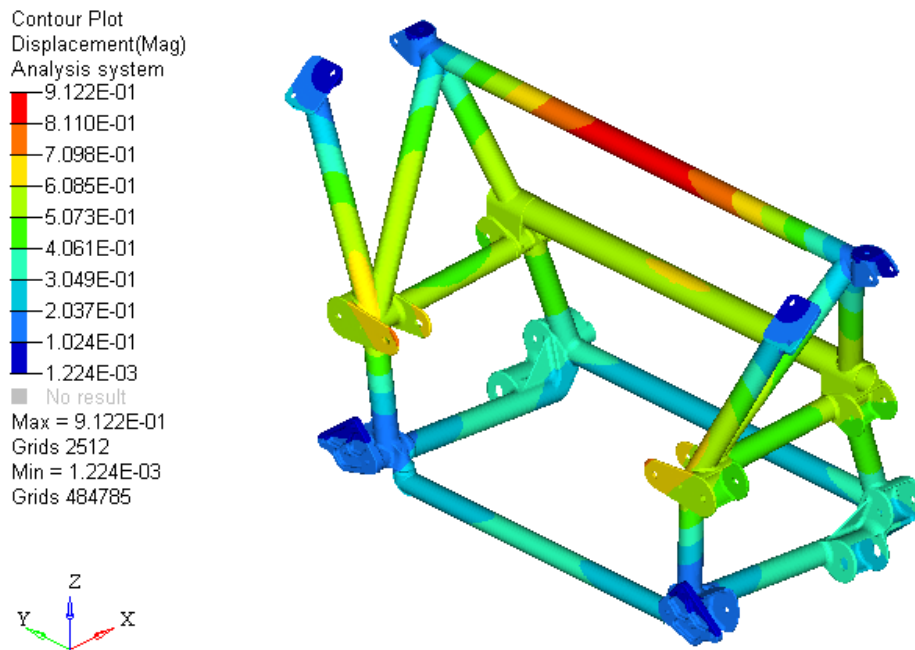


Figure 114: Longitudinal Impact Displacements.

- Maximum Displacement:  $f = 4.556$  mm.

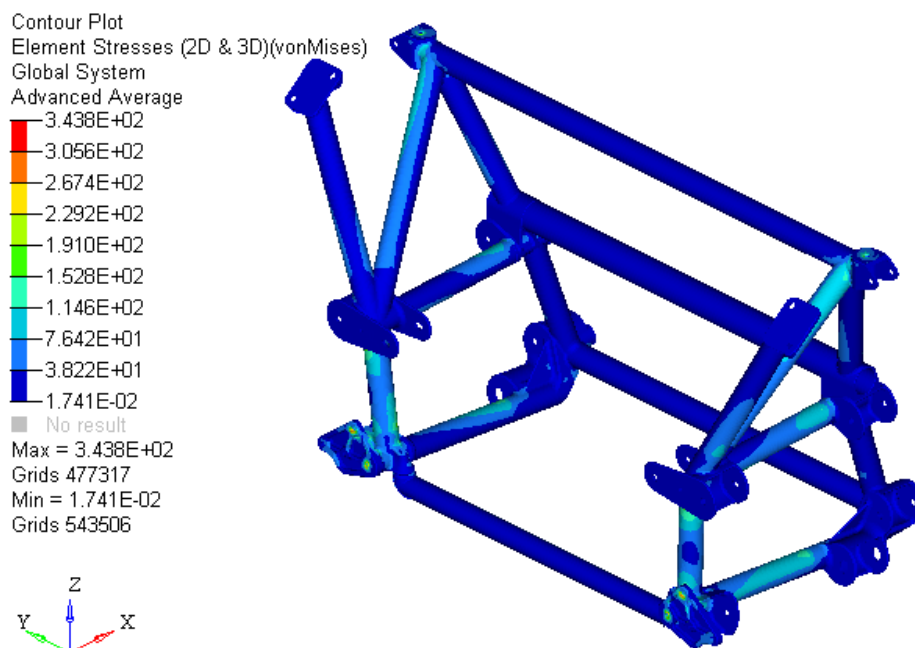


Figure 115: Longitudinal Impact Stresses.

### 6.1.8 Conclusions

FEM Analysis Results							
Hardpoints Displacements [mm]						Maximum Tension [MPa]	Max Displacement [mm]
Test	$UCA_f$	$UCAr$	$LCA_f$	$LCAr$	$ITR$	$\sigma_{MAX}$	$f$
Acceleration 1,2g	0,025	0,036	0,014	0,056	0,059	164	0,073
Braking 1,5g	0,024	0,033	0,029	0,041	0,042	127	0,052
Cornering 1,5g	0,137	0,708	0,199	1,080	1,206	156	1,336
Bump 4g	0,031	0,064	0,057	0,094	0,091	396	0,11
Lateral Impact	0,436	2,451	0,712	3,651	4,105	539	4,556
Longitudinal Impact	0,544	0,515	0,159	0,305	0,327	343	0,912

Table 25. FEM Analysis Results.

With all the data recorded in a single table is then possible to evaluate the behavior of the Rear Frame under the imposed Loadcases, starting from the general Maximum Displacements and Maximum Stresses.

It is immediately noticeable that the overall displacements of the Acceleration Slip and Braking cases are indeed low (less than a tenth of a millimeter): the main explanation is attributable to the modules of the forces applied which are the lower between the cases and, furthermore, it is outlined that the constraints might overrate the Stiffness in these case and so to fully analyze a case with consistent vertical force it is needed to model also the Central Cell. This was not possible due to lack of time, computer power and it would have significantly increased the costs. Along with small displacement even the Stresses are low (<170 MPa) and then is possible to consider the model coherent.

The Cornering 1.5g is as expected from experience the most stressful of the Dynamics cases, this is represented by a greater value of maximum displacement (1.35 mm), but the value of maximum stress is alike the previous cases: this is because the greater displacement is given by the combined action of the higher load but also of the greater arm of the Lateral forces with respect to the SPC, thus given an equal value of deformation the displacement will be higher.

The Bump 4g case confirms the hypothesis of the need for a complete model in order to completely characterize the Frame response to loads with vertical main direction, in fact the displacement is lower than expected being the Force applied an order of magnitude larger than the prior cases. The value of the maximum stress is higher than the average observed up to now, but the stresses are mainly concentrated between the Top Mount joint and the Top Mount SPC.

The Lateral and Longitudinal Impact cases are giving the expected results, since the Test is directed more towards a crash simulation than a dynamics condition, being the displacements 4.5 and 1mm. There is difference on the maximum stress value (540 MPa for the Lateral, 345 MPa for the other) due to the direction of the Forces: the Rear Frame is embossed with respect to the Force in Y



---

direction while it is perfectly aligned with the X direction, thus the latter Load is faced by all the structure.

The importance of the analysis of the Hardpoints displacements is given by the fact that it is expected a limited change in their position (few millimeters) while the Vehicle is undergoing common driving conditions, in order not to modify the Kinematics of the Suspensions. It is possible to address a trend aligned with that of the general maximum displacement, noticing that the displacements will be greater the farther the Hardpoint is from the SPC, accordingly to the principle that with the same strain the displacement of a point will increase with its distance from the center of rotation.

The larger Hardpoints displacement are recorded for the Cornering 1.5g, the Lateral and the Longitudinal Impacts, already identified as the most severe Loadcases. The values of the Lateral Impacts exceed the limits, but it is not an issue since it is not a Dynamics case, but a crash, and the tensions are within Yielding Stress. The values for the Cornering are around the limits yet they are not a concern: it has been neglected the effect of the Anti-Roll Bars and the presence of the Powertrain, therefore the actual displacement in real driving condition can be considered acceptable.

Finally, for the cases of Acceleration Slip, Braking and Bump it is not possible to outline in the graphs the distributions of the stresses, this is due to the fact that the stresses are concentrated around the SPC and in order to outline the distributions it must be applied a filter that masks the values higher than a certain value: said value would be so low that the interest in defining the Stresses Distributions is negligible.

## 6.2 Motor Mounts FEM Analysis

The Motor Mounts described in Chapter 3 are not directly involved in any of the Loadcases, since the Powertrain contribution to the Frame stiffness is neglected, nevertheless considering that they are made out of Aluminum it is of interest to perform at least a simple FEM analysis to check if the weight reduction has decreased the components stiffness beyond limits. In order to do so it is observed a simple Loadcase based on the maximum Torque out of the Reducer in Transient Conditions, neglecting a Safety Factor due to the Maximum Performance of the Vehicle is exploited unfrequently and for a reduced time period. The maximum torque Transmitted is rounded to 2720 Nm, and it is acting on an arm of 400mm. Hence the Force applied to each side, Front and Rear, of the powertrain group is 6800 N: on the Front Mounts it will be split half for each Mount, on the Rear Mount it is applied directly. Since all 3 the components are made of ALU7075 the material in the model is equal for all with parameter referred to the *Table9*: Density 2.7 kg/dm<sup>3</sup>; Young Modulus 72 GPa; Poisson's Ratio 0.3; UTS 530 MPa and Yielding Stress 460 MPa.

### 6.2.1 Left Motor Mount

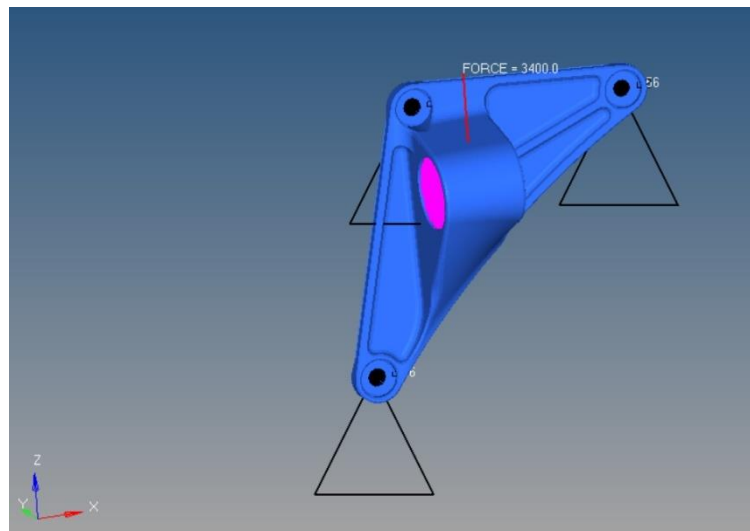


Figure 116. Left Motor Mount FEM Analysis Model.

The model of the Mounts, starting from the Left Motor Mount, are all based on the same ideas, the component is imported in FEM environment and after a brief correction of the geometry a 2D Mesh made of mixed QUAD and TRIA elements is generated. The 3D Mesh is obtained over the 2D Mesh guide and the elements created are simple TETRA elements.

The Vertical load is applied by means of a RBE2 rigids spider on the internal surface of the eyelet, and with a separate set of RBE2 rigids the SPC are put in place of the 3 passing through holes for the Screws.

Observing *Figure117* is possible to measure the maximum displacement on the rib under the eyelet with value 0.149 mm, and in the same place the maximum stress is 149 MPa.

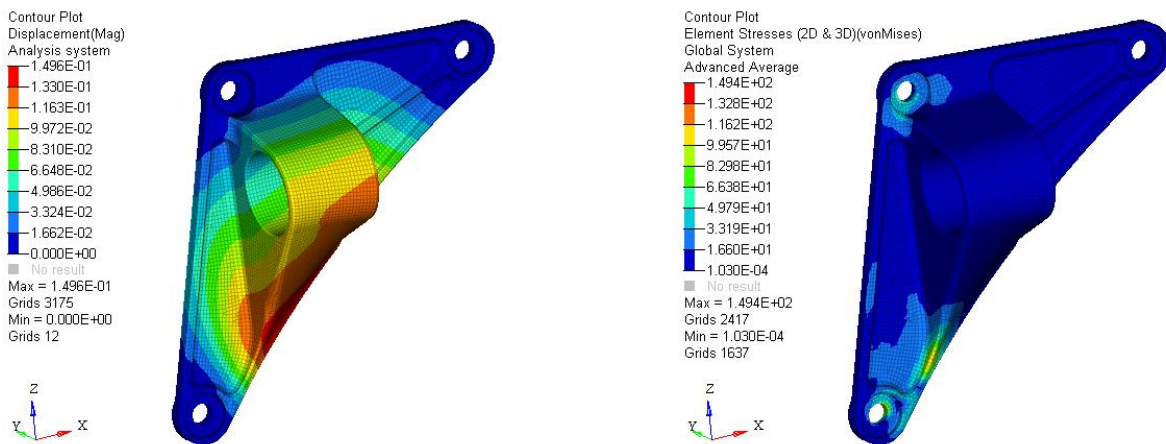


Figure 117. Left Motor Mount FEM Analysis Results.

### 6.2.2 Right Motor Mount

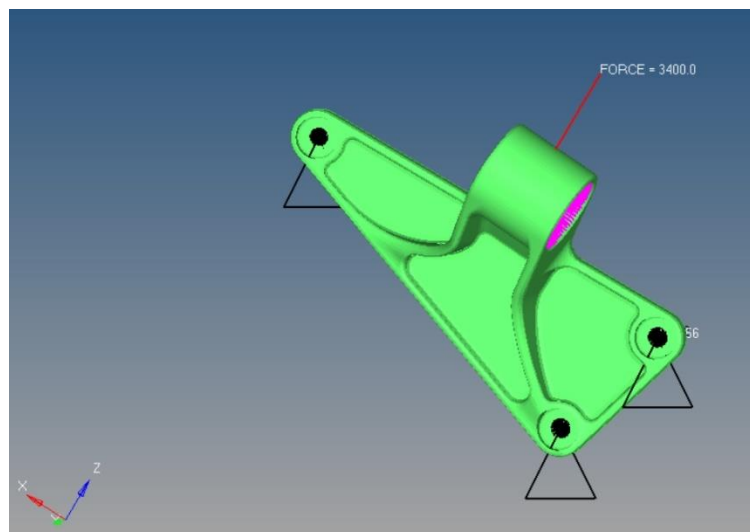


Figure 118. Right Motor Mount FEM Analysis Model.

The model of the Right Motor Mount is in practice the same as for the prior component: the base 2D Mesh is made of mixed QUAD and TRIA elements that helps the building of the 3D TETRA Mesh.

The Load is the same as before and it is applied on the bore of the eyelet via RBE2 Rigids, meanwhile also in this case the SPC are put on the 3 holes with which the Mount is fixed on the Powertrain.

The analysis results in *Figure119* give the values for maximum displacement 1.171 mm on the eyelet and maximum stress 291 MPa on the shorter of the ribs under the eyelet.

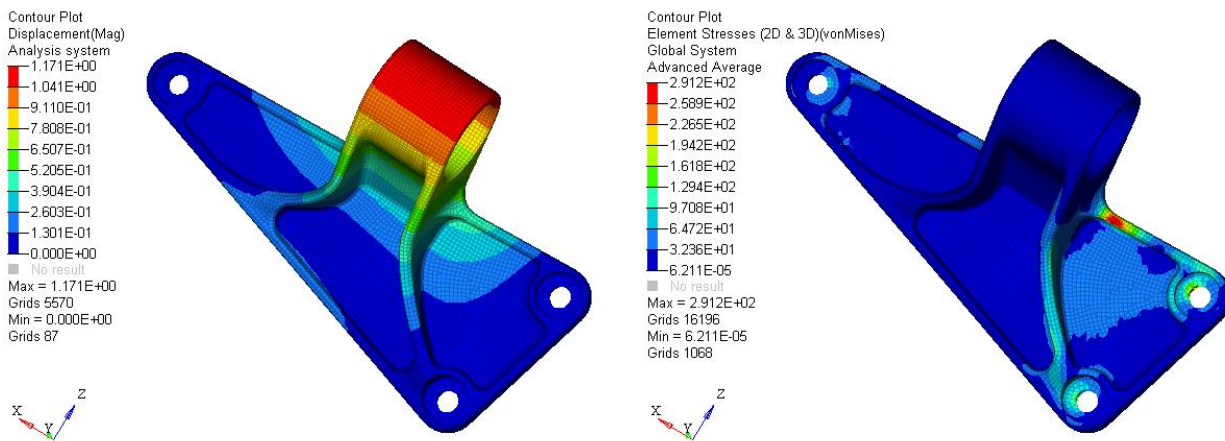


Figure 119. Right Motor Mount FEM Analysis Results.

### 6.2.3 Rear Motor Mount

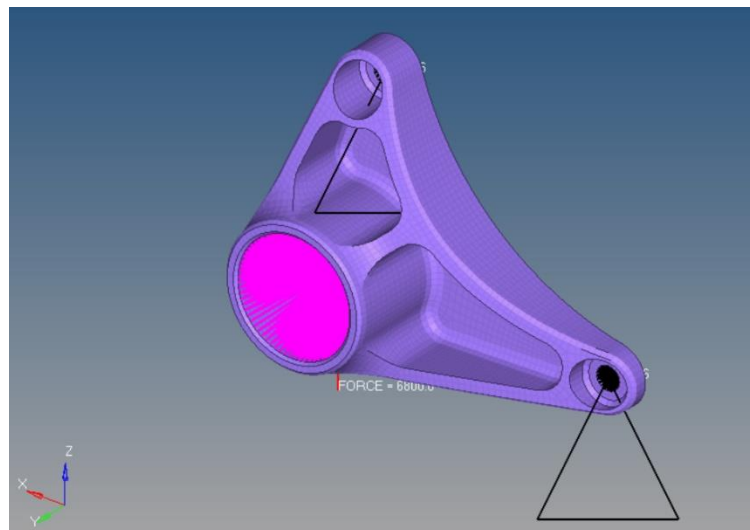


Figure 120. Rear Motor Mount FEM Analysis Model.

The last of the Motor Mounts has a slightly different geometry but the model is created with the same features of the others: 2D mixed QUAD and TRIA mesh as base for a 3D Mesh made of TETRA.

The load applied this time is twice in model and opposite in direction with respect to previous components, but it is still applied on the bore of the eyelet, the SPC are placed on the only 2 holes designed to fasten the Mount on the Reducer.

Finally, the general results are a maximum displacement of 0.502 mm in the lower part of the eyelet and a maximum stress of 281 MPa in the higher of the 2 counterbored holes.

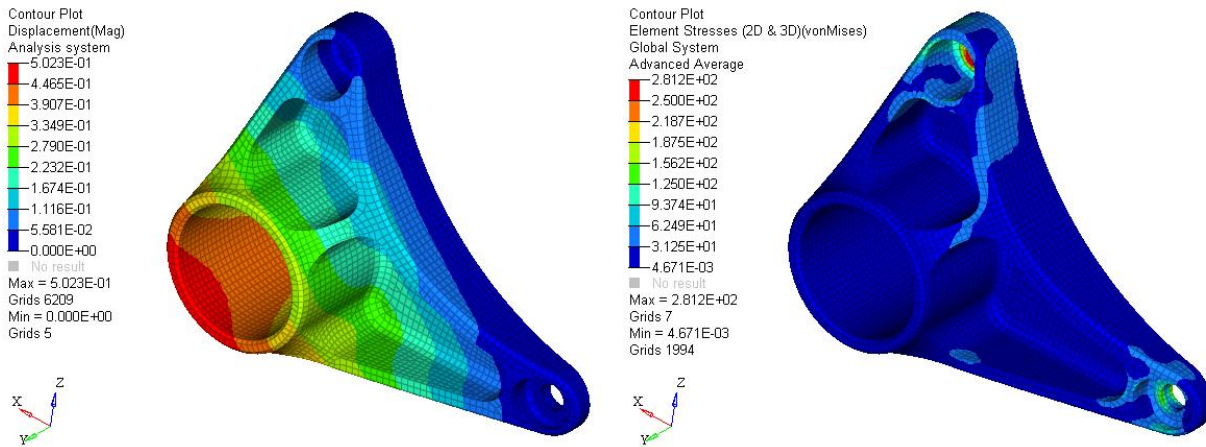


Figure 121. Rear Motor Mount FEM Analysis Results.

## 6.2.4 Conclusions

Motor Mounts Results		
Component	Displacement [mm]	Maximum Tension [MPa]
Front Left Mount	0,149	149
Front Right Mount	1,171	291
Rear Mount	0,502	281

Table 26, Motor Mounts FEM Analysis Results.

The results of the analysis are quite good since for all the components is outlined a Tension Distribution coherent with the Loadcase, moreover the displacements are within reasonable limits, apart for the Front Right Mount that would probably need a combination of thicker or more numerous ribs to deal with its particularly embossed shape. It must be added that reasonably also the Rear Frame is participating in sustaining the Motor Torque, hence applying all the load only on the Mounts it is already a conservative approach: in reality the value of this displacement will be lower. Finally, the Maximum Stresses are all thoroughly within the Yielding stress (460 MPa) by a Safety Factor of at least 1.5.

In conclusion, the choice of the material ALU7075 is confirmed to be good, exploiting correctly its characteristics, being lightweight and with remarkable mechanical properties.





## 7. CHAPTER 7 – TORSIONAL STIFFNESS

### 7.1 Torsional Stiffness Assessment

#### 7.1.1 Reference and Model

In general a Vehicle Chassis must perform in terms of structural integrity, but it is also a key element influencing Handling and overall Car performance. In order to quantify this property it is introduced into the discussion the measurement of the Chassis Torsional Stiffness.

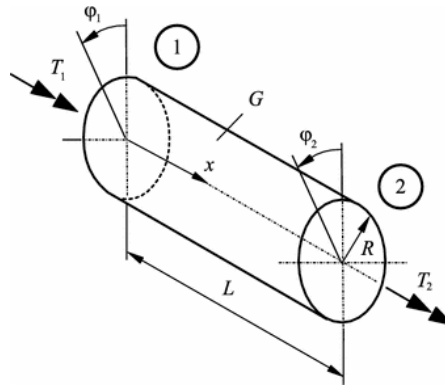


Figure 122. Torsional Bar Model.

The Torsional Stiffness, indicated with  $K_t$ , in the case of a simple torsional bar (Figure 122) it is function of the torsional load  $M_t$  in Nm applied in one or both of the 2 ends, of the Shear Modulus  $G$  in MPa, the Polar Inertia of the cross section  $I_p$  in  $\text{mm}^4$ , and the length of the bar  $l$  in mm. Therefore are obtained the main relations between these parameters:

$$\theta = \frac{M_t}{K_t}, \quad \text{with } K_t = \frac{G \cdot I_p}{l}.$$

This means that the angular displacement  $\theta$  in rad or deg is equal to the ratio between the load and the Torsional Stiffness, which can be measured in several units: N/mm, Nm/rad or Nm/deg.

Considering an actual vehicle the model must be enhanced in order to get a proper description of its behavior. Usually the Model considered is the 3-Springs Model in which are considered 3 different torsional springs connected in Series, each representing the Torsional Stiffness of a different part of the vehicle, i.e.: the Front Axle, the Central Cell and the Rear Axle.

With reference to Figure 123 it is possible to understand the influence of the Chassis Torsional Stiffness on the vehicle. In practical terms the stiffness is the resistance to twisting action, this leads to the consideration that the Chassis must be as rigid as possible since a non-neglectable deformation of the Cell would add another degree of freedom, leading to a more complex model in which a proper prediction of the car Handling would be hard to get or impossible at worst. Moreover, the Dampening of the loads is a task of the suspensions and not of the Chassis, a softer structure would absorb part of the load without dampening it and a sensible deformation of the chassis would be introduced, hence the Chassis would undergo Fatigue cycles which may results in failure.

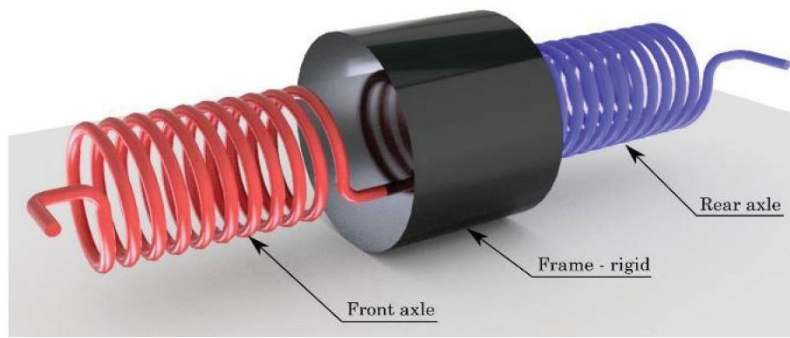


Figure 123. 3-Springs Torsional Model.

In the particular Frame under analysis it is possible to exploit the 3-Springs Model to evaluate the new value of Torsional Stiffness obtained after the alteration of the Chassis. It is proper to define the stiffness of the Front Frame,  $K_f$ , that of the CoP Central Cell,  $K_c$ , and that of the Rear Frame,  $K_r$ . Given that they are 3 springs in series the model the same “Force”, in this case Torque, is acting on all 3 the component, hence the relationship between the springs is that the overall Compliance  $C_{tot}$  is equal to the sum of the single Compliances, being the Compliance the inverse of the Stiffness.

Thus it gives that:  $C_{tot} = C_f + C_c + C_r \text{ deg/Nm}$ , and then  $K_t = \frac{1}{\frac{1}{K_f} + \frac{1}{K_c} + \frac{1}{K_r}} \text{ Nm/deg}$ .

Given the model to compute the value of Torsional Stiffness is necessary to investigate the market to look for a reference value of  $K_t$  that guides all the designing process of the Front and Rear Frame. Being the CoP in Aluminum alloy and the car type a 2-seated coupé an existing vehicle that can be seen as a reference is the Audi R8 MY2014, that has a torsional stiffness equal to 40000 Nm/deg. Another close model is the Porsche 911, generation 997, with  $K_t$  roughly 33000 Nm/deg, therefore it comes that the target value should be between 30000 and 40000 Nm/deg. Finally, looking to a car of a way higher tier can help to measure how much an increase of stiffness over the targeted range would mean in terms of increase of the design and production costs, the Bugatti Veyron is a clear example setting a Top limit of 60000 Nm/deg, from which it is important not to get too close.



Figure 124. Benchmark Models: Left: Audi R8; Right: Bugatti Veyron.

### 7.1.2 Rear Frame Torsional Stiffness

The next step towards evaluating the Chassis Torsional Stiffness is to get the values of the 3 Compliances, starting from the Rear Frame under discussion. The best choice is without any doubt to build a pre-production prototype of the Frame and to perform a Torsional Stiffness Test on a testbench, unfortunately this was not possible due to issues related to production time and costs, not being explicitly requested by the Customer all the procedure has been discarded. In place of that is possible to simulate the Test adopting the FEM Analysis and exploiting the model already built to test the Frame under driving conditions.

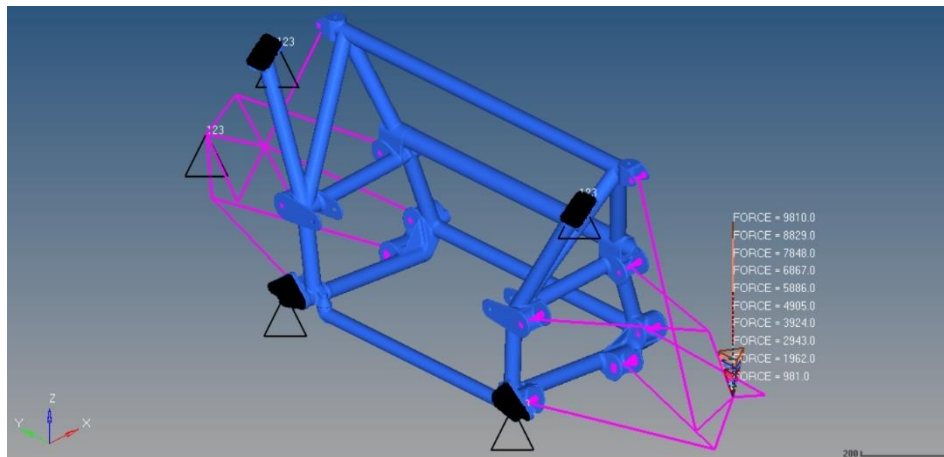


Figure 125. Torsional Test FEM Model.

The main features of the model are that the Frame is considered as a whole component, as already welded, the Suspensions are assumed Infinitively Rigid, thus they transfer all the Load on the Frame. The 3D Mesh is formed by TETRA elements and the material properties are those of the 25CD4 already described in Chapter 6.

The model still presents some differences with respect to the previous one: the Rigids and SPC applied at the Top Mount Interface are removed, because during a first run of the simulation the results obtained were greater than the expected values of more than 1 order of magnitude. The assumption made has been that the presence of said SPC is dramatically overestimating the Frame stiffness, therefore in order to get a reasonable result it has been removed, introducing some error on the  $K_t$  measure.

The Loadcases considered are a set of increasing Forces applied on one wheel hub of the Rear Axle generating a Torque equal to the Force multiplied by the Track, which values are computed as a weight fixed in said place. The values of the weight are in a range from 100 kg to 1000 kg, with an increment of 100 kg, defining a total of 10 Loadcases. In order to defining the SPC it is first needed to understand how the Test on the Testbench is usually performed.

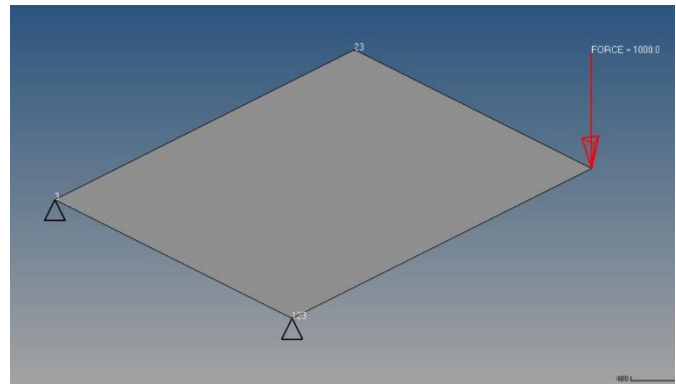
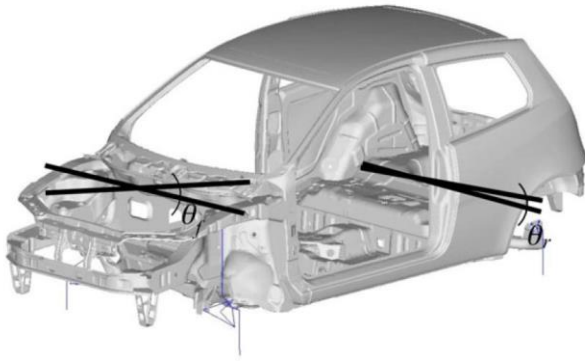


Figure 126. Torsional Test. Left: Test on the Testbench; Right: Scheme of the correct SPCs.

The Torsional Test on the Testbench is made by locking one of the Rear Cross Beams translation in all 3 directions (DoF 1,2,3), while the other is only blocked in vertical direction (DoF 3). One of the Front Cross Beams is locked in vertical and lateral directions (DoF 2,3) and the last free Hub is applied the weight, which acts in vertical direction generating a torque on the Axle: measuring the rotation of the Front axle and the Torque applied is possible to obtain the Torsional Stiffness of the Chassis.

Such a procedure is not perfectly replicable in our case:

- It is not possible to model the Central Cell in FEM environment;
- Central Cell data are unavailable;
- Focusing on the Rear Frame it is necessary to invert the Constraint between Front and Rear Axle.

Thus, it is not possible to build a model with correct Load and SPC like that in *Figure126, Right*, instead the result is the one in *Figure125*, with the vertical load applied on one Hub and all the 3 DoF blocked on the other. Additional SPC are maintained on the Interface Nodes, since as for the precedent analyses the focus is on the Rear Frame only and the behavior of the Central Cell and Front Frame are neglected. The result is a measure of the stiffness higher than the real one but traded off with the absence of the Top Mount SPC.

The results of the FEM Analysis are reported in the following table and graph.

Torsional Test FEM Analysis Results						
Weight	Force	Torque	Displacement	Displacement	Angular Dis.	$K_t$
<i>kg</i>	<i>N</i>	<i>Nm</i>	<i>mm</i>	<i>m</i>	<i>rad</i>	<i>Nm/rad</i>
100	981	1716,75	2,486E-01	0,000249	0,000142	12084925,66
200	1962	3433,5	4,972E-01	0,000497	0,000284	12084925,91
300	2943	5150,25	7,458E-01	0,000746	0,000426	12084926,31
400	3924	6867	9,945E-01	0,000995	0,000568	12083711,71
500	4905	8583,75	1,243	0,001243	0,00071	12084927,62
600	5886	10300,5	1,492	0,001492	0,000853	12081688,58
700	6867	12017,25	1,74	0,00174	0,000994	12086318,64
800	7848	13734	1,989	0,001989	0,001137	12083715,61
900	8829	15450,75	2,238	0,002238	0,001279	12081692,24
1000	9810	17167,5	2,486	0,002486	0,001421	12084933,71

Table 27. Torsional Test FEM Analysis Results.

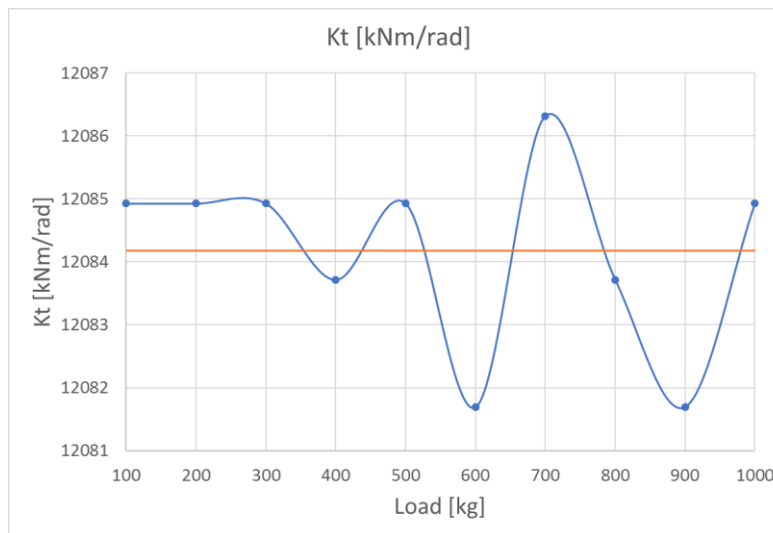


Figure 127. Rear Frame Torsional Stiffness Results and Mean Value.

The value of the displacement  $f$  of the point in which the vertical Force is applied is measured by means of tools of the Post-Processing environment, recorded in the table and converted in  $m$ . The Angular Displacement  $\theta$  is obtained as:  $\theta = \tan^{-1}\left(\frac{f}{t}\right)$  rad, where  $t$  is the Rear Track of the Car. Knowing the Torque  $M_t$  applied to the model  $M_t = F * t$  Nm, it is possible to get the value of Torsional Stiffness as:

$$K_r = \frac{M_t}{\theta} \text{ Nm/rad.}$$

The measure is repeated for each Loadcase so that a set of values for the stiffness are obtained, the final result will be the arithmetical average of the 10 values, giving:

$$K_r = 12084 \text{ kNm/rad.}$$

### 7.1.3 Chassis Torsional Stiffness

In order to compare the values with the target value of 40 kNm/deg all the values are converted in kNm/deg, starting from  $K_r = 211 \text{ kNm/deg}$ . After the evaluation of the Rear Frame torsional Stiffness it is needed to get the values for the Central Cell and the Front Frame. It follows that:

- The value of  $K_c$  for the Cell is unknown and not possible to be measured, it is necessary to introduce a hypothesis that must be verified while validating the overall Stiffness measure: from experience it can be considered that a Central Cell in Aluminum would have a value of 1/3 with respect to a Frame made of Steel. Hence:

$$K_c = \frac{1}{3} * K_r = \frac{211}{3} = 70 \frac{\text{kNm}}{\text{deg}}.$$

- The value of the Front Frame, in Steel alloy 25CD4, is made with procedure similar with the one applied for the Rear Frame, the FEM Analysis gives:

$$K_f = 147 \frac{\text{kNm}}{\text{deg}}.$$

Adopting the relationships given by the definition of the 3-Springs Model is possible to compute the final assessment for the overall Torsional Stiffness:

- The values of the 3 Compliances are calculated

$$C_f = \frac{1}{K_f} = 0.00680 \frac{\text{deg}}{\text{kNm}}; C_c = \frac{1}{K_c} = 0.01429 \frac{\text{deg}}{\text{kNm}}; C_r = \frac{1}{K_r} = 0.00474 \frac{\text{deg}}{\text{kNm}}$$

- The equivalent Compliance is:

$$C_{tot} = C_f + C_c + C_r = 0.02583 \frac{\text{deg}}{\text{kNm}}$$

- Finally the overall Torsional Stiffness is:

$$K_t = \frac{1}{C_{tot}} = 38.718 \frac{\text{kNm}}{\text{deg}}$$

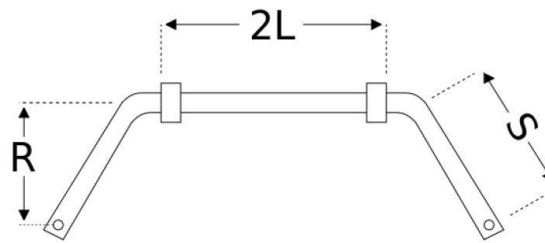
The value obtained is satisfactory with respect to the expectation and target value (40 kNm/deg), but it is of course influenced by all the hypothesis made in order to build the model and compute the value, hence the number is serving as a reference to understand that the order of magnitude of the Torsional Stiffness is right. As a final note two important considerations: first, the stiffness of the Rear Frame might be overestimated, but part of the error is recovered in real conditions because of the presence of the Powertrain; and last, the esteem of the overall Stiffness may be overestimated, but even in this case part of the error is recovered by the presence of the Interiors, glass windows and most of all the Battery Pack and its support frame.



## 7.2 Torsional Stiffness Validation

### 7.2.1 Antiroll Bars

The validation of the Torsional Stiffness value obtained in the prior subchapter starts observing the design process of the Antiroll Bars, which are involved along with the Chassis and the rest of the suspensions with the Handling of the vehicle. The design of the Antiroll Bars is based on the Model of Mike Pilbeam, that allows to link bar stiffness with its geometry.



$$Q = \frac{10^4 \times T^2 \times K^2 \times d^4}{R^2 \times L}$$

Figure 128. Pilbeam Model and Formula.

The model describes a U-shaped bar with diameter  $d$  in inch, central length  $2L$  in inch and lateral arm  $S$  in inch, with effective arm  $R$  in inch. The Formula permits to calculate the stiffness  $Q$  of the bar expressed in pounds over inches lb/inch relying also on the values of the Track  $T$  in inch and  $K$ , the leverage ratio between wheel and Bar attach. Due to the employment of the Imperial System it is implied that all that values are converted back and forth between International and Imperial Systems as befits.

The design starts with the setting of a target Stiffness value and then by means of the model and the geometry decided during the DMU Analysis the equivalent Bar Diameter is obtained. Notice that the Bar geometry and stiffness are not definitive, they are intended to be verified by means of On-road Tests and changed if necessary, with the purpose to adjust Handling Performance.

The target Bar stiffness  $K_{ARB}$  is derived from the esteemed value of Torsional Stiffness of the Chassis, by means of L.M Gianetti design experience: the Chassis Stiffness is sort of distributed on the 4 wheels, hence divided by 4 in magnitude, the resulting wheel stiffness is linked to the axle Antiroll Bar stiffness by a corrective factor equal to 10.

It will be:

$$K_t = 38718 \frac{Nm}{deg}, \quad K_{ARB} = \frac{K_t}{4 \times 10} = 968 \frac{Nm}{deg} = 55463.5 \frac{Nm}{rad}.$$

The conversion from Nm/rad to N/mm involves the Effective Arm R, given by Bar geometry, and brings to the target value:  $K_{ARB}[N/mm] = \frac{K_{ARB}[\frac{Nm}{rad}] * 1000}{R^2} = 1717.5 \frac{N}{mm}$ , rounded to  $1800 \frac{N}{mm}$ .

Rear Antiroll Bar Data						
Q		d		T		K
N/mm	lb/inch	mm	inch	mm	inch	--
1800	10265,5	18,22	0,717	1750	69,29	0,809
R		L		S		--
mm	Inch	mm	inch	mm	inch	--
179,7	7,075	411,5	16,201	200	7,874	--

Table 28. Rear Antiroll Bar Data.

In *Table28* are collected all the data needed to complete the computation, apart for the value of d which is the result obtained. In order to get d it is required to invert the Pilbeam formula and use as input the geometry parameters coming from the design constraints and the target stiffness previously calculated. Thus it is:

$$d = \left( \frac{Q * R^2 * L}{10^4 * T^2 * K^2} \right)^{\frac{1}{4}} = 0.717 \text{ inch} = 18.22 \text{ mm}.$$

The diameter computed is referring to a bar with whole circular cross section, which has the drawback to have a considerable weight. In order to reduce the weight a good solution is to consider a hollow circular cross section with Polar Inertia close to the one of the whole cross section. Such

Inertia is calculated as:  $I_p = \frac{\pi * d^4}{32} = 10300.8 \text{ mm}^4$ .

The final section is that of a tube with diameter 20 mm and thickness 2.5 mm, being:

$$I_p = \frac{\pi * (D^4 - d^4)}{32} = \frac{\pi * (20^4 - 15^4)}{32} = 10732.4 \text{ mm}^4.$$

Having set the values for Bar length, cross section and effective satisfying the requested torsional stiffness the design of the Rear Antiroll Bar is completed.

---

### 7.2.2 On Road Testing

The GFG Style Vision R2030 as stated in the introduction is a one-off prototype car, in this type of projects it is expected to face unpredicted issues and dealing with them from the early stages of design till the last components installment. Especially in the final phase of the vehicle assembly the Testing of all the car subsystems is fundamental: it allows to validate the design with any hypothesis made alongside, it permits to adjust any settings defined during the design process, may them be those of the suspensions setup or of the Hydraulics or Electronics Systems, and between others possibilities it brings out problems that would have showed up only to the final user.

The opportunity to perform simple on road tests or more complex track tests is exploited, for example, with the aim to verify if the Antiroll Bars Stiffness computation leads to a proper vehicle dynamic behavior. The perceived Handling of the car guides the final choice of Antiroll Bars assuming the following rule:

- Increasing the Front ARB Stiffness leads the vehicle towards Understeering behavior, or reduces the Oversteering;
- Increasing the Rear ARB Stiffness brings the vehicle closer to Oversteering or reduces Understeering.

The best choice, as always, is a trade-off between several elements but with clear aim for an even load transfer: the phenomena of Under or Oversteering are linked to unevenness between loads acting on the Front and the Rear axles.

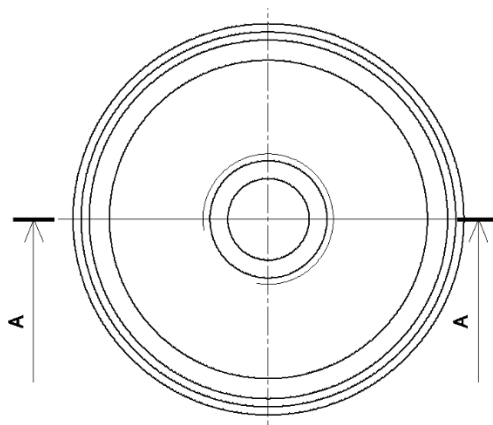
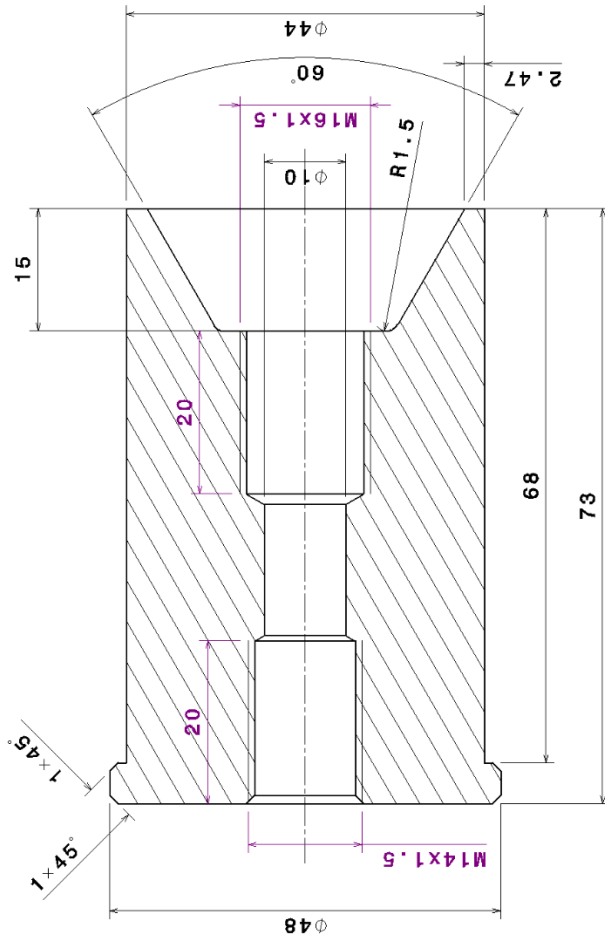
A poor performance in Handling during on road testing might cause a consistent change in Antiroll Bar Stiffness final settings with respect to the computed values, meaning that the error in assessment of the Chassis Torsional Stiffness would be non-negligible.

Along with several other issues the Validation of the Chassis Torsional Stiffness esteem and the correction of the ARB Stiffness have been tracked in place of final on road tests. The vehicle has been driven by an experienced Pilot capable to correctly address any odd behavior of the car and moreover, the test not only have been conducted on road but also on gravel: with the purpose to check the OFF-ROAD suspensions setting the car has been driven into a quarry.

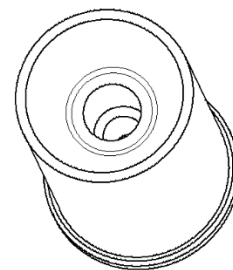
In conclusion, after the end of the tests there were not any considerable changes to be made on the ARBs, since the vehicle behavior was alright, hence the assessment of the Chassis Torsional Stiffness can be considered correct at least in terms of empirical proof. The only considerable way to definitively confirm the value is to perform a Torsional Stiffness test on testbench, but as already discussed, unfortunately, that was not possible due to time and costs issues.





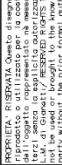

**Vista in sezione A-A**  
**Scala: 2:1**



Vista isometrica  
Scala: 1:1



- Per quote mancanti riferirsi modello matematico.
- Eliminare spigoli vivi con smusso  $0,5 \times 45^\circ$  o R  $0,5$ .
- Raggi non quotati R1, smussi non quotati  $1 \times 45^\circ$ .
- Quote da intendersi dopo trattamenti se previsti.

							
DESCRIZIONE/DESCRIPTION <b>ATTACCO SCOCCA SALDATO POST DUOMO</b>		TIPO/TYPE <b>LMG_R2030</b>		N° DI SERIE/SERIAL N° <b>01_055</b>		TAVOLA TECNICA/TECHNICAL DRAWING <b>BOCCA LAVORATA</b>	
MATERIALE/MATERIAL <b>AL 6082</b>		DATA/DATE <b>18/11/19</b>		SCALA/SCALE <b>2:1</b>		DIMENSIONI IN MM <b>0-20 -0,1 -21-50 -0,16 51-&gt; -0,2 :0,30°</b>	
TRATTAMENTO TERMICO/THERMAL TREATMENT <b>--</b>		DISEGNATORE/DRAWER <b>EM</b>		MISURA/MASB <b>-- kg</b>		FILETTI INTERNI <b>6H</b>	
TRATTAMENTO SUPERFICIALE/ SURFACE TREATMENT <b>--</b>		CONTROLLATO /CHECKED <b>--</b>		FORMATO/FORMAT <b>A3</b>		FILETTI ESTERNI <b>6g</b>	













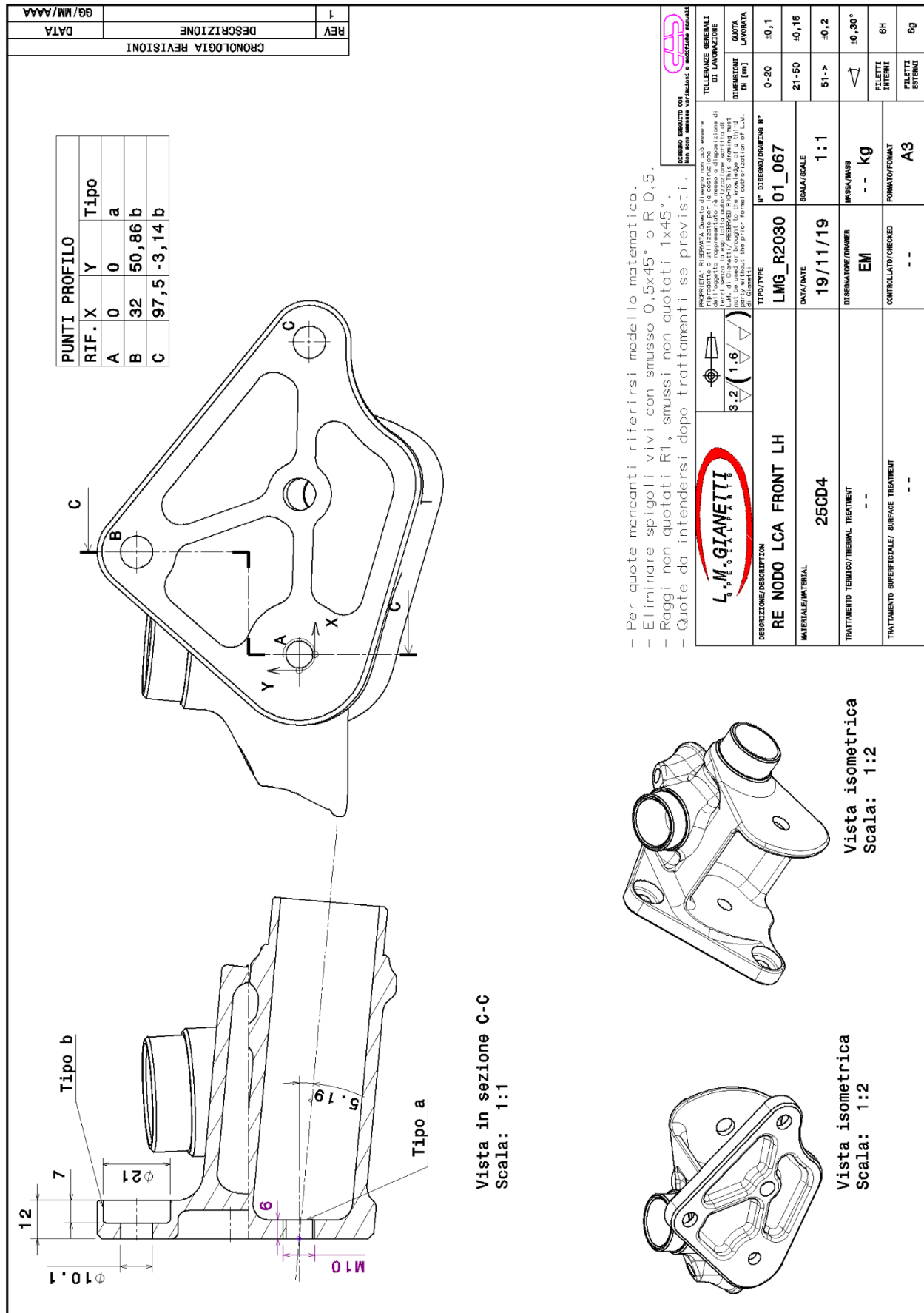




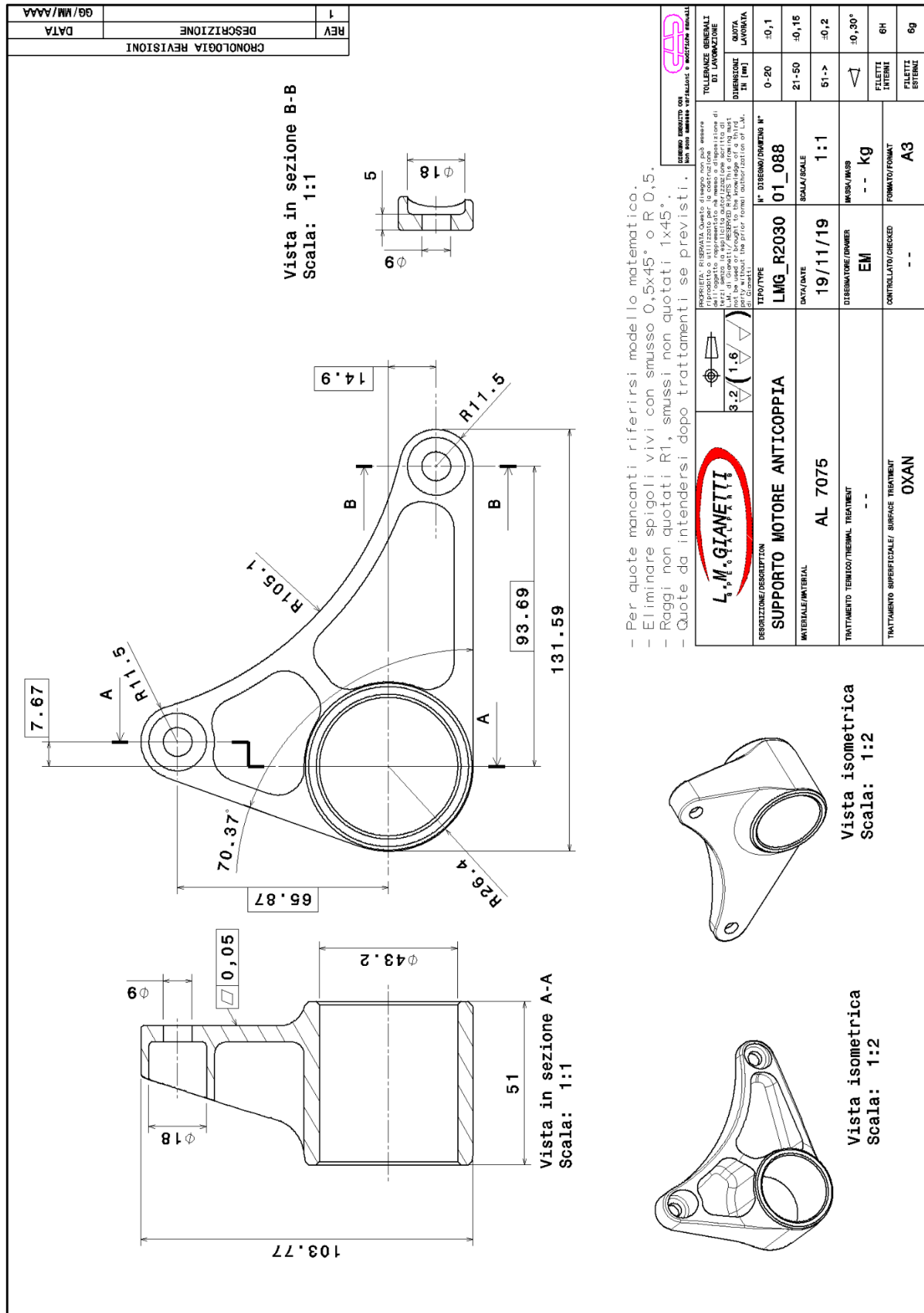






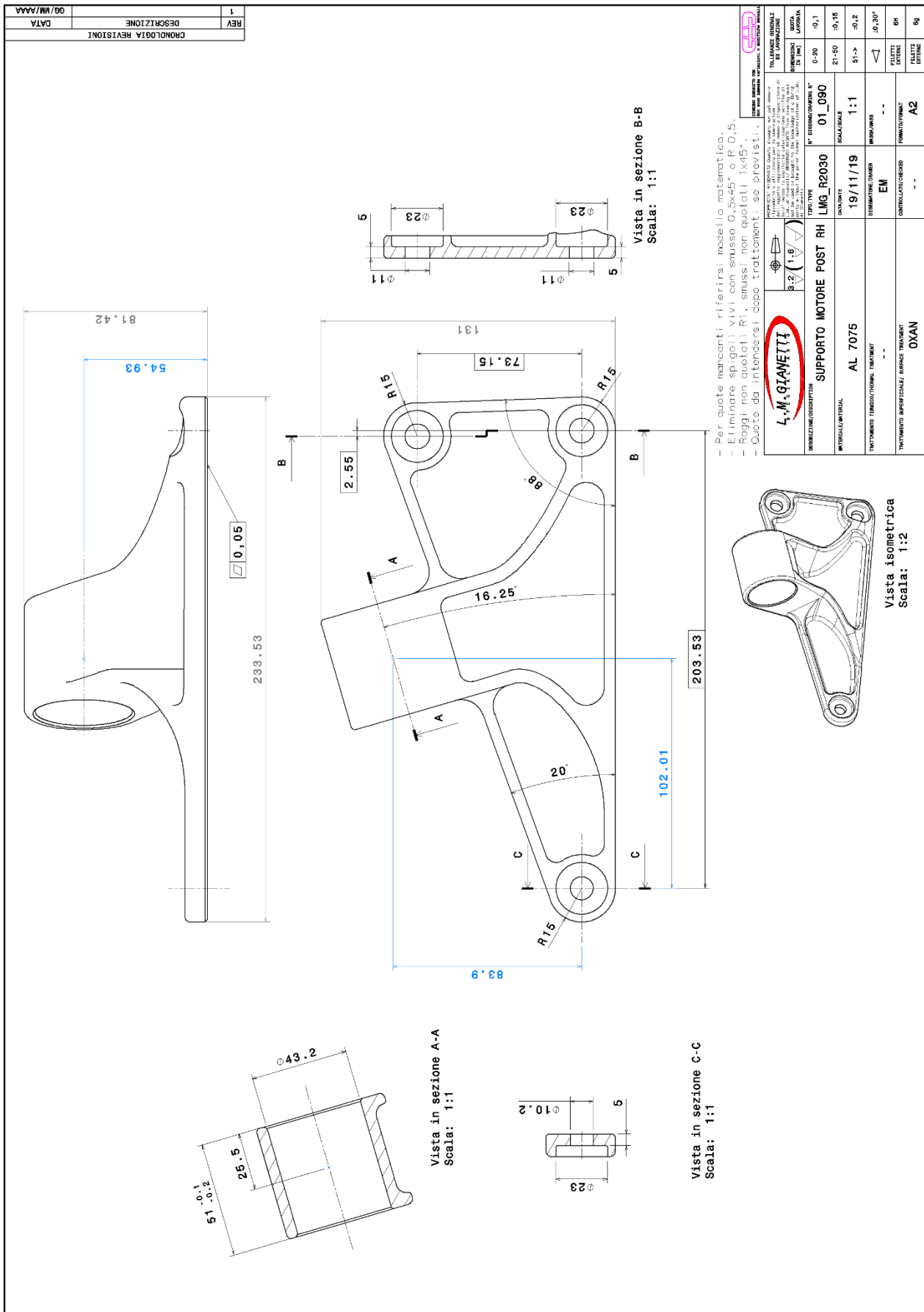












---

## Bibliography

### *Images*

<https://lmdigianetti.it>

<https://www.gfgstyle.it>

[https://it.wikipedia.org/wiki/Liquidi\\_penetranti](https://it.wikipedia.org/wiki/Liquidi_penetranti)

<https://www.conceptcarz.com/z22700/audi-r8-v8.aspx>

<https://finder.porsche.com>

[https://it.wikipedia.org/wiki/Bugatti\\_Veyron](https://it.wikipedia.org/wiki/Bugatti_Veyron)

[https://link.springer.com/chapter/10.1007/978-3-642-31797-2\\_4](https://link.springer.com/chapter/10.1007/978-3-642-31797-2_4)

### *Commercial components*

<https://www.powerflexitalia.it>

<https://www.nmbitalia.it>

<https://www.kw-suspensions.it>

<https://www.borgwarner.com>

<https://www.kvt-fastening.ch>

### *Data*

<https://mullenusa.com>

<http://www.qiantumotor.com>

<https://www.airoldimetalli.it>

<http://www.mtacciai.com>

<https://www.saf-fro.com>

<http://www.tws-saldatura.com>

---

*Books*

«*The Automotive Chassis vol.1 and 2*» - G. Genta

«*Race Car Vehicle Dynamics*» - Milliken

«*Modern Electric Hybrid Electric and Fuel Cell Vehicles*» - Ehsani, Gao, Emadi

«*Microelectronic Circuit Design*» - Richard C. Jaeger

«*Acciai E Leghe Non Ferrose*» - Nicodemi

«*Principi Generali Di Metallurgia*» - Nicodemi

«*The Automotive Body - Volume II - Systems Design*» – Morello, Rosti, Pia, Tonoli

«*Analysis of Torsional Stiffness of the Frame of a Formula Student Vehicle*» – VSB-Technical University of Ostrava, Czech Republic

«*Design and Optimization of Anti-Roll Bar*» - Kaunas University of Technology

«*Dinamica del veicolo*» – Guiggiani

«*Mechanics of vehicle*» - Tabork

«*L'assetto*» - Falcinelli

«*Vademecum per disegnatori e tecnici*» - L. Baldassini

«*Manuale dell'ingegnere meccanico*» - P. Andreini

*Course Material*

*Elementi di Costruzione di Macchine*, E. Brusa

*Tecnologia Meccanica*, E. Azteni

*Car body Design and Aerodynamics* – A. Tonoli

## Acknowledgements

I would like to use this last page to add a final consideration about my studies career's path. In first place I would like to thank part of the *Politecnico di Torino* professors, represented by Professor Andrea Tonoli, for their teachings. The first important experience I made during this last years has been to work in the *Zer037 4WD Hybrid Polito Student Team*, I want to thank my teammates and the *Italtecnica* owner Mario Cavagnero for allowing me to take part to this project. Finally, I want to express my gratitude to *L.M. Gianetti* owners Andrea, Luisa and Paolo Gianetti for the great opportunity of working in their company and my colleagues Gianluca Rao, Marco Viarengo and Mattia Viteritti for the guide in the development of this Thesis.

In conclusion, the last word of thanks is dedicated to my fellows of the Politecnico and mostly to my family, for the help in overcoming these last years.

## Ringraziamenti

*Voglio usare quest'ultima pagine per aggiungere un'ultima considerazione sul mio percorso di studi. In primo luogo voglio ringraziare parte dei Professori del Politecnico di Torino, rappresentati dal Professor Andrea Tonoli, per i loro insegnamenti. La prima esperienza importante che ho avuto negli ultimi anni è stata lavorare nel Team Studentesco Zer037 4WD Hybrid Polito, voglio ringraziare i miei compagni e il proprietario di Italtecnica Mario Cavagnero per avermi permesso di partecipare a questo progetto. Infine voglio esprimere la mia gratitudine ai proprietari di L.M. Gianetti Andra, Luisa e Paolo Gianetti per la grande opportunità di lavorare nella loro azienda e i miei colleghi Gianluca Rao, Marco Viarengo e Mattia Viteritti per la guida datami nella compilazione di questa Tesi.*

*Concludendo dedico le ultime parole di ringraziamento ai miei compagni del Politecnico e in maniera maggiore alla mia famiglia, per l'aiuto ricevuto nel superare questi ultimi anni.*